

ESKOM

NUCLEAR SITES
SITE SAFETY REPORTS

COASTAL ENGINEERING
INVESTIGATIONS

THYSPUNT

Report No. 1010/2/102

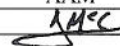
OCTOBER 2009



PRESTEDGE RETIEF DRESNER WIJNBERG (PTY) LTD
CONSULTING PORT AND COASTAL ENGINEERS

Coastal Engineering Investigations - Thyspunt Report No. 1010/2/102					
Revision	Date	Author	Checked	Status	Approved
00	March 2008	CWK/SAL	AAM/GKP	Draft for Comment	AAM
01	March 2008	CWK/SAL	AAM/GKP	For Use	AAM
02	March 2008	CWK/SAL	AAM/GKP	For Use	AAM
03	December 2008	CWK/SAL/RLH	AAM/GKP	For Use	AAM
04	March 2009	CWK/SAL/RLH	AAM/GKP	For Use	AAM
05	October 2009	RLH/CWK/SAL	AAM/GKP	For Use	AAM

Keywords: Nuclear Sites, Coastal Engineering, Thyspunt



ESKOM

NUCLEAR SITES SITE SAFETY REPORTS

COASTAL ENGINEERING INVESTIGATIONS THYSPUNT

TABLE OF CONTENTS

	PAGE NO
1. INTRODUCTION.....	1
1.1 Scope of Work	1
1.2 Limitations	2
1.3 Conventions and Terminology	2
2. PHYSIOGRAPHY AND MARINE/COASTAL GEOLOGY	3
2.1 General Site Description	3
2.2 Coastline and Seabed Characteristics	3
3. POSSIBLE CHANGES TO HYDROGRAPHIC CONDITIONS DUE TO CLIMATE CHANGE .	4
3.1 Introduction.....	4
3.2 Adopted Parameters for Long Term Climate Change.....	4
4. HYDROGRAPHIC CONDITIONS.....	5
4.1 Tides	5
4.2 Storm Surge	5
4.3 Long Waves.....	6
4.3.1 Definition	6
4.3.2 Analysis.....	6
4.3.3 General Discussion of Residuals.....	7
4.3.4 Results for Thyspunt	8
4.4 Extreme Waves.....	9
4.5 Wave Transformation across the Surf-Zone.....	9
4.6 Wave Set-up.....	9
4.7 Wave Run-up.....	10

4.7.1	Calculation of Run-up from Profile Data	10
4.7.2	Model Input Conditions	10
4.7.3	Analysis of Profile Slopes	10
4.7.4	Results	11
5.	INTAKE AND OUTFALL DESIGN CONSIDERATIONS.....	13
5.1	Classification of Intake and Outfall Structures	13
5.2	General Requirements	13
5.2.1	Quantity of Intake Water	13
5.2.2	Quality of Intake Water	13
5.3	Damage to Cooling Water Intakes and Outfall Structures.....	15
5.4	Sedimentation Risk	15
5.4.1	Tsunami Deposition	15
5.4.2	Tsunami Erosion	16
5.5	Blockage of Cooling Water Intake	18
5.5.1	General Considerations	18
5.5.2	Marine Debris.....	19
5.5.3	Biofouling	20
5.6	Sea Temperatures.....	20
6.	COMBINATIONS OF MAXIMUM AND MINIMUM WATER LEVELS	21
6.1	Introduction	21
6.2	Design Basis for Extreme Events	21
6.3	Combination of Extreme Events	22
6.3.1	Reference Water Level and Return Periods	22
6.3.2	Dependant Events.....	23
6.3.3	Independent Events	23
6.3.4	Long Term Sea Level Rise and Climate Change Parameters.....	24
6.3.5	Confidence Levels.....	25
6.4	Results	26
6.5	Discussion of Results	27
7.	COASTLINE STABILITY AND CROSS-SHORE SEDIMENT TRANSPORT	28
7.1	Introduction	28
7.2	Long-term Coastline Trends	29
7.2.1	Physical Process	29
7.2.2	Methodology	29
7.2.3	Accuracy	29
7.2.4	Coastline Trends.....	30
7.2.5	Discussion of Results	31
7.3	Seasonal Variation in Coastline	31

7.3.1	Physical Process	31
7.3.2	Methodology	32
7.3.3	Coastline Trends.....	32
7.3.4	Quantification of Seasonal Variations.....	32
7.4	Storm Event Erosion	33
7.4.1	Physical Process	33
7.4.2	Methodology	34
7.4.3	Storm Events	35
7.4.4	Storm Analysis	36
7.5	Long-term Sea-level Rise	37
7.5.1	Physical Process	37
7.5.2	Methodology	38
7.5.3	Storm Erosion Including Climate Change.....	40
7.6	Discussion of Results	41
8.	CONCLUSIONS.....	42

REFERENCES**FIGURES****APPENDIX A: Global Climate Change: Consequences for Coastal Engineering Design**

LIST OF TABLES

Table 3.1	:	Adopted parameters for climate change to year 2100	4
Table 4.1	:	Predicted tidal levels for Port Elizabeth	5
Table 4.2	:	Long wave data set information	7
Table 4.3	:	Extreme long-wave residuals at five SANHO tide gauge locations around South Africa	7
Table 4.4	:	Extreme long wave residuals at Port Nolloth	8
Table 4.5	:	Significant wave height from deep water to shallow water location used in run-up calculations for Profile 03	9
Table 4.6	:	Profile slopes for run-up calculations	11
Table 4.7	:	Calculated run-up values excluding climate change wave conditions	11
Table 4.8	:	Calculated run-up values including climate change wave conditions	12
Table 5.1	:	Tsunami deposition study: Event identification	15
Table 5.2	:	Summary of deposition thickness	16
Table 5.4	:	Summary of inundation	17
Table 5.5	:	Summary of erosion characteristics	17
Table 6.1	:	Extreme high and low water level results	26
Table 7.1	:	Maximum seasonal variations in horizontal displacements of the measured beach profiles	33
Table 7.2	:	SBEACH calibration parameters	35
Table 7.3	:	Maximum storm erosion horizontal displacements - Excluding climate change	37
Table 7.4	:	Parameters for long-term horizontal erosion due to sea level rise	39
Table 7.5	:	Maximum storm erosion horizontal displacements - Including climate change	40
Table 7.6	:	Maximum expected horizontal coastline erosion at Thyspunt beach for the expected installation life	41

LIST OF FIGURES

- Figure 2.1 : Seabed features
- Figure 4.1 : Locations of SANHO tide gauges used in the extraction of long wave extreme values
- Figure 4.2 : Complete residuals of three minute data for 5 SANHO tide gauge locations around South Africa
- Figure 4.3 : Comparison of residual values for three long wave events for 3 SANHO tide gauge sites around South Africa
- Figure 4.4 : Comparison of residual values for a meteo-tsunami event for 5 SANHO tide gauge sites around South Africa
- Figure 4.5 : Comparison of residual values for a bound long wave event for 5 SANHO tide gauge sites around South Africa
- Figure 4.6 : Extreme value analysis of negative long wave residuals at Port Elizabeth
- Figure 4.7 : Extreme value analysis of positive long wave residuals at Port Elizabeth
- Figure 4.8 : Extreme value analysis of negative long wave residuals at Port Nolloth
- Figure 4.9 : Extreme value analysis of positive long wave residuals at Port Nolloth
- Figure 4.10 : Run-up calculations: Plan view of profiles used
- Figure 4.11 : Selected coastline profiles for run-up calculations
- Figure 4.12 : Extreme high water level beach run-up - Excluding climate change
- Figure 4.13 : Extreme high water level beach run-up - Including climate change
- Figure 5.1 : Biofouling plates recovered from Thyspunt
- Figure 7.1 : Combined image of the Thyspunt site showing beach locations used for the coastline study
- Figure 7.2 : Plan view of historical coastline trends from aerial photographs - Slangbaai
- Figure 7.3 : Plan view of historical coastline trends from aerial photographs - Slangbaai
- Figure 7.4 : Plan view of historical coastline trends from aerial photographs - Slangbaai
- Figure 7.5 : Plan view of historical coastline trends from aerial photographs - Slangbaai
- Figure 7.6 : Plan view of historical coastline trends from aerial photographs - Slangbaai
- Figure 7.7 : Plan view of historical coastline trends from aerial photographs - Slangbaai
- Figure 7.8 : Plan view of historical coastline trends from aerial photographs - Thyspunt coast
- Figure 7.9 : Plan view of historical coastline trends from aerial photographs - Thyspunt coast
- Figure 7.10 : Plan view of historical coastline trends from aerial photographs - Thysbaai
- Figure 7.11 : Plan view of historical coastline trends from aerial photographs - Thysbaai
- Figure 7.12 : Plan view of historical coastline trends from aerial photographs - Cape St Francis
- Figure 7.13 : Plan view of historical coastline trends from aerial photographs - Cape St Francis
- Figure 7.14 : Plan view of historical coastline trends from aerial photographs - Cape St Francis
- Figure 7.15 : Plan view of historical coastline trends from aerial photographs - Krommebaai
- Figure 7.16 : Plan view of historical coastline trends from aerial photographs - Krommebaai
- Figure 7.17 : Satellite image of the Thyspunt site showing profile locations for Slangbaai used for the coastline study

- Figure 7.18 : Measured beach profiles showing seasonal variations: Profiles 01, 03, 05, 07 (refer to Figure 7.17 for positions of profiles)
- Figure 7.19 : Measured beach profiles showing seasonal variations: Profiles 09 to 12 (refer to Figure 7.17 for positions of profiles)
- Figure 7.20 : Measured beach profiles showing seasonal variations: Profiles 18 to 19 (refer to Figure 7.17 for positions of profiles)
- Figure 7.21 : Satellite image of the Thyspunt site showing profile locations for Thysbaai used for the coastline study
- Figure 7.22 : Measured beach profiles showing seasonal variations: Profiles 23a, 26 to 28 (refer to Figure 7.21 for positions of profiles)
- Figure 7.23 : Measured beach profiles showing seasonal variations: Profiles 30, 32, 34, 36 (refer to Figure 7.21 for positions of profiles)
- Figure 7.24 : Measured beach profiles showing seasonal variations: Profiles 38, 40 (refer to Figure 7.21 for positions of profiles)
- Figure 7.25 : Seasonal erosion/accretion variation from mean: 2008 - 2009: Distance from beacon at +1 m MSL (Slangbaai)
- Figure 7.26 : Seasonal erosion/accretion variation from mean: 2008 - 2009: Distance from beacon at +1 m MSL (Thysbaai)
- Figure 7.27 : Beach profile instability due to extreme storm events
- Figure 7.28 : Duynefontein storm erosion model verification: Extrapolation of measured beach Profile 15 from available bathymetric data - Plan view
- Figure 7.29 : Duynefontein storm erosion model verification: Measured wave and water levels April 2008 - July 2008
- Figure 7.30 : Duynefontein storm erosion model verification: Comparison of modelled profile response of SBEACH calibration parameters against measured profile data
- Figure 7.31 : Duynefontein storm erosion model verification: Comparison of measured storm events and modelled storm progressions
- Figure 7.32 : Duynefontein storm erosion model verification: SBEACH modelled beach response profiles for measured storms and modelled storms
- Figure 7.33 : Thyspunt beach storm erosion Profile 05 - excluding climate change: Comparison of SBEACH response profiles using varying D50 values
- Figure 7.34 : Schematic diagrams of original Bruun's rule and implemented modification
- Figure 7.35 : Coastal morphology: Application of Bruun's rule to Profile 05 from existing bathymetric data
- Figure 7.36 : Thyspunt beach storm erosion Profile 05 - including climate change: Comparison of SBEACH response profiles using varying D50 values

1. INTRODUCTION

Eskom have embarked on a Nuclear Sites Programme (NSP) as part of their overall Nuclear Programme. The purpose of the NSP is to identify the most suitable nuclear sites to meet the requirements of sufficiency for a “Strategic reserve of banked potential sites” through a Nuclear Siting Investigation programme implemented to internationally accepted standards, according to best practice and in line with authority requirements (e.g. the National Nuclear Regulator) as appropriate.

To this end, Eskom have embarked on a programme to prepare licenceable Site Safety Reports (SSR’s) for three sites, namely Duynefontein, Bantamsklip and Thyspunt. SSR’s are licensing documents that are submitted to the national nuclear regulatory authority in support of obtaining a site licence. The data incorporated into the SSR’s contain site-related information spanning the site life-cycle phases from Nuclear Siting Investigations through construction, commissioning, operation, decommissioning, to site reuse and thereafter.

Prestedge Retief Dresner Wijnberg (Pty) Ltd (PRDW), as part of a multi-disciplinary team preparing the SSR’s, are responsible for the Oceanography and Coastal Engineering Chapter of the Site Safety Report (SSR), which is required to be prepared in accordance with Eskom’s Technical Specification for this work.

This report on the Coastal Engineering Investigations, along with the Numerical Modelling of Coastal Processes Report (PRDW, 2009a), provide details of the studies undertaken in support of the SSR Chapter on Oceanography and Coastal Engineering for the Thyspunt site. Due to space constraints the SSR chapter summarises the study methodology and results, whilst the two supporting reports provide additional details.

1.1 Scope of Work

The scope of work is to characterise the following parameters at the Thyspunt site:

- Physiography and marine/coastal geology
- Possible changes to hydrographic conditions due to climate changes
- Hydrographic conditions
- Intake and outfall design considerations
- Combinations of maximum and minimum water levels
- Coastline stability and cross-shore sediment transport.

1.2 Limitations

As required by Eskom's Technical Specification for this work, this study analyses return periods up to $1:10^6$ years for water levels, waves and beach erosion. Since these predictions are based on measured or hindcast datasets covering periods as short as three years, the predictions for longer return periods need to be interpreted with extreme caution.

1.3 Conventions and Terminology

The following conventions and terminology are used in this report:

- H_{m0} is the significant wave height, determined from the zeroth moment of the wave energy spectrum.
- T_p is the peak wave period, defined as the wave period with maximum wave energy density in the wave energy spectrum.
- D_N is the diameter for which N% of the sediment, by weight, has a smaller diameter, e.g. D_{50} is the median grain diameter.
- Time is South African Standard Time (Time Zone -2)
- Seabed and water levels are measured relative to Chart Datum, which corresponds to Lowest Astronomical Tide (LAT) for Port Elizabeth. Chart Datum is 0.836 m below Mean Sea Level or Land Levelling Datum (South African Tide Tables, 2009).
- The map projection system is as follows:

Map projection:	Gauss Conformal
Datum:	Hartebeesthoek 94
Spheroid:	WGS84
Scale factor:	1
Central meridian:	25 °E
Reference system:	WG25
Co-ordinates:	Eastings (X, increasing eastwards) Northings (Y, increasing northwards)
Distance units:	International metre

2. PHYSIOGRAPHY AND MARINE/COASTAL GEOLOGY

2.1 General Site Description

The Thyspunt site is situated approximately 12 km west of St Francis Bay and 5 km east of Oyster Bay.

The site is located on an exposed section of coastline that faces towards the prevailing south-westerly deep sea swell waves. Owing to the significant headlands at Cape Seal (near Plettenberg Bay) and Cape St Francis (refer to PRDW (2009a) for location map), this stretch of coastline forms an isolated coastal cell with no significant sediment feeds or losses likely to occur into or out of the cell from adjacent sections of coastline. There are no major rivers discharging to this section of coastline. The sediment transport regime in the vicinity of the Thyspunt site has been extensively modelled and is discussed in PRDW (2009a). There are lengths of exposed rocky outcrops on the coastline, with a few beaches along the bays protected by rocky headlands. These beaches could however be susceptible to erosion during storm events.

2.2 Coastline and Seabed Characteristics

The area is underlain by quartzitic sandstones of the Kouga formation. This is overlain by up to about 50 m of unconsolidated to consolidated sediments consisting of sand, calccrete and calcarenite of the Nanaga Formation. Figure 2.1 indicates the main seabed features at the Thyspunt site (FUGRO Survey, 2006). Although seabed features nearshore of the site are not indicated, a wide band of rock with intermittent sediment is the main seabed feature just east of Thyspunt (see Figure 2.1). Offshore of the rock reef the seabed is composed of consolidated and partly consolidated sediments.

A thin line of sometimes swampy and mostly marshy vegetation, not wider than 40 m, lies between the coast and the vegetated sand dunes. The densely vegetated stabilized dunes strike ENE and extend northwards from the marshy area. At approximately 300 m inland to the north, lie the larger dunes reaching more than 50 m above Mean Sea Level.

Seabed slopes vary along the site with steeper slopes evident on the exposed rocky outcrops and gentler slopes on Slangbaai and Thysbaai beaches. Between -5 m CD and +10 m CD average values range from 1:25 to 1:13 with a maximum slope, from measured profiles, of 1:6.

3. POSSIBLE CHANGES TO HYDROGRAPHIC CONDITIONS DUE TO CLIMATE CHANGE

3.1 Introduction

In the past, engineers relied on the assumption that the natural environment, although highly variable, remains statistically static and that probability distributions for prime environmental factors such as wind speed, wave height, flood frequency and sea level are unchanging with time. Efforts have therefore centred on the already difficult problem of estimating the underlying natural statistical variability of these phenomena through long-term measurement programs, sophisticated numerical modelling and statistical simulation. The proven rise in carbon dioxide levels and the possibility of the Earth being subject to an enhanced "greenhouse" effect has brought some aspects of this basis of design into question. Extrapolation of probability distributions to exposure times very much longer than the data base may be invalid in a changing environment unless some specific account can be taken of those changes. Scientific opinion suggests that changes to climate may occur within the design life of many coastal and ocean engineering activities. Consequently, consideration of the possible impacts of climate change should be included in the design process (Engineers Australia, 2004).

The oceanographic and coastal engineering parameters which may be influenced by climatic changes over the next 90 to 100 years are described in Appendix A. The adopted parameters for this site safety assessment are tabulated in Section 3.2. The 90 to 100 year horizon takes account of the likely life of the nuclear facility (60 years) and cognisance of the phasing in of facilities over the next 20 plus years.

3.2 Adopted Parameters for Long Term Climate Change

The adopted parameters for long term climate change for purposes of the SSR are summarized in the following table.

TABLE 3.1: ADOPTED PARAMETERS FOR CLIMATE CHANGE TO YEAR 2100

Parameter	Change
Sea level rise to 2100	+ 0.8 m
Sea temperature	+ 3°C
Wind speed	+ 10%
Wave height	+ 17%
Storm surge	+ 21%

These values are based on the information available at present, and need to be continually reassessed as new data and research results become available.

4. HYDROGRAPHIC CONDITIONS

Only details of hydrographic conditions required for the coastal engineering calculations are provided below. Details on other hydrographic conditions including waves, storm surge, tsunamis, currents and seawater temperature are described in PRDW (2009a).

4.1 Tides

The closest port to the Thyspunt site for which long-term tidal data is available is Port Elizabeth. The predicted tidal levels at Port Elizabeth are as follows (South African Tide Tables, 2009):

TABLE 4.1: PREDICTED TIDAL LEVELS FOR PORT ELIZABETH

Parameter	Level [m CD]	Level [m MSL]
Lowest Astronomical Tide (LAT)	0.00	-0.84
Mean Low Water Springs (MLWS)	0.21	-0.63
Mean Low Water Neaps (MLWN)	0.79	-0.05
Mean Level (ML)	1.04	0.20
Mean High Water Neaps (MHWN)	1.29	0.45
Mean High Water Springs (MHWS)	1.86	1.02
Highest Astronomical Tide (HAT)	2.12	1.28

These levels are calculated relative to Chart Datum, which is 0.836 m below Mean Sea Level or Land Levelling Datum (South African Tide Tables, 2009). The values for MSL are accurate to the precision as supplied in the South African Tide Tables.

HAT is the highest level which can be predicted to occur under average meteorological conditions and under any combination of astronomical conditions (South African Tide Tables, 2009). HAT is not the extreme upper level which can be reached, as storm surges and other meteorological or geological (e.g. tsunami) conditions may cause considerably higher levels to occur.

LAT is the lowest level which can be predicted to occur under average meteorological conditions and under any combination of astronomical conditions (South African Tide Tables, 2009). LAT is not the extreme lower level which can be reached, as negative storm surges and other meteorological or geological (e.g. tsunami) conditions may cause considerably lower levels to occur.

HAT and LAT will only be reached once every 18.6 years, although levels within approximately 0.14 m of HAT and 0.14 m of LAT will be reached annually.

4.2 Storm Surge

Storm surge is for the purpose of this report defined as the influence of meteorological effects such as winds and barometric pressure that results in actual sea level being above or below the predicted astronomical tide level.

For the calculations of extreme high and low water events, extreme values for positive and negative storm surge residuals (the difference between the actual water level and the predicted tide) have been calculated from hourly tide gauge data. Refer to PRDW (2009a) for full details.

4.3 Long Waves

This section describes exclusively the maximum expected elevation due to long waves (refer to definition below). The analysis and run-up resulting from the Probable Maximum Tsunami is evaluated independently (PRDW, 2009a).

4.3.1 Definition

Long waves are, for the purpose of this report, defined as fluctuations in still water level with periods between 3 to 60 minutes. Long waves typically include: edge waves, shelf waves, bound waves and tsunami (both tectonically and meteorologically generated).

Meteo-tsunami are meteorologically initiated long waves which can subsequently propagate as edge or shelf waves. Meteo-tsunami can also produce patterns in tide gauge records closely analogous to tectonic tsunamis, with multiple waves impinging on the coast for a number of hours (PRDW, 2009a).

Bounded long waves are generated by gradients in radiation stress found in wave groups, causing a lowering of the mean water level under high waves and a raising under low waves (CEM, 2003). The bounded wave travels at the group speed of the wind waves, hence is bound to the wave group. The occurrences of bounded long waves are therefore expected to occur during a storm.

4.3.2 Analysis

High frequency (1 - 3 minute) measured data from tide gauges at Port Nolloth, Simon's Town, Cape Town, Mossel Bay and Port Elizabeth have been processed to determine the occurrence and severity of long waves (refer to Figure 4.1 for tide gauge locations). The data has been kindly provided by the Hydrographer of the South African Navy (who is not responsible for any transcription errors or errors due to calculations using the data). The data has been "cleaned" (by removing "spikes" and other errors), and the residuals (difference between the measured data and a 60 minute running mean) have been extracted. Details of the available data sets for each of the tide gauges are presented in Table 4.2 and illustrated in Figure 4.2.

TABLE 4.2: LONG WAVE DATA SET INFORMATION

Location	Start Date	End Date	Duration [years]
Port Nolloth	2006-01-01	2009-08-31	3.32
Cape Town	2008-03-31	2009-08-31	1.35
Simon's Town	2006-01-01	2009-08-31	3.45
Mossel Bay	2007-05-16	2009-08-31	1.96
Port Elizabeth	2005-06-09	2009-08-31	4.20

An extreme value analysis was completed on the residuals of the data using the MIKE EVA software package from DHI (refer to PRDW (2009a) for details regarding the EVA software). Extreme values for return periods of 1:1, 1:10, 1:100 and 1:10⁶ years have been calculated and are tabulated below for all five tide gauge locations. As the measured datasets are only between 1.35 and 4.2 years in duration, results from extrapolation to return periods longer than 5 to 10 years should be interpreted with caution.

TABLE 4.3: EXTREME LONG-WAVE RESIDUALS AT FIVE SANHO TIDE GAUGE LOCATIONS AROUND SOUTH AFRICA

Return period [years]	Location	Positive Residuals [m]		Negative Residuals [m]	
		Best estimate	Upper 95% confidence	Best estimate	Upper 95% confidence
1	Port Nolloth	0.37	0.51	0.29	0.41
	Cape Town	0.37	0.45	0.40	0.51
	Simon's Town	0.18	0.21	0.18	0.21
	Mossel Bay	0.45	0.55	0.46	0.58
	Port Elizabeth	0.33	0.39	0.30	0.33
10	Port Nolloth	0.74	0.99	0.62	0.88
	Cape Town	0.52	0.64	0.59	0.74
	Simon's Town	0.26	0.31	0.26	0.30
	Mossel Bay	0.65	0.78	0.71	0.89
	Port Elizabeth	0.50	0.59	0.37	0.40
100	Port Nolloth	1.14	1.49	1.03	1.39
	Cape Town	0.67	0.82	0.77	0.94
	Simon's Town	0.33	0.39	0.32	0.38
	Mossel Bay	0.81	0.97	0.94	1.16
	Port Elizabeth	0.65	0.77	0.41	0.44
10 ⁶	Port Nolloth	2.91	3.64	3.16	3.77
	Cape Town	1.27	1.47	1.42	1.67
	Simon's Town	0.57	0.70	0.54	0.66
	Mossel Bay	1.34	1.62	1.83	2.21
	Port Elizabeth	1.15	1.44	0.51	0.59

4.3.3 General Discussion of Residuals

Figure 4.3 illustrates the typical residual values and periods associated with long-wave events. The figure shows recorded events at Port Nolloth, Mossel Bay and Port Elizabeth, with the events attributed to: a meteo-tsunami, bound long-waves and tectonic tsunami respectively. The tectonic tsunami is seen (NGDC, 2009) to have originated in Sumatra, Indonesia, from an 8.4 magnitude earthquake which occurred at approximately midday (GMT) on the 12th of August, 2007. As the tide gauges are located inside harbours, the measured data is likely to include localised effects such as resonance of the adjacent bay or harbour basin.

Figure 4.4 illustrates the progression of a meteo-tsunami from Port Nolloth to Port Elizabeth and demonstrates the typical travel times associated with these events and the relative magnitude of the residuals at each of the five SANHO tide gauge stations.

Figure 4.5 illustrates the progression of bound long-waves associated with a measured storm event and associated magnitude of the residuals at each of the five SANHO tide gauge stations.

Although Figure 4.4 indicates the initial location of the identified meteo-tsunami event as near Port Nolloth, there is currently insufficient information to suggest that the initiation mechanisms are specific to the coastal area around Port Nolloth. It is reasonable, and conservative, to assume that these initiating events could as readily occur at any location around the coast of South Africa. For this reason, the maximum predicted long-wave event tabulated in Section 4.3.4 and utilised in the calculation of combinations of maximum surface elevations expected at the proposed nuclear installation corridor, is the Port Nolloth $1:10^6$ year event.

4.3.4 Results for Thyspunt

For the evaluation of the impact of long waves at Thyspunt, three minute sampled data (2006-01-01 to 2009-08-31) from the Port Nolloth tide gauge have been used. This approach is considered to be conservative

As only 3.45 years of continuous data are currently available, results from extrapolation to return periods longer than 10 years should be interpreted with caution. The upper 95% confidence level to the best estimate is calculated using the Monte Carlo method. The results of the extreme value analysis for Port Elizabeth, not tabulated, are presented in Figures 4.6 and 4.7. The results for Port Nolloth are presented in Figures 4.8 and 4.9 and Table 4.4.

TABLE 4.4: EXTREME LONG WAVE RESIDUALS AT PORT NOLLOTH

Return Period [years]	Positive Residuals [m]		Negative Residuals [m]	
	Best estimate	Upper 95% confidence	Best estimate	Upper 95% confidence
1	0.37	0.51	0.29	0.41
10	0.74	0.99	0.62	0.88
100	1.14	1.49	1.03	1.39
10⁶	2.91	3.64	3.16	3.77

The large uncertainty in the EVA analysis for the longer return periods, particularly evident in the lower 5% confidence level plots in Figures 4.6 to 4.9, is indicative of the short period of data available compared to the extended return periods considered.

4.4 Extreme Waves

In this section sea and swell waves generated by wind and having periods between 4 and 25 s are described. The wave climate at the site was determined by refracting a 15 year offshore hindcast dataset to the -30 m CD depth contour opposite the site and then performing an extreme value analysis on the dataset. The modelling procedure and the results are described in PRDW (2009a). Wave data have also been recorded at two locations at the site since February 2008. Full details are provided in PRDW (2009a).

4.5 Wave Transformation across the Surf-Zone

The cross-shore hydrodynamic engine of the LITPACK model (as described in PRDW, 2009a) was used to transfer each of the extreme wave conditions at the -30 m CD position inshore to the -5 m CD position, where the resulting wave conditions are required as input to the wave run-up computations.

The inputs for the LITPACK model are the beach profile and the wave conditions at -30 m CD. The water level is set to HAT plus any addition for storm surge and climate change where applicable. (Refer to Chapter 3 and Table 6.1). The calculations are performed using variable grid spacing with values between 1 m and 2 m. Note that the wave heights extracted at -5 m CD for calculations of run-up are broken wave heights and represent a depth-limited condition (refer to Table 4.5).

TABLE 4.5: SIGNIFICANT WAVE HEIGHT FROM DEEP WATER TO SHALLOW WATER LOCATION USED IN RUN-UP CALCULATIONS FOR PROFILE 03

Return period [years]	H_{m0} [m] at -30 m CD and -5 m CD							
	Excluding climate change				Including climate change			
	Best estimate		Upper 95% confidence		Best estimate		Upper 95% confidence	
	-30 m CD	-5 m CD	-30 m CD	-5 m CD	-30 m CD	-5 m CD	-30 m CD	-5 m CD
1	6.7	5.9	6.9	6.0	7.8	6.6	8.1	6.7
10	8.2	6.4	8.7	6.6	9.6	7.2	10.2	7.4
100	9.6	6.8	10.5	7.1	11.2	7.6	12.3	7.9
10⁶	14.4	8.1	17.5	8.9	16.9	9.2	20.5	10.1

4.6 Wave Set-up

The cross-shore wave model used (refer to Section 4.5), includes the effect of wave set-up. Although this result for wave set-up is not used explicitly, including this parameter takes into account the effect of a higher water level on the wave transformation in the surf zone in itself.

In the present study, wave run-up is calculated using empirical equations from laboratory investigations with irregular wave input (refer to Section 4.7). Total vertical run-up is correlated to a non-dimensional height based on physical measurements inclusive of the effect of set-up. Therefore, no separate analysis of wave set-up is required as it is implicit in the equations for wave run-up.

4.7 Wave Run-up

Wave run-up is calculated on the average beach slopes of five beach and coast profiles for the Thyspunt site and the transformed wave conditions (refer to Section 4.5). The plan view of the selected profiles is shown in Figure 4.10. The final value of vertical wave run-up is seen to be highly dependent on the chosen slope of the profile. In order to maintain consistency of approach for all of the profiles, the slope was taken as the average value between points at -5 m CD to +10 m CD.

4.7.1 Calculation of Run-up from Profile Data

Hughes (2004) re-examined existing wave run-up data for regular, irregular and solitary waves on smooth, impermeable plane slopes. A model is used to derive a new wave run-up equation in terms of a dimensionless wave parameter representing the maximum, depth-integrated momentum flux in a wave as it reaches the toe of the slope.

The approach by Hughes (2004) assumes a smooth impermeable slope. For an impermeable slope, the wave run-up will typically be more than for an equivalent permeable slope. This approach is considered conservative as these calculations for wave run-up will give values greater than for rough, permeable slopes.

For calculation of wave run-up for plunging/spilling waves refer to Equation 40 in Hughes (2004). In Hughes (2004), $R_{u,2\%}$ is the vertical elevation from sea water level exceeded by 2% of the run-ups.

4.7.2 Model Input Conditions

The above-mentioned method (Hughes, 2004), with modelled wave conditions at -5 m CD as input, is used for calculating design wave run-up $R_{u,2\%}$.

Run-up for each of the combined events (refer to Section 6.3) has been analysed for given wave and water-level input conditions for each profile. The values for H (local significant wave height) and h (water depth at -5 m CD) have been extracted from the LITPACK results files and used to assess maximum wave run-up (refer to Section 4.5).

4.7.3 Analysis of Profile Slopes

Initial assessment of the results shows a high dependence on the average beach slope of the profile under consideration. Smoothing of profile features such as bars and naturally formed berms reduces the slope and tends to reduce the wave run-up, whereas using the maximum feature slope tends to greatly increase the levels of calculated run-up.

Since the intake structure details and terrace level structures are not yet defined, no coastline structures have been superimposed onto the profiles and considered in the calculations. The results will be subject to review once the design of the intake and terrace has advanced and any coastline structures can be incorporated into the assessment.

A number of cross-sections have been taken along the Thyspunt site coastline. Beach slopes for each of the cross-sections have been assessed (refer to Figure 4.11 for profile details). Table 4.6 summarises slope information for all of the profiles. The mean values of the profile slopes between -5 m CD and +10 m CD are used in the run-up calculations.

TABLE 4.6: PROFILE SLOPES FOR RUN-UP CALCULATIONS

	-30 m CD to -20 m CD		-20 m CD to -5 m CD		-5 m CD to +10 m CD	
	Mean	Max	Mean	Max	Mean	Max
Profile 01	1:50	1:6	1:10	1:7	1:25	1:6
Profile 02	1:50	1:8	1:17	1:10	1:25	1:7
Profile 03	1:10	1:6	1:40	1:8	1:13	1:7
Profile 04	1:60	1:15	1:60	1:14	1:25	1:7
Profile 05	1:25	1:17	1:70	1:14	1:26	1:7

The occurrence clearly visible horizontal rock shelves (Profiles 01 and 02), in the surf zone tend to greatly reduce the average slope used for the calculation of run-up.

4.7.4 Results

Results are indicated in Figure 4.12 (excluding the effects of climate change) and Figure 4.13 (including the effects climate change), and tabulated below (refer to Chapter 3 for details regarding increase water levels due to climate change).

TABLE 4.7: CALCULATED RUN-UP VALUES EXCLUDING CLIMATE CHANGE WAVE CONDITIONS

	Run-up [m above Still Water Level]							
	Best estimate				Upper 95% confidence			
	Return Period [years]				Return Period [years]			
	1	10	100	10⁶	1	10	100	10⁶
Profile 01	4.70	4.98	5.21	5.96	4.75	5.07	5.37	6.40
Profile 02	4.49	4.86	5.10	5.86	4.59	4.96	5.25	6.32
Profile 03	6.04	6.59	7.04	8.48	6.15	6.78	7.34	9.36
Profile 04	2.60	2.79	2.95	3.48	2.63	2.86	3.06	3.80
Profile 05	3.60	3.87	4.08	4.73	3.65	3.96	4.22	5.10

The run-up varies for each of the profiles due to wave refraction effects and most importantly the beach slope between -5 m CD to +10 m CD, (refer to Section 4.7.3). The noticeable offshore reef visible in Profile 04 and Profile 05 cause wave breaking prior to the -5 m CD slope initiation point, reduced significant wave heights and consequently reduced run-up values.

TABLE 4.8: CALCULATED RUN-UP VALUES INCLUDING CLIMATE CHANGE WAVE CONDITIONS

	Run-up [m above Still Water Level]							
	Best estimate				Upper 95% confidence			
	Return Period [years]				Return Period [years]			
	1	10	100	10 ⁶	1	10	100	10 ⁶
Profile 01	5.28	5.60	5.87	6.73	5.34	5.71	6.04	7.25
Profile 02	5.09	5.48	5.74	6.64	5.21	5.59	5.92	7.24
Profile 03	6.79	7.41	7.92	9.64	6.90	7.62	8.27	10.71
Profile 04	2.97	3.19	3.38	4.01	3.01	3.27	3.51	4.39
Profile 05	4.01	4.31	4.54	5.29	4.07	4.41	4.70	5.72

Since the exact position of the nuclear terrace is unknown at present, the single maximum run-up from all of the profiles has been used to calculate the maximum water levels in Table 6.1. The maximum run-up occurs for Profile 03, due to increased profile slope and an almost normal angle to the incident wave direction. Significantly lower run-up values occur on the beach profiles (Profile 04 and Profile 05).

5. INTAKE AND OUTFALL DESIGN CONSIDERATIONS

5.1 Classification of Intake and Outfall Structures

Since no engineering feasibility studies on the intake and outfall structures have been completed by Eskom to date (October 2009), two conceptual layouts were developed which serve to illustrate the thermal plumes and recirculation that can be anticipated for typical combinations of intake and outfall types. The intakes considered are offshore tunnels, while the outfalls considered are a nearshore channel and nearshore channel. Note that these conceptual layouts will need to be refined based on geotechnical and engineering considerations.

- Layout 1 – offshore tunnel intake (-30 m CD), nearshore pipeline outfall (-5 m CD)
- Layout 2 – offshore tunnel intake (-30 m CD), nearshore channel outfall (-5 m CD)

Further details of these layouts, along with the thermal plume, recirculation and sediment transport modelling results for these layouts are provided in PRDW (2009a).

5.2 General Requirements

5.2.1 Quantity of Intake Water

For a new installed power output of 10 000 MWe, the anticipated seawater cooling flow rate is 456 m³/s (refer to PRDW (2009a) for details).

In the case of intake and outfall tunnels, the diameter of the tunnels is designed to avoid the risk of sediments settling in the tunnel (minimum velocity of 2.5 to 3 m/s). On the other hand, the velocity in the tunnels needs to be limited in order to reduce head losses in the tunnels. For the purposes of maintenance redundancy, it is assumed each reactor unit will be provided with an intake and/or outfall tunnel to allow the reactor and tunnel to go into maintenance outage independently of the other units.

5.2.2 Quality of Intake Water

5.2.2.1 Clean Water

Most nuclear power plants obtain condenser cooling water from the open sea, in which case pre-screening of the intake water using travelling screens, mechanically cleaned bar screens, or passive well screens is necessary. In many instances, the screening chamber is located on or near shore and the intake pipe may extend out hundreds of meters into the sea.

It is recommended (Bosman and Wijnberg, 1987) to:

- Remove sediment particles larger than 0.15 mm (by dredged stilling basin or settling pond)
- Remove marine organisms larger than 5 mm
- Prevent marine fouling in pressure ducts.

The intake design will have to respond to the maximum allowable sediment concentrations for the pumps. The pumps of the existing Koeberg nuclear power station can cope with sediment concentrations up to 50 ppm (Eskom, 2006). No information on the maximum allowable sediment concentrations for the planned installation is available.

A dredged stilling basin or an onshore settling pond will be required to enable capture of sediment particles by settlement. Offshore intake systems will take in water of better quality and will require less pre-treatment than a nearshore intake system. The conventional method of intake is the open intake of seawater by active or passive screens of different kinds. These are subject to marine biological activity and suspended matter, which needs to be removed or reduced by pre-treatment. Impingement of marine life in offshore intakes can be reduced by proper design of the velocity cap. The velocity cap, the cover placed over the vertical terminal of an offshore intake pipe, converts vertical flow into horizontal flow at the intake entrance to reduce fish entrainment. This velocity ranges from 0.15 to 0.45m/s (ASCE, 1982). The velocity cap is sized to ensure a maximum horizontal velocity of 0.3 m/s or less is achieved.

Chlorine, produced by electrolysis, is typically used to keep the cooling system free of marine growth. Maintenance of the pipelines can add a significant factor to the overall costs. The offshore tunnel intake option should include adequate redundancy to allow for periodic maintenance/cleaning of the tunnel and intake system.

5.2.2.2 *Recirculation Risk*

Two different configurations of intake and outfall structures have been considered for the Thyspunt site and are dealt with in more detail in the Numerical Modelling Report (PRDW, 2009a). For each of these configurations, the thermal plume dispersion has been modelled for a typical winter, summer and calm weather conditions in order to evaluate the recirculation risk of heated cooling water to the cooling water intake point of the new nuclear installation.

5.3 Damage to Cooling Water Intakes and Outfall Structures

In the case of offshore intake or outfall structures, the structures need to be positioned in a depth where extreme wave conditions will have no damaging impact on the structure or any of its components which might jeopardize the intake or discharge of cooling water. In the case of a nearshore basin or channel type structures (rock structures), the structure will be designed to a “no-damage” criteria (less than 5% damage). The damage is defined as a percentage of the eroded volume (CEM, 2006).

5.4 Sedimentation Risk

Tunnelled intake structures have been positioned offshore in water depths of -25 m CD to -30 m CD. Suspended sediment concentrations at these depths and sedimentation risks have been assessed (PRDW, 2009a). Refer to Chapter 7 for details regarding sedimentation and coastline stability for Thysbaai.

Bottom shear by a strong tsunami current may be significant in shallow water. The deposition of a large amount of sediment could affect the safety features of the plant. In particular, the deposition of sediment around cooling water structures or the water inlet and outlet might disrupt the operation of the plant.

5.4.1 Tsunami Deposition

As part of the investigation into sedimentation risk from tsunami waves a literature study has been completed. Historic cases of deposition from tsunami events from the 1998 Papua New Guinea Tsunami, 2001 Peru Tsunami and the most recent 2004 Indonesian Tsunami have been researched and a summary of the relevant results presented. The events associated with these tsunamis are described in Table 5.1.

TABLE 5.1: TSUNAMI DEPOSITION STUDY: EVENT IDENTIFICATION

Tsunami event	Ocean	Earthquake Magnitude	Maximum water level relative to Mean Sea Level (m)
1998 - Papua New Guinea	Pacific	7.0 + landslide	15
2001- Peru	Pacific	8.4	7
2004 - Indonesia	Indian	9.2	10

5.4.1.1 Papua New Guinea, 1998, Peru, 2001

Details of the maximum and minimum deposition vary between resources examined for the study. The maximum values measured have recorded values of up to 1 m, with average historic values of approximately 0.25 m (Morten *et al*, 2007).

5.4.1.2 *Indonesia, 2004*

After the 2004 Indonesian Tsunami, field data of tsunami inundation and sediment deposits along the west Sumatra coast were collected (USGS, 2005).

At Kuala Mersi, approximately 100 km south of Banda Aceh, a 15 m high tsunami wave inundated a distance of nearly 2 km across a coastal plain that was only 3 - 4 m above sea level. The tsunami eroded the beach face and left a deposit that varied in thickness from less than 0.01 m to 0.34 m across the coastal plain.

At Lhoknga and Leupueung, the maximum thickness of the tsunami deposits of sediment observed along surveyed lines was about 0.7 m. Most of them were composed of beach-sand including shells and corals. At the village of Lampuuk, 0.73 m of sediment was deposited over soil.

In Sri Lanka, run-up elevation measured varied from less than 3 m to more than 12 m (increasing on the East Coast of Sri Lanka towards the south). Measured water levels near the coastline varied from less than 3 m to more than 10 m (increasing on the East Coast of Sri Lanka towards the south, and on the south coast toward the East). Erosion was often concentrated in a relatively narrow zone near the coast.

At Mankerni (Sri Lanka), a grassy area was eroded about 1 m in the vertical in a zone about 20 to 30 m wide near the coast. Tsunami sediment deposits started about 50 m inland, and decreased in thickness from about 0.10 m total thickness to about 0.02 m thickness at about 150 m inland.

5.4.1.3 *Discussion of Results*

According to the sediment surveys undertaken for different modern tsunamis events, a maximum value of 1 m for tsunami sediment deposition is verified. The table below summarises deposition patterns from the study.

TABLE 5.2: SUMMARY OF DEPOSITION THICKNESS

Tsunami Event	Location	Deposition thickness [m]
Papa New Guinea, 1998		0.25
Peru, 2001		1.00
Indonesia, 2004	Kuala Mersi, Sumatra	0.01 to 0.34
	Lhoknga and Leupueung, Sumatra	0.70
	Lampuuk, Sumatra	0.73
	Mankerni, Sri Lanka	0.02 to 0.10

5.4.2 Tsunami Erosion

5.4.2.1 *Inundation Scour*

Scour comparisons were undertaken for Banda Aceh and Lhoknga, Sumatra. These two adjacent coastal communities are located very near the tsunami source which bore the brunt of severe

inundation flow and suffered large areas of complete destruction from the 2004 Indonesian Tsunami (FEMA, 2006).

The Lhoknga coast experienced the highest run-up elevations recorded in the event (>20 m).

All observed scour depths appear to be less than 3 m, at both Banda Aceh and Lhoknga. The scour patterns were in areas of relief, near structures, and with vast areas of eroded coastlines.

A scour evaluation was performed for 20 sites selected to represent a range of locations, inundation conditions and scour depth measured after the 2004 Indonesian Tsunami in India, Andaman/Nicobar, Thailand and Sumatra (FEMA, 2006).

The selected site parameters provided a broad range of run-up heights (up to 20 m) and inundation distances (up to several kilometers). However, all evaluated scour features were located within 200 m of the coastline, except at the Lhoknga mosque in Sumatra which was approximately 600 m from the coastline. Soil conditions included various gradations of silty sands, sand and gravels typical of coastal environments. Table 5.3 provides a summary of the water levels and inundation distances observed (FEMA, 2006):

TABLE 5.3: SUMMARY OF INUNDATION

Location	Run-up height	Overland flow depth	Inundation distance
India	2 to 5 m	0.2 to 2 m	Up to 800 m
Andaman/Nicobar	3 to 15 m	Not available	Not available
Thailand	5 to 10 m	2 to 5 m	Up to 5000 m
Sumatra	5 to 20 m	2 to 15 m	Up to 10,000 m

Topography generally consisted of low (1 to 2 m) fore-dunes, some areas of slightly raised profiles on higher more stabilized dunes, associated with relatively flat beach plains. Vegetation adjoining beaches varied from mostly agricultural fields and coconut plantations, with some areas of more dense tropical forests or shrubbery. Some areas of steep or rocky coastlines also produced damaging scour, though not as predominant as in the broad low lying inundation (refer to Table 5.4).

TABLE 5.4: SUMMARY OF EROSION CHARACTERISTICS

Run-up Height (m)	Dist. to Coastline (m)	Scoured Soil Type	Surface Cover	Observed Scour (m)	Scour Feature
4 to 5	30 to 100	Med to Fine Sand	Beach / very large beach	0.5 to 1.5	Road / Railway scour
5 to 12	5 to 180	Coarse/Med to Med/Fine Sand	Beachfront	0.5 to 2	Footing / Bridge scour
15	50 to 75	Coarse/Med to Med/Fine Sand	Beachfront with spit	1.5 to 2.5	Abutment washout/sinkhole
4	5	Med to fine sand w/gravel	Beachfront w/seawall	1	Seawall road scour
11	5	Silty gravel base & boulders	Jungle slope, rocky coast	4	Road scour

5.4.2.2 *Sub-aerial Scour*

Though not measured or assessed in the case studies referenced, sub-aerial scour due to tsunami are likely to be destructive to coastal structures (Yim, 2006). Offshore tsunami scour differs from ordinary coastal structure scour, which occurs gradually caused by periodic waves and steady current loads. In a tsunami or storm surge, the leading wave may scour away much of the supporting materials around the base of the structure such that catastrophic failure occurs with following waves due to hydrodynamic drag forces. Deposition usually occurs within sub-aerial scour holes shortly after initially scouring, thus making measurements and investigations of sub-aerial scour difficult.

Sub-aerial scour is particularly site specific (Yeh *et. al.*, 2003). Yeh *et. al.* (2003) make reference to the 1960 Chilean Tsunami where a 10 m deep scour hole occurred in the mouth of the Kesen-numa port in Japan, but little other scour damage for the site was observed.

Currently, no simple formula exists for scour prediction. Much experimental work needs to be conducted to provide data for empirical prediction and analysis (Yim, 2006).

5.4.2.3 *Discussion of Results*

Inundation scour depth observations appear to be largely limited to less than 2.5 m for run-up values of maximum 15 m. These are seen to occur within 200 m of the coastline and at less than half the maximum inundation distance.

Sub-aerial scour is currently poorly understood and information is scarce due to the inherent difficulties in measuring offshore scour information.

5.5 **Blockage of Cooling Water Intake**

Measures to prevent the complete blockage of the cooling water intake will depend on the type of intake structure. A brief overview of the measures to be considered in the intake design development to mitigate blockage risks is provided below.

5.5.1 General Considerations

In case of an offshore intake structure, cooling water is taken from much larger depths (25 m to 30 m water depth). This reduces the risk of blockage of the intake structure significantly. Suspended sediment concentrations at these levels are much lower, reducing the amount of sediment drawn in by the pumps and thus reducing the dimensions of the required settlement basins. The cover placed over the vertical terminal of an offshore intake tunnel/pipe is called a “velocity cap”. The cover converts vertical flow into horizontal flow at the intake entrance to reduce fish entrainment. It has been noted that fish will avoid rapid changes in horizontal flow and velocity cap intakes have been shown to provide 80-90% reduction in fish impingement.

Chlorine produced through electrolysis, is typically used to keep the cooling system free of marine growth.

5.5.2 Marine Debris

Consideration of potential blockages due to marine debris needs to be included in the design of the intake.

A study by the World Association of Nuclear Operators (WANO) in 2006 found that in the period 2004 to 2006, there were 44 occurrences of blockages at nuclear installations (EPRI, 2008). Of the 44 events, 37 of these were attributed to aquatic life, including algae, seaweed and other grasses, mussels, jellyfish, crustaceans (shrimps and crabs) and fish. The remaining blockage events were caused by depositions of sand and silt and ingress of crude oil.

An environmental impact assessment for the proposed Thyspunt site indicated that the following ecological species are to be found at Thyspunt (Eskom, 2008):

- Inter-tidal Zone - Algae, Gastropod, Barnacle, Mussel, Giant Periwinkle, Plough Shell
- Benthic environment - Colonial Ascidiars, Hydroids, Sponges, Coralline Algae
- Open Water - Chokka Squid, Dusky Kob, Silver Kob, Cape Salmon, Shad, White Steenbras, Bronze Bream, Bottlenose Dolphin, Common Dolphin, Humpback Whale, Southern Right Whale.

WANO has identified four main categories for tackling the problem of blockages (EPRI, 2008), namely:

- Implementing proactive methods, including prediction tools and low level event trending, to understand potential threats and to take pre-emptive actions to mitigate their effects;
- Confirming plant system and equipment design are sufficient to address potential events;
- Verifying that maintenance strategies maintain and enhance equipment performance and
- Establishing operational criteria, procedure guidance and personnel training to address potential events and to incorporate industry operating experience.

The Electric Power Research Institute (EPRI, 2008) is in the process of carrying out a project which is aiming at identifying best management practices for preventing cooling water intake blockages. The draft report, though due to be complete by June 2009, is at present still unavailable. The recommendations put forward by WANO and the outcome of the EPRI project will form an important and valuable input to the intake design and prevention of cooling water intake blockages through the plant life.

There is no extra-ordinary marine debris identified at the site which the intakes could not be designed to cope with and which would be expected to cause a complete blockage of the intake.

5.5.3 Biofouling

Biofouling has been measured at the Thyspunt site by mooring 20 cm x 20 cm asbestos plates 3 m and 8 m below the water surface in 10 m water depth. These plates are periodically removed, photographed and the thickness of marine growth measured. The biofouling organisms are then scraped off the plates and stored in sample bottles with formaldehyde for further analysis if required. Further details are provided in PRDW (2009a).

Results are currently available for plates deployed on 1 July 2008 and recovered on 23 October 2008, i.e. approximately 4 months in the sea. Photographs of the plates are shown in Figure 5.1. The average biofouling thickness measured on the plate deployed 3 m below the surface was 7.5 mm, while the plate deployed 8 m below the surface had an average thickness of 2.8 mm. These measurements are ongoing.

Further to the continued vandalism and loss of the biofouling plates, the plates were mounted directly onto a seabed positioned frame. The plates and frame was deployed on 14 June 2009 and will be retrieved in November 2009.

5.6 Sea Temperatures

The following data have been provided for the seawater intakes temperatures of a typical Pressurised Water Reactor (PWR) (Eskom, 2007):

- maximum cooling water temperature: 30°C
- minimum cooling water temperature: -0.4°C
- extreme conditions for safety assessment: 34.5°C

The two factors influencing the intake temperature are the ambient temperature at the intake depth and possible recirculation from the outfall back to the intake, refer to PRDW (2009a) for details.

6. COMBINATIONS OF MAXIMUM AND MINIMUM WATER LEVELS

6.1 Introduction

The IAEA (2003) safety guide on 'Flood Hazard for Nuclear Power Plants on Coastal and River Sites' gives some general guidelines concerning combined events to be considered in deriving the design basis flood for a nuclear installation. These guidelines have been used in deriving the design basis for extreme high water levels.

6.2 Design Basis for Extreme Events

In deriving the design basis flood for a nuclear installation, combined events should be considered as well as single events. Combinations of events should be carefully analysed with account taken of the stochastic and nonlinear nature of the phenomena (IAEA, 2003).

For evaluating combined flooding events on coastal, estuary and river sites, distinctions may be made between (IAEA, 2003):

1. Extreme events (such as storm surges, river floods and tsunamis)
2. Wind waves related or unrelated to the extreme events
3. Maximum seiche (in the case of an enclosed or semi-enclosed body of water)
4. Reference water levels (including tides if significant).

Appropriate combinations of extreme events with wind waves and reference water levels should be taken into consideration. The probability range of each combination should be estimated (IAEA, 2003).

The design basis flood for a given site may result not from the occurrence of one extreme event but from the simultaneous occurrences of more than one severe event each of which is in itself less than the extreme event. The interdependence or independence of the potential flood causing phenomena should be examined according to the site specific features (IAEA, 2003).

For independent events, the probability that they will occur in such conditions that their effects will be additive is related to the duration of the severity level of each event. The events to be combined should be selected appropriately with account taken not only of the resultant probability but also of the relative effect of each secondary event on the resultant severity of the flood. For example for estuary sites, combinations that should be examined should include both maritime and river conditions. If the consequences of these combinations are significant and the combined probability of the results is not very low, they should be taken into account (IAEA, 2003).

Wind wave activity should be considered in association with all the flood events. For surge, wind waves are dependent events and the waves that are generated by the storm producing the surge should be considered (IAEA, 2003).

In this report both Tsunami and long waves are considered independent events. Long waves are categorised as independent events because the generation mechanisms (atmospheric pressure fluctuations, propagation of edge waves and shelf waves) are independent on the atmospheric and ocean conditions leading to storm induced surges and associated maximum wind wave. Only wind waves with a shorter recurrence interval should thus be considered in the combination. Independent events are combined with the 1:10 year return period of dependant events.

The potential for instability of the coastline should be evaluated and if the occurrence of these events affects the flood at the site they should be combined with other primary flood causing events (IAEA, 2003).

Considerable engineering judgement is necessary in selecting the appropriate combinations (IAEA, 2003).

6.3 Combination of Extreme Events

From all of the above-mentioned potential flooding hazards the most severe and relevant hazards for the nuclear installation at the Thyspunt site are combined to obtain the maximum water levels at the site required for flooding risk assessment and the minimum levels for loss of cooling water assessment.

The following hydrographic conditions contribute to the combined water level:

- Sea level rise: Refer to Section 3.2
- Tidal levels: Refer to Section 4.1
- Storm surge: Refer to Section 4.2
- Wave set-up and run-up: Refer to Sections 4.6 and 4.7
- Long wave: Refer to Section 4.3
- Tsunami: Refer to Section 6.3.3

6.3.1 Reference Water Level and Return Periods

Following international recommendations (IAEA, 2003) a conservatively high reference water level should be considered for each combination of dependant events. In this case the Highest Astronomical Tide (HAT) is added to obtain the extreme high water level (see Table 4.1). Similarly Lowest Astronomical Tide (LAT) has been used as a conservative low water level for combinations leading to loss of cooling water.

Independent events should be considered in combination with waves having a shorter recurrence interval (IAEA, 2003). USNRC (2007) recommends that the 90th percentile of high tides be used as the initial water surface elevation when evaluating tsunami run-up, which for Thyspunt is +0.98 m MSL. Based on these recommendations, for extreme high water levels, independent events are combined with a tide of +0.98 m MSL and a 1:10 year combination of dependant events (see Table 6.1). For extreme low water, independent event water levels are combined with the 90th percentile of low tides (-0.58 MSL) and the 1:10 combination of dependent events.

6.3.2 Dependant Events

Storm surge is for the purpose of this report defined as the effective term for the meteorological effects such as winds and barometric pressure that results in actual sea level being above (positive) or below (negative) the predicted astronomical tide level.

Storm surge, wave set-up and wave run-up are considered to be dependent events since they are all associated with the passage of frontal weather systems (refer to Chapter 4). For this reason, storm surge is combined with wave set-up and wave run-up having the same return period when calculating maximum water levels on exposed beaches. In the case of the extreme low water condition on an exposed beach, the individual effects of wave draw-down are not included, as the set-up (a positive elevation) would negate the effects of the draw down.

All dependant events have been calculated for 1, 10, 100 and 10⁶ year return periods. As long waves are considered independent events (refer to Section 6.2) they are not included in the results of Table 6.1.

6.3.3 Independent Events

As both tsunami and long waves are considered independent events, the maximum value obtained from either: the run-up from the maximum probable tsunami or the positive elevation associated with the 1:10⁶ year return period long wave is used in obtaining design flood levels. Similarly the minimum of either: the run-down from the maximum probable tsunami or the negative elevation associated with the 1:10⁶ year return period long wave is used to ascertain the lowest water levels.

PRDW (2009a) investigated the tsunami risk at the site based on local and distant tsunamigenic sources provided by the Council for Geoscience. Values for the maximum predicted tsunami run-up level from a distant tsunamigenic source are available in PRDW (2009a). As discussed in PRDW (2009a), there is presently insufficient data to assess the risk from local tsunamigenic sources, e.g. submarine slumps. The maximum predicted tsunami run-up level from a distant tsunamigenic source is +2.5 m (PRDW, 2009a).

The tsunami run-up level used in the combination of events is the maximum of the estimated long wave positive water level (refer to Section 4.3), and the maximum credible earthquake induced tsunami run-up (+2.0 m, above). For the inclusion of climate change parameters, the adopted increase for long waves is consistent with that used for storm surge (refer to Section 3.2 and Appendix A). Refer to Table 6.1 for values used.

The maximum predicted tsunami draw down level from a distant tsunamigenic source is -2.0 m (PRDW, 2009a). As discussed in PRDW (2009a), there is presently insufficient data to assess the risk from local tsunamigenic sources, e.g. submarine slumps.

The tsunami draw down level used in the combination of events is the maximum of the estimated long wave negative water level (refer to Section 4.3), and the maximum credible earthquake induced tsunami draw down (-2.0 m, above). For the inclusion of climate change parameters, the adopted increase for long waves is consistent with that used for storm surge (refer to Section 3.2 and Appendix A). Refer to Table 6.1 for values used.

As long wave are inclusive of tsunami and meteo-tsunami, all references to tsunami in the following section regarding combination of events will imply the above mentioned maximum of the independent events. Refer to Section 6.3.1 for combination of tsunami event and storm events.

6.3.4 Long Term Sea Level Rise and Climate Change Parameters

All combinations have also been evaluated for climate change conditions. An additional component is added for sea level rise and the effect of higher waves and winds on wave set-up, wave run-up and storm surge was taken into consideration (Refer to Chapter 3).

In the analysis of extreme low water level, no component for long term sea level rise has been added to the still water level in order to have the design values for the worst case scenario. Other components of climate change having an impact on the extreme low water level are taken into consideration, like increase on wind speeds increasing the negative storm surge (winds blowing from the land).

6.3.5 Confidence Levels

Extreme values for wave height and storm surge have been obtained by fitting a Weibull distribution to the available data sets (refer to PRDW (2009a) for details). The output of the procedure is the best estimate value as well as the upper 95% confidence value. This means that 4 different values are calculated for each component in the extreme water level:

1. Best estimate – Excluding climate change
2. Upper 95% confidence level – Excluding climate change
3. Best estimate – Including climate change
4. Upper 95% confidence level – Including climate change

6.4 Results

Reference is made to Table 6.1 summarizing results for extreme high water levels for the design return periods for beach Profile 03.

TABLE 6.1: EXTREME HIGH AND LOW WATER LEVEL RESULTS

Return Period [years]	Individual component of extreme water level calculations	Units	Excluding climate change		Including climate change	
			Best estimate	Upper 95% confidence	Best estimate	Upper 95% confidence
1	HAT ^(Port Elizabeth)	m MSL	1.28	1.28	1.28	1.28
	Sea level rise	m	0.00	0.00	0.80	0.80
	Positive storm surge	m	0.57	0.60	0.69	0.73
	Set-up and run-up	m	6.04	6.15	6.79	6.90
	Extreme high water level	m MSL	7.89	8.03	9.56	9.71
	LAT ^(Port Elizabeth)	m MSL	-0.84	-0.84	-0.84	-0.84
	Negative storm surge	m	-0.53	-0.55	-0.64	-0.67
	Extreme low water level	m MSL	-1.37	-1.39	-1.48	-1.50
10	HAT ^(Port Elizabeth)	m MSL	1.28	1.28	1.28	1.28
	Sea level rise	m	0.00	0.00	0.80	0.80
	Positive storm surge	m	0.74	0.80	0.90	0.97
	Set-up and run-up	m	6.59	6.78	7.41	7.62
	Extreme high water level	m MSL	8.62	8.86	10.39	10.67
	LAT ^(Port Elizabeth)	m MSL	-0.84	-0.84	-0.84	-0.84
	Negative storm surge	m	-0.73	-0.80	-0.88	-0.97
	Extreme low water level	m MSL	-1.57	-1.64	-1.72	-1.80
100	HAT ^(Port Elizabeth)	m MSL	1.28	1.28	1.28	1.28
	Sea level rise	m	0.00	0.00	0.80	0.80
	Positive storm surge	m	0.90	1.00	1.09	1.21
	Set-up and run-up	m	7.04	7.34	7.92	8.27
	Extreme high water level	m MSL	9.22	9.62	11.10	11.56
	LAT ^(Port Elizabeth)	m MSL	-0.84	-0.84	-0.84	-0.84
	Negative storm surge	m	-0.93	-1.06	-1.13	-1.28
	Extreme low water level	m MSL	-1.77	-1.90	-1.96	-2.12
10 ⁶	HAT ^(Port Elizabeth)	m MSL	1.28	1.28	1.28	1.28
	Sea level rise	m	0.00	0.00	0.80	0.80
	Positive storm surge	m	1.43	1.75	1.73	2.12
	Set-up and run-up	m	8.48	9.36	9.64	10.71
	Extreme high water level	m MSL	11.19	12.40	13.45	14.91
	LAT ^(Port Elizabeth)	m MSL	-0.84	-0.84	-0.84	-0.84
	Negative storm surge	m	-1.73	-2.23	-2.09	-2.70
	Extreme low water level	m MSL	-2.57	-3.07	-2.93	-3.53
Tsunami event	90 th percentile high tides	m MSL	0.98	0.98	0.98	0.98
	Sea level rise	m	0.00	0.00	0.80	0.80
	Positive storm surge ¹	m	0.74	0.80	0.90	0.97
	Tsunami ²	m	2.91	3.64	3.52	4.40
	Set-up and run-up	m	6.59	6.78	7.41	7.62
	Extreme high water level	m MSL	11.22	12.20	13.61	14.77
	90 th percentile low tides	m	-0.58	-0.58	-0.58	-0.58
	Negative storm surge ¹	m	-0.73	-0.80	-0.88	-0.97
	Tsunami ²	m	-3.16	-3.77	-3.82	-4.56
	Extreme low water level	m MSL	-4.47	-5.15	-5.28	-6.10

Notes:

- 1) Based on a 1:10 year return period
- 2) Maximum value of 1:10⁶ year return period long wave and maximum probable tsunami run-up and run-down values

6.5 Discussion of Results

Maximum extreme high water level is seen to occur during a 1:10⁶ year storm event (refer to Table 6.1). Maximum extreme low water is seen to occur during a tsunami event.

One approach to deal with the uncertainties associated with future climate change is adaptive design, for example provision can be made for a seawall in front of the terrace which can be raised in future as necessary. The phased development of the site also allows for the design of the second and third phases to respond to the more accurate climate change predictions that will be available in future.

For the inclusion of climate change in the calculations of extreme flood levels, values are based on the information available at present, and need to be continually reassessed as new data and research results become available. Refer to Section 3.2 for the climate change parameters used in the assessment of the extreme flood levels. Though incorporated implicitly within the calculations for run-up, storm surge and wave heights, any new data regarding sea level rise can for preliminary estimates be added to the calculated levels in Table 6.1.

Climate change is described in detail in Appendix A. For this SSR the upper end projection from the IPCC (2007) of 0.8 m sea level rise to 2100 is used to estimate the maximum wave run-up levels at the site (see Table 6.1 and Section 3.2). These run-up levels do not take into account the presence of the nuclear installation, since this has not yet been designed.

The design of the nuclear installation will need to consider the following:

- The extent to which the infrastructure will modify the topography of the site and thus modify the run-up levels, e.g. excavations or revetments.
- The type and position of intake and outfall structures.
- The volume rate of wave overtopping of the specific structures (in addition to wave run-up levels).
- An evaluation of the risk to the specific design of an extreme upper limit sea level rise of 2 m by 2100. Depending on the specific design, it may be cost effective to design for this extreme level from the start, or to plan future design adaptations or make specific contingency plans.

As discussed in Appendix A, it is highly unlikely that sea level rise will occur suddenly and there will thus be many years warning should the sea level start to rise faster than the predicted rates.

7. COASTLINE STABILITY AND CROSS-SHORE SEDIMENT TRANSPORT

7.1 Introduction

The morphology of the coastline is a result of many individual sediment transport events caused by a succession of waves. In this sense, the shape of the beach and nearshore region may be thought of as representing a form of averaging over time (Reeve *et al.*, 2004). The stability of a length of coastline will depend on the difference between the volumes of sediment entering and leaving this section owing to the net cross-shore and longshore sediment transport due to waves, currents and wind. The coastline will be eroding, accreting or remaining in equilibrium. If equilibrium exists, it is most likely to be a dynamically stable equilibrium, whereby the coastline is evolving continuously in response to varying winds, waves and currents (Reeve *et al.*, 2004). Nevertheless, the typical coastline is relatively constant over a period of months or years, although the position of the coastline at any particular point will vary about this average.

In order to assess the impacts of the driving mechanisms of coastline stability, the following physical processes of erosion/accretion are considered:

- Long-term coastline trends
- Seasonal variation in the coastline
- Storm event erosion
- Effects on coastline movement due to long term sea level rise.

Of the above, the storm events and sea-level rise trends can be effectively modelled. Due to the nature of long-term coastline trends and seasonal variation, the most feasible approach to a quantitative estimation of stability related from these processes requires detailed measurements from historic profiles spanning many years. As this amount of historic profile data are not available, only a preliminary quantitative assessment can be made with the existing limited data series.

Recent profile measurements for the months of January, April, July and October of 2008 and January, April and July of 2009, have been processed and analysed for a number of beacon locations. These include 40 combined beacons for Slangbaai and Thysbaai. The profiles are the first available for the ongoing profile survey as part of the oceanographic data collection programme. The data collection programme commenced in January 2008 and is scheduled to run until August 2010 (31 months of data).

Further to the physical monitoring of beach profiles in Slangbaai and Thysbaai, a number of aerial photographs have been utilised in qualitatively assessing the long term erosional/accretional processes for: Slangbaai, Thysbaai, Cape St. Francis and Krommebaai (refer to Figure 7.1).

7.2 Long-term Coastline Trends

7.2.1 Physical Process

Long-term coastline trends are typically processes which are likely to persist over a number of years, and which result in erosion and accretion rates in the order of a few meters per year. Reeve *et al.*, (2004) suggest that records as long as 20 years are sometimes required to establish an average longshore transport rate with reasonable accuracy. Due to the long time scales and complex process interaction associated with long-term coastal changes, numerical modelling is problematic and has a limited reliability of results. Statistical analysis of past records for historically collected data is considered to be the most accurate method for establishing coastline trends due to long-term processes (Coastal CRC, 2006).

7.2.2 Methodology

Three contour lines, namely: the vegetation line, the high water mark and the +5 m MSL contour line, were digitised on each of the available geo-referenced aerial photographs. Profile comparison lines, positioned on each beach at approximately 200 m intervals, were superimposed onto the available images for comparison between consecutive aerial photographs.

The position of the vegetation line, 5 m contour and the high water mark were compared at each profile comparison line in each photo taking into account the beach slope variation, tidal ranges and seasonal variations in order to deduce any accretion or erosion trend.

By comparing the vegetation line and the high water mark (based on wetted area) with the profile comparison lines in each photo, an assessment was made of long term coastline processes within the time difference of the photographs. Based on this methodology a general overview of the stability of the coastline was made and specific areas of interest categorised as having: eroded, accreted or remained dynamically stable.

7.2.3 Accuracy

The accuracy of the comparison of the high water mark is dependent on available information regarding tidal data and storm information at the time of the respective photographs. As this information is not currently available, the accuracy is limited by the maximum possible horizontal movement of the high water mark between MHWS and MHWN (refer to Section 4.1) and possible variations in storm surge, wave set-up and wave run-up. For the beaches at Thyspunt with a maximum tidal variation (MHWS to MHWN) of approximately 0.6 m, an approximate vertical variation due to storm surge, set-up and run-up of 2 m, and considering an average slope of 1:20, the accuracy of the method is limited to approximately 50 m. Additional sources of error include rectification and image

resolution. The combined magnitude of imaging errors is found to be in the order of an 8 m horizontal residual (Crowell *et al.*, 1991).

7.2.4 Coastline Trends

Coastline trends were assessed on this basis for the following four beaches, (refer to PRDW (2009a) for location map):

1. Slangbaai
2. Thysbaai
3. Thyspunt Coast
4. Cape St Francis
5. Krommebaai

7.2.4.1 *Slangbaai*

Slangbaai is a 5.5 km long beach located 11 km west of the Thyspunt site. Photos available for this area are dated from 1980 and 2004-2007. As insufficient information regarding the 5 m contour line is available, only the vegetation and high water lines have been used to ascertain coastline trends. The vegetation line is seen to have accreted over the period 1980 to 2007. The high water line shows erosion over the period (refer to Figures 7.2 to 7.7).

7.2.4.2 *Thyspunt Coast*

There are two small beaches along the rocks in front of the nuclear installation corridor. Aerial photos for 1980 and 2007 are shown in Figures 7.8 and 7.9. The images are available as reference to measured profiles (refer to Section 7.3).

7.2.4.3 *Thysbaai*

Thysbaai is a 2 km long beach located at the Thyspunt site. Photos available for this area are dated from 1980, 2004 and 2007. The vegetation line and 5 m contour are both seen to have remained dynamically stable during the observation period. The high water mark is seen to have eroded during the period of 1980 to 2007 (refer to Figures 7.10 and 7.11. No information is available regarding the high water mark for the year 2004. It is noted, however, that there are several rip cells on the Thysbaai beach with frequent cusp and spit formations. This may contribute to the appearance of erosion on the aerial photographs.

7.2.4.4 *Cape St Francis*

Cape St Francis is a 2.5 km long beach located 5.5 km east of Thyspunt. Photos available for this area are dated from 1980, 1999 and 2006. The vegetation line is seen to have accreted or remained dynamically stable over the observation period. The high water mark is seen to have remained

dynamically stable over the observation period (refer to Figures 7.12 to 7.14). Where information is available, there is evidence that the 5 m contour has eroded during the observation period.

7.2.4.5 *Krommebaai*

Krommebaai a 2 km long beach located 6 km east of the Thyspunt site. Photos available for this area are dated from 1980, 1999 and 2006. The vegetation line is seen to have accreted during the period of 1980 to 1999. The 5 m contour line, where information is available, is seen to have remained dynamically stable in the southern part of the Krommebaai beach (refer to Figure 7.15) from 1980 to 1999. No information is available for 2006. The 5 m contour for the northern extent of the Krommebaai beach is seen to have eroded over the period 1980 to 1999 (refer to Figure 7.16). Where information is available, the high water mark is seen to have eroded over the period from 1980 to 2006.

The erosion at Krommebaai has been observed locally and reported with a rate of between 2 to 3 m per year over the last 25 years (SFBT, 2008).

7.2.5 Discussion of Results

By comparing the vegetation line and the high water mark (based on wetted area) on each set of photos, an assessment was made of whether the beach eroded, accreted or remained dynamically stable.

Although a rigorous method has been followed in the assessment of coastline trends using aerial photographs, the method is subjective. The above observations of coastline trends are qualitative and must be interpreted as such.

For Slangbaai and Thysbaai, the closest beaches to the nuclear installation corridor, though signs of both erosion and accretion are noticed in the analysis of the aerial photographs, these are believed to be indications of long term variations about dynamically stable beach shapes (refer to Section 7.1).

7.3 Seasonal Variation in Coastline

7.3.1 Physical Process

Seasonal variations can be seen as coastline modification events with averaging periods typically in the order of months. These are generally due to seasonal variations in wave conditions and the occurrence of erosional storms separated by periods of low wave accretion events. In South Africa the majority of erosion related storms occur in the winter months, with summer months predominated by accretionary periods of low wave height conditions (Rossouw, 1989). As in long-term coastline trends, a statistical analysis based on measured profile data is the primary method of determining seasonal variations.

With the limited profile data currently available only a preliminary quantitative assessment of seasonal variation for the Thyspunt coastal sites is possible. For coasts that do exhibit a seasonal signature, the large perturbations caused by storm events require repetitive surveys over many years to extract this seasonal signature (CEM, 2002).

7.3.2 Methodology

As mentioned in Section 7.1, recent profile measurements for the months of January, April, July and October of 2008 and January, April and July of 2009, have been processed and analysed for a number of beacon locations along the beaches for the Thyspunt site. For an overview of profile locations for Slangbaai and details of the available measured profiles refer to Figures 7.17 to 7.20. For Thysbaai, refer to Figures 7.21 to 7.24.

Distances from the respective beacon locations have been calculated from interpolated values obtained at 0 m MSL, +1 m MSL, +2 m MSL and +3 m MSL for each of the available measurements. An average distance has then been calculated from these interpolated values. The difference between this calculated average and the measured distance, for each survey date, has been used in order to calculate seasonal variations.

7.3.3 Coastline Trends

Figures 7.25 and 7.26 show the variations for horizontal displacements for beach profiles at Slangbaai and Thysbaai and front of the proposed nuclear installation corridor. Figure 7.25 specifically shows variations for Slangbaai and Profiles 18 and 19. Generally the beach exhibits a typical winter storm erosion pattern, with erosion of the majority of profiles between April and October, winter storm months, and accretion from October to April. Similar erosion patterns are noticeable on the Thysbaai beach.

Between July and October 2008, significant erosion is observed for the Slangbaai and Thysbaai coastline. This is expected to be as a result of a significant storm which occurred on 30 August 2008. The profile changes observed during this period relate to storm induced movement of material from the inter-tidal and upper beach zone to an offshore bar. This material is expected to return onshore with time.

7.3.4 Quantification of Seasonal Variations

Maximum (+ve: accretional), and minimum (-ve: erosional) deviations from the calculated average (Section 7.3.2) for each of the profiles over the survey periods of 2008 and 2009 are provided in Figures 7.25 and 7.28 and Table 7.1.

TABLE 7.1: MAXIMUM SEASONAL VARIATIONS IN HORIZONTAL DISPLACEMENTS OF THE MEASURED BEACH PROFILES

Profile no.	0 m MSL		+1 m MSL		+2 m MSL		+3 m MSL	
	Erosion [m]	Accretion [m]						
01 ¹	-9.43	14.95	-9.49	6.66	-8.78	10.78	-1.08	1.03
03	-48.61	42.87	-44.91	27.03	-36.11	21.86	-4.92	9.04
05	-14.75	21.23	-16.42	21.46	-19.34	26.19	-4.95	3.45
07	-29.72	41.31	-25.53	19.95	-27.18	22.62	-27.55	40.81
09	-12.92	13.14	-11.22	18.57	-11.67	23.60	-4.41	8.13
10	-8.21	4.73	-13.07	17.67	-24.16	25.38	-33.56	36.77
11	-15.26	9.41	-11.89	12.85	-9.90	18.48	-4.82	6.97
12	-28.65	38.14	-15.57	17.49	-14.64	9.47	-4.84	3.58
18	-9.28	9.71	-6.30	6.08	-6.82	8.79	-8.47	8.69
26 ²	-19.60	19.15	-12.37	21.85	-11.12	29.44	-2.68	3.22
27	-13.47	12.58	-8.19	14.10	-12.10	15.53	-2.51	4.79
28	-11.17	12.47	-7.09	9.78	-5.88	8.71	-2.30	2.06
30	-24.34	15.10	-13.38	8.82	-7.07	6.00	-4.91	3.66
32	-10.28	9.03	-8.25	4.97	-7.81	5.70	-5.83	3.07
34	-15.52	11.84	-15.50	14.86	-12.48	18.93	-3.01	2.10
36	-11.60	12.73	-13.81	11.76	-7.81	14.16	-3.81	4.63
38	-48.09	50.77	-39.84	30.50	-31.05	12.76	-15.66	6.57
40	-14.43	10.63	-5.89	21.54	-1.72	8.79	-0.39	0.32

Notes (refer to Figures 7.17 and 7.21):

1. Profiles 01 to 12 refer to profiles on Slangbaai beach
2. Profiles 26 to 30 refer to profiles in Thysbaai beach

The available profile data indicates that the maximum seasonal erosion from the *average* of the survey data on the Thysbaai Beach is approximately -48 m (at the +0 m MSL level at Profile 38). Profiles 19 and 23a (excluded from Table 7.1) are seen to be on an elevated rocky shelf at approximately +0 m MSL (see Figure 7.20 and 7.22), no erosion is evident from the profile measurements.

Profile measurements for Thyspunt are on-going, (refer to Section 7.1), however the data utilised on the profile analysis above can be seen as the first complete season of measured data.

7.4 Storm Event Erosion

7.4.1 Physical Process

Severe storms can cause significant modifications of the littoral zone, particularly to the profile of the beach (IAEA, 2003). Sediment transport at a point in the nearshore zone is a vector with both longshore and cross-shore components. Although the long-term beach profile might be stable, severe storm conditions can cause cross-shore sediment transport resulting in a 'storm profile' (see Figure 7.27). The evolution of the beach profile can have an impact on the nearshore waves. An increase of nearshore waves has a direct impact on wave run-up.

7.4.2 Methodology

At Thyspunt the coastline is generally rocky and not highly susceptible to erosion under normal storm conditions. Only during episodic events would back of coast dunes possibly be vulnerable. The beach at Thysbaai is however subject to both seasonal and storm cross-shore erosion. SBEACH, a beach response model for storm events (CERC, 1993), has been used to model storm erosion for the combined storm events (refer to Section 6.3) for the 1:1, 1:10, 1:100 and 1:10⁶ year return periods at a specific profile at the Thysbaai site.

As SBEACH is fundamentally a cross-shore storm erosion model it is necessary to calibrate the model with profile information from a relatively straight beach where profile changes are predominantly due to cross-shore transport and unlikely to be caused by long-shore sediment gradients. The Duynefontein site exhibits such characteristics and has thus been used to calibrate the SBEACH model. Based on the profiles obtained from historic measurements for the Duynefontein site (PRDW, 2009b) a representative beach profile has been chosen for calibration of SBEACH (refer to Figure 7.28 for a plan view of the location of the profile (PRDW, 2009b) used for model calibration).

7.4.2.1 Calibration: Beach Profile and Sediment Properties

In order to calibrate the model, historic information of beach profiles is needed. Measured profiles from April 2008 and July 2008 have been used (PRDW, 2009b). The profiles have then been interpolated onto existing bathymetric and topographic data to obtain a full profile for modelling.

Since SBEACH requires a constant grain size across the profile a representative D_{50} grain size has been used in the calibration of the model. From measured sediment sample data for the profile considered, a D_{50} of 0.3 mm is considered as representative. This grain size has been used consistently in the calibration process.

7.4.2.2 Calibration: Wave Conditions

Wave conditions for the period from April 2008 to July 2008 have been extracted from a previous wave refraction study, described in the modelling report for Duynefontein (PRDW, 2009c). For initial calibration of the model a complete time series of significant wave heights and peak wave periods for every 6 hours has been used. Figure 7.29 shows a plot of the significant wave heights and peak wave periods used over the modelling period.

7.4.2.3 Calibration: Water Levels

SBEACH models the wave setup and run-up internally, whilst the combined tidal, wind setup and pressure setup are specified as a time-varying boundary condition. For input water level conditions measured tidal data from Cape Town has been interpolated as hourly boundary data for the period coinciding with the calibrated wave data. Figure 7.29 shows a plot of the tidal data used over the modelling period.

7.4.2.4 Calibration: Model Parameters

The primary model parameters for SBEACH are the transport rate coefficient, K , the coefficient for slope dependence, ϵ , and the transport rate decay coefficient multiplier, λ . A sensitivity test was performed using values corresponding to the minimum recommended value, the default value and the maximum recommended value for each of the model parameters with the other parameters set to default. For the transport rate decay coefficient multiplier, λ , an intermediate value between the minimum and maximum recommended values was modelled, as the default value is equal to the maximum recommended value (CERC, 1993).

TABLE 7.2: SBEACH CALIBRATION PARAMETERS

Calibration Parameter	Minimum Value	Intermediate Value	Maximum Value
K [m^4/N]	0.50E-06	1.75E-06 ⁽¹⁾	2.5E-06
ϵ [m^2/s]	0.001	0.002 ⁽¹⁾	0.003
λ [-]	0.1	0.3	0.5 ⁽¹⁾

Notes:

- 1) Model default values

7.4.2.5 Calibration: Discussion of Results

Results show:

- High dependence on K
- Marginal dependence of ϵ
- Little dependence on λ

Refer to Figure 7.30 for results of the calibration analysis. The default values (refer to Table 7.2) for all calibration parameters show sufficient correlation for modelling purposes. For the further modelling of storm induced erosion, these values are used.

7.4.3 Storm Events

Further calibration of the model input conditions is achieved using shorter time scales with actual storm and water levels, obtained from the wave refraction model (PRDW, 2008c), and measured tidal data for Cape Town.

As knowledge of storm progression, i.e. duration, increase in H_{m0} and T_p , is not known before hand for the design storm conditions, a method is utilised whereby a measured storm is compared to a modelled storm using the equivalent wave energy for the measured storm (MacHutchson, 2006).

7.4.3.1 Measured Storm Conditions

Individual storm events extracted from the data set for April to July 2008 (refer to Section 7.4.2.2) have been used for more detailed calibration and verification of final model storm parameters. The four

highest energy storms, as calculated with the equivalent wave energy calculations, have been isolated and applied to the SBEACH model (refer to Figure 7.30).

7.4.3.2 Modelled Storm Conditions

Equivalent design storms are modelled using an equivalent wave energy storm progression, with the maximum H_{m0} for the measured storm events, and the $H_{m0} - T_p$ relationship obtained from PRDW (2008c). Further to the maximum H_{m0} and T_p , a representative storm duration, and storm threshold value for H_{m0} are required. Storm threshold is defined as being equal to the annual average H_{m0} for the area (MacHutchson, 2008). For the calibration of storm data from the Duynfontein site the storm threshold has been extracted from existing measured data and corresponds to an H_{m0} of 1.8 m.

Furthermore, MacHutchson (2006), categorised South African storm events with respect to a defined steepness ratio, difference in maximum H_{m0} and storm threshold H_{m0} over duration, for specific individual coastal regions in South Africa based on historical data. The steepness ratio used in calculations for both the modelled calibration storm events and design modelled storm events corresponds to that determined for the south coast region. Using this steepness ratio, typical storm durations based on storm maximum H_{m0} , T_p and mean H_{m0} are calculated (refer to Figure 7.31).

7.4.3.3 Results

The SBEACH modelled erosion patterns for the *modelled storm progressions* show close agreement with the SBEACH modelled erosion patterns for the *measured storm events* (refer to Figure 7.32). Good agreement is seen with erosion of the dune and set-back at high water levels. Based on these results from initial tests, the assumption of a linear equivalent wave energy storm progression for individual storm events appears justifiable. Using the method described, storm progressions for extreme design wave conditions are modelled.

7.4.4 Storm Analysis

7.4.4.1 Beach Profile and Sediment Properties

Model runs have been completed with an interpolated profile based on detailed topographic measurements of the dunes and surveyed data of the coast seaward of the beach (refer to PRDW, 2009a). Profile 05 (refer to Figures 4.10 and 4.11) has been used for storm analysis.

From sediment grading data for Thyspunt, (PRDW, 2009a) representative samples show D_{50} values of 0.2 to 0.4 mm. D_{50} values of 0.2, 0.3 and 0.4 mm have been specified in three SBEACH models for the profile.

7.4.4.2 Wave Conditions and Water Levels

Values of the maximum H_{m0} and T_p for the 1:1, 1:10, 1:100 and 1:10⁶ year storm conditions have been used in determining the modelled storm profiles for Thysbaai. Refer to Section 4.1 for water levels and PRDW (2009a) for wave conditions. Storm threshold values are specified as the local mean H_{m0} for Thysbaai at 2.4 m (PRDW, 2009a).

A sinusoidal tidal variation has been modelled for each of the storm conditions, with a period of 12 hours and maximum amplitude of half of HAT - LAT. The peak of the storm, the maximum H_{m0} and T_p values, correspond to HAT for the water levels with an inclusion due to maximum storm surge (refer to Section 4.1).

7.4.4.3 Discussion of Results

Figure 7.33 shows erosion patterns for the surf zone for Profile 05 and the three D_{50} values. Maximum horizontal erosion at any level for all model runs are tabulated below:

TABLE 7.3: MAXIMUM STORM EROSION HORIZONTAL DISPLACEMENTS - EXCLUDING CLIMATE CHANGE

D_{50}	Units	Return Period [years]			
		1:1	1:10	1:100	1:10 ⁶
0.2 mm	[m]	-16	-20	-23	-34
0.3 mm	[m]	-9	-11	-14	-23
0.4 mm	[m]	-5	-7	-8	-15

As can be seen in Table 7.3, the maximum absolute value of shoreline recession due to a single storm event occurs during the 1:10⁶ year.

As SBEACH assumes a standard grain size, and the model is calibrated for measured profiles in the surf zone, no vertical position of the tabulated horizontal change is given. Similarly, and considering avalanching of the dune during storm erosion, the maximum horizontal values should conservatively be seen as occurring from the foredune crest.

7.5 Long-term Sea-level Rise

7.5.1 Physical Process

The effect of increased water levels due to climate change (see Section 3.2) needs to be accounted for. These effects are shown to be highly complex and inclusive of local geomorphological and sedimentological characteristics (Cooper and Pilkey, 2004). However, the majority of coastline response studies to sea-level change are based on the simplified fundamental assumption that a beach will maintain an equilibrium profile dependent on the dominant wave climate. As such, provided that the rate of sea-level rise is small, the beach profile will translate vertically and horizontally landward such that this equilibrium profile is maintained.

7.5.2 Methodology

One of the best known shore response models to climate induced sea level change was proposed by Bruun in 1962 (CEM, 2002). This model, though noted as omitting factors other than wave action affecting sediment transport (CEM, 2002), has nonetheless been widely used in predicting long-term sea level change tendencies.

It remains the “only practical way of yielding a rapid, semi-quantitative assessment of shore response to a rise in sea level” (Cooper and Pilkey, 2004). Based on the complexity of long-term sea level rise due to climate change and the unknowns regarding rates of change, and effects on wave and climate conditions it is suggested that Bruun-type calculations give, at best, order of magnitude estimates of shoreline retreat (CEM, 2002).

7.5.2.1 Bruun’s Rule

The use of Bruun’s rule is based on the following assumptions:

- The upper beach erodes because of a landward translation of the profile
- Sediment eroded from the upper beach is deposited immediately offshore; the eroded and deposited volumes are equal (i.e. longshore transport is not a factor).
- The rise in the seafloor offshore is equal to the rise in sea level. Thus, offshore, the water depth stays constant.

$$R = \frac{L_*}{B + H_*} S \quad \text{Equation 1}$$

Where:

R is the horizontal coastline retreat [m]

S is the increase in sea level [m]

L_* is the cross-shore distance to the water depth H_* [m]

B is the berm height of the eroded area [m]

7.5.2.2 Applied Modification to Bruun’s Rule

Reformatting the Bruun Rule in a simplified form (CEM, 2002) gives:

$$x = \frac{zX}{Z} \quad \text{Equation 2}$$

Where:

z is the change in water level [m]

x is the ultimate profile retreat [m]

X is the corresponding distance determined from the depth of closure to the upper point of profile adjustment (refer to Figure 7.34). [m]

Z is the vertical distance from the depth of closure to the upper point of profile adjustment (refer to Figure 7.34). [m]

The upper point of profile adjustment is taken to be the crest of the foredune. The modified Bruun Rule, shown above, is a simple geometric rule to account for sea level changes and related beach response profiles. From the depth of closure, the minimum depth at which no measurable or significant changes in the bottom depth occurs, the profile is relocated such that sediment is conserved and the profile is assumed to reach an equilibrium profile at the new water level. The following equation is used to calculate the depth of closure (CEM, 2002):

$$d_l = 2.28H_e - 68.5 \left(\frac{H_e^2}{gT_e^2} \right) \quad \text{Equation 3}$$

Where:

d_l is the annual depth of closure below the mean water level [m]

H_e the non-breaking significant wave height that is exceeded 12 hours per year (0.137 %) [m]

T_e the associated wave period [s]

g gravitation acceleration [m.s⁻²]

For calculations of modified profile changes based on Bruun's Rule for sea level change, H_e is predicted from the 1:1 year return period wave (refer to Section 4.4). The parameters and solution for the calculation of long term horizontal displacement due to sea level rise are given in Table 7.4

TABLE 7.4: PARAMETERS FOR LONG-TERM HORIZONTAL EROSION DUE TO SEA LEVEL RISE

Parameter	Value
H_e	6.85 m
T_e	16.05 m
g	9.81 m.s ⁻²
d_l	14.35 m
Z	26.54 m
z	0.8 m
X	730 m
x	22 m

Figure 7.35 shows the horizontal and vertical translation of Profile 05. For the assumed sea level rise of **0.8 m** (Section 3.2), the maximum horizontal change is calculated to be approximately **22 m**.

7.5.3 Storm Erosion Including Climate Change

Extreme wave conditions exacerbated by climate change events (refer to Section 3.2), have been used to model the storm erosion patterns for Profile 05 and the climate changed beach profile. Refer to Figure 7.36 for details of erosion patterns for the representative D_{50} values as specified in Section 7.4.4.1. As the equilibrium profile is assumed to translate vertically and horizontally due to climate induced sea level rise, the maximum horizontal values should conservatively be seen as occurring from the foredune crest.

Maximum horizontal erosion for all model runs is tabulated below:

TABLE 7.5: MAXIMUM STORM EROSION HORIZONTAL DISPLACEMENTS - INCLUDING CLIMATE CHANGE

D_{50}	Units	Return Period [years]			
		1:1	1:10	1:100	1:10 ⁶
0.2 mm	[m]	-18	-25	-30	-41
0.3 mm	[m]	-11	-14	-16	-29
0.4 mm	[m]	-7	-9	-10	-19

The maximum absolute value for erosion is seen to occur during the 1:10⁶ year return period storm for a D_{50} of 0.2 mm.

7.6 Discussion of Results

Results for the following physical processes of erosion/accretion events considered in the section above are tabulated:

- Long-term coastline trends (Section 7.2)
- Seasonal variation in the coastline position (Section 7.3)
- Storm event erosion based on 1:10⁶ year with grain size 0.2 mm (Section 7.4)
- Effects on coastline movement due to long term sea-level rise (Section 7.5)

TABLE 7.6: MAXIMUM EXPECTED HORIZONTAL COASTLINE EROSION AT THYSPUNT BEACH FOR THE EXPECTED INSTALLATION LIFE

	Long-term Trend	Seasonal Erosion	Storm Event Erosion	Long Term Sea level rise	Total Coastline Erosion
Excluding climate change	Dynamically stable	48 m	34 m	N/A	82 m
Including climate change	Dynamically stable *	≥ 48 m **	41 m	22 m	≥ 111 m

Notes:

* Future changes in wave direction could modify the long-term trend (no information available at present);

** Likely to exceed 48 m based on future increase in wave height (see Section 3.2);

Coastline recession data and models due to climate induced sea-level change are based on the information available at present, and need to be continually reassessed as new data and research results become available.

8. CONCLUSIONS

The following conditions for the Thyspunt site have been addressed in this report and where applicable numerical models have been used to generate results:

- Physiography and marine/coastal geology
- Possible changes to hydrographic conditions due to climate changes
- Hydrographic conditions
- Intake and outfall design considerations
- Combinations of maximum and minimum water levels
- Coastline stability and cross-shore sediment transport

Hydrographic conditions for the proposed Thyspunt site have been analysed as well as the impact of climate change on these conditions within the lifetime of the planned nuclear installation. The risk of flooding assessment and availability of cooling water have been undertaken according to internationally specified standards as documented in the IAEA (2003).

The results of these investigations, along with the Numerical Modelling of Coastal Processes Report (PRDW, 2009a), provide inputs to the SSR Chapter on Oceanography and Coastal Engineering.

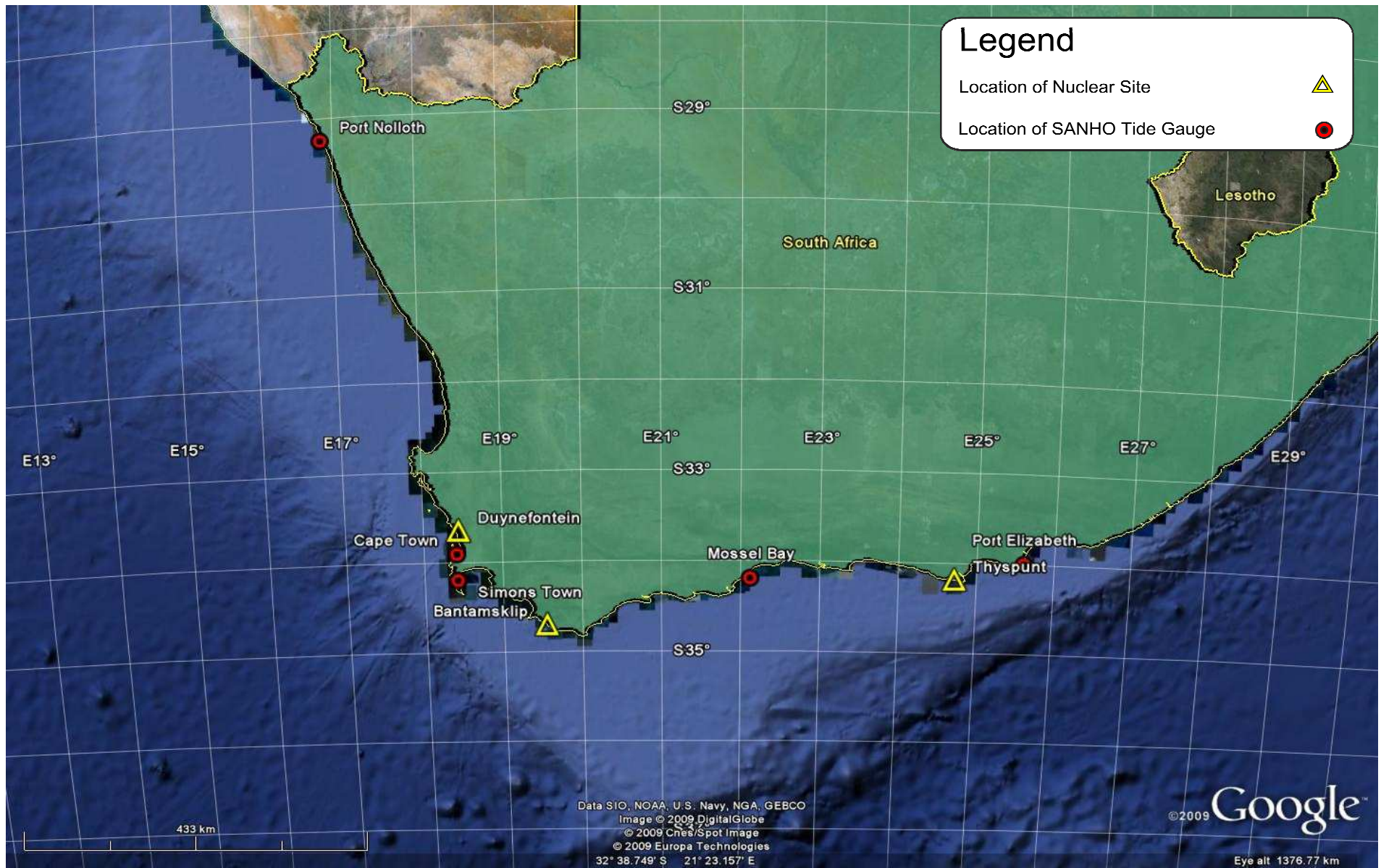
REFERENCES

1. ASCE (1982) Design of Water Intakes for Fish Protection, American Society of Civil Engineers, 1998
2. Bosman, D. E. and Wijnberg, A. R (1987) Gouriqa Marine Reports, Volume V. Nuclear Coastal Engineering NSE – 1 Project. Cost model for marine Cooling Systems for S.A. Nuclear Sites, November 1987
3. CEM (2002) CEM Part IV Chapter 3 - Coastal Morphodynamics, US Army Corps of Engineers, April 2002
4. CEM (2003) CEM Part II Chapter 2 - Meteorology and Wave Climate, US Army Corps of Engineers, July 2003
5. CEM (2006) CEM Part VI Chapter 5 - Fundamentals of Design, US Army Corps of Engineers, June 2006
6. CERC (1993) SBEACH: Numerical Model for Simulating Storm-Induced Beach Change, Report 3, User's Manual, US Army Corps of Engineers, 1993.
7. Coastal CRC (2006) The evolution of Jumpinpin Inlet, McCaully, E. and Tomlinson, R. Cooperative Research Centre for Coastal Zone, Estuary and Waterway Management, 2006.
8. Cooper and Pilkey (2004) Sea-level rise and shoreline retreat: time to abandon the Bruun Rule, Cooper J. A. G and Pilkey O. H, *Global and Planetary Change*, 43 (2004) 157-171
9. Crowell, M., S.P. Leatherman, and M.K. Buckley, 1991. Historical Shoreline Change: Error Analysis and Mapping Accuracy. *Journal of Coastal Research*, Vol. 7, No. 3, pp. 839-852.
10. Engineers Australia (2004) Guidelines for Responding to the Effects of Climate Change in Coastal and Ocean Engineering, The National Committee on Coastal and Ocean Engineering, Engineers Australia.
11. EPRI (2008) Best Management Practice for Preventing Cooling Water Intake Blockage, Electric Power Research Institute, Palo Alto, California, January 2008
12. Eskom (2006) Koeberg Site Safety Report, Chapter 8, Oceanography and Cooling Supply, Rev 3.
13. Eskom (2007) Areva, EPR Technical Description, Rev A, Received from Eskom, August 2007.
14. Eskom (2008) ESKOM Holdings Limited; Environmental Impact Assessment for the Proposed Nuclear Power Station ('Nuclear 1') and Associated Infrastructure; Marine Ecology Study; September 2008.
15. FEMA (2006) "Tsunami Inundation Scour of Roadways, Bridges and Foundations Observations and Technical Guidance from the Great Sumatra

-
- Andaman Tsunami”, EERI Earthquake Engineering Research Institute / FEMA [Federal Emergency Management Agency](#), 2006
16. FUGRO Survey (2006) Marine Geophysical Survey THYSPUNT Seabed Features, FUGRO SURVEY AFRICA (PTY) LTD, Commissioned for ESKOM HOLDINGS LTD., November 2006
17. Hughes (2004) Estimation of wave run-up on smooth, impermeable slopes using the wave momentum flux parameter, S. A. Hughes, 2004, *Coastal Engineering*, 51, 1085-1104
18. IAEA (2003) Flood Hazard for Nuclear Power Plants on Coastal and River Sites. International Atomic Energy Agency. IAEA Safety Standards Series No. NS-G-3.5.
19. IPCC (2007) Climate Change 2007 - The Physical Science Basis, Contribution of Working Group I to the Fourth Assessment Report of the IPCC
20. MacHutchson (2006) The Characterisation of South African Storms, K. R MacHutchson, MSc. Thesis, University of Stellenbosch, 2006
21. Morton, R. A, Gelfenbaum, G, Jaffe, B. E, Physical criteria for distinguishing sandy tsunami and storm deposits using modern examples, *Sedimentary Geology*, 2007.
22. NGDC (2009) National Geophysical Data Centre (NGDC), NOAA Satellite and Information Service, The Significant Earthquake Database, Available from <http://www.ngdc.noaa.gov/nndc/>
23. PRDW (2009a) Eskom, Nuclear Sites, Numerical Modelling of Coastal Processes - Thyspunt, Prestedge Retief Dresner Wijnberg (Pty) Ltd, Report 1010/2/101 Rev 04.
24. PRDW (2009b) Eskom, Nuclear Sites, Coastal Engineering Investigations - Duynfontein, Prestedge Retief Dresner Wijnberg (Pty) Ltd, Report 1010/4/102 Rev 03.
25. PRDW (2009c) Eskom, Nuclear Sites, Numerical Modelling of Coastal Processes - Duynfontein, Prestedge Retief Dresner Wijnberg (Pty) Ltd, Report 1010/4/101 Rev 03.
26. Reeve D, Chadwick A and Flemming C ,2004. Coastal Engineering, Processes, Theory and Design Paractice, D Reeve, A Chadwick and C Fleming. SPON Press, 2004
27. Rossouw (1989) Rossouw, J. Design Waves for the South African Coastline. Dissertation approved for the degree Doctor of Philosophy at the University of Stellenbosch, March 1989.
28. SFBT (2008) Saint Francis Bay Trust - The Beach Erosion Forecast at <http://www.stfrancisbay.org/index.htm>
29. South African Tide Tables (2009) SAN HO-2, Published by the Hydrographer, South African Navy, ISBN 0-97809584817-4-8.
30. USGS (2005) The 26 December 2004 Indian Ocean Tsunami: Initial Findings from Sumatra, Based on Survey Conducted January 20-29, 2005,

- USGS U.S. Geological Survey, 2005, Available from:
<http://walrus.wr.usgs.gov/Tsunami/sumatra05/>
31. USNRC (2007) US Nuclear Regulatory Commission (2007) NUREG-0800, Part 2.4.6, Probable Maximum Tsunami Hazards, Washington
32. Yeh, H, Tonkin S, Kato, F and Sato, S, Tsunami Scour Mechanisms Around a Cylinder, Journal of Fluid Mechanics (2003), 496 : 165-192
33. Yim (2006) Modelling and Simulation of Tsunami and Storm Surge Hydrodynamic Loads on Coastal Bridge Structures, Yim, S., 2006, Technical Memorandum of Public Works Research Institute.

FIGURES

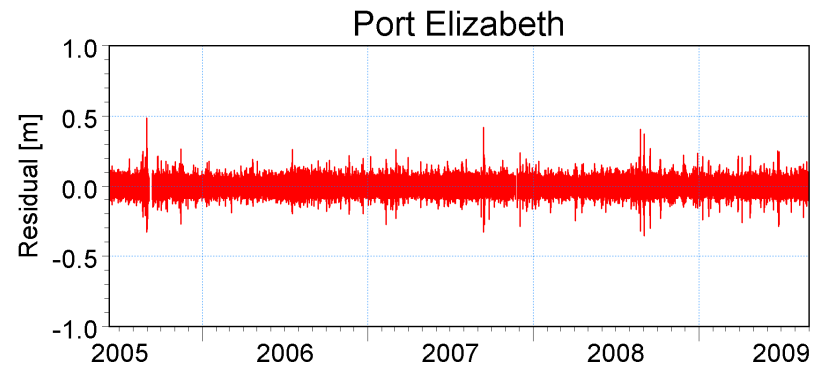
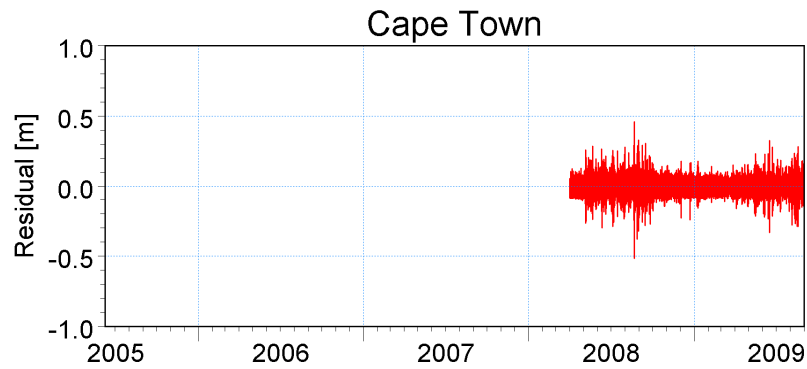
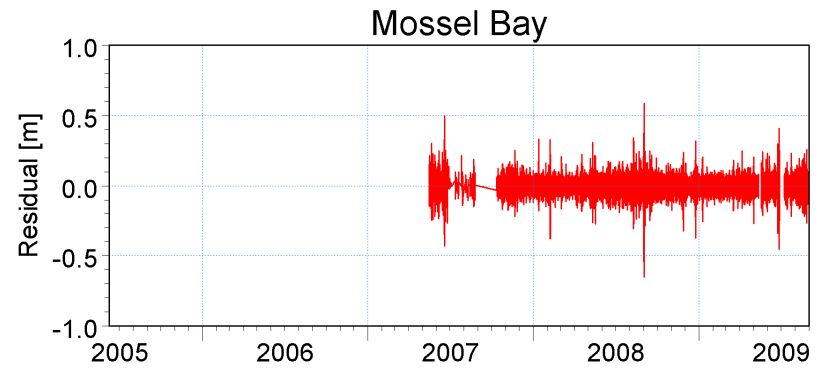
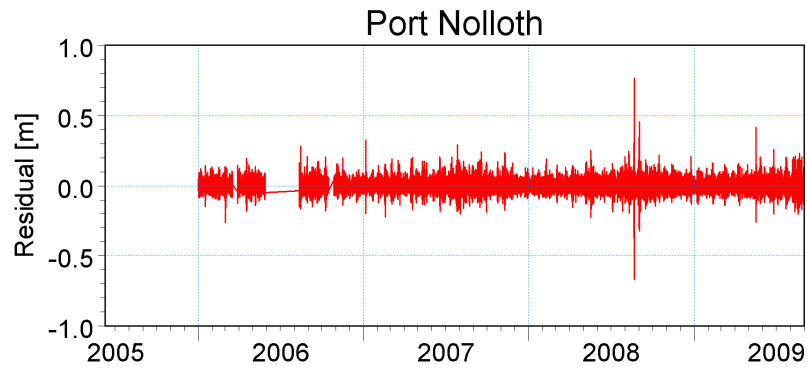


Title:

Locations of SANHO tide gauges used in the extraction of long wave extreme values

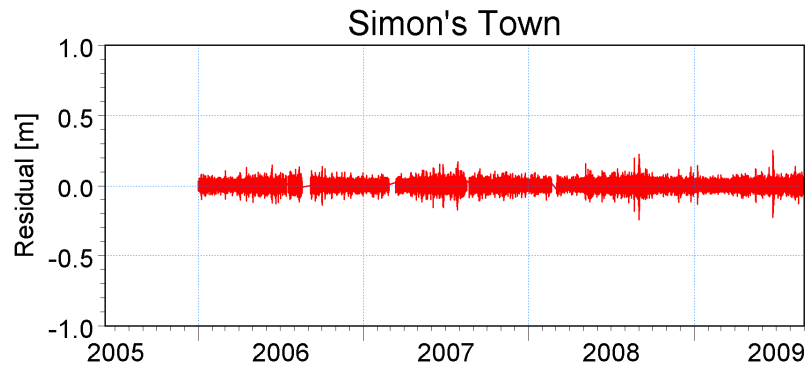
Figure No.

4.1



X:\PRDW Projects\Current\SA (1010) Nuclear Sites
SSRs\Working\Engineers\RLH\Meteotsunami\Data\Sites\ResidualComparisonAll1t.png

X:\PRDW Projects\Current\SA (1010) Nuclear Sites
SSRs\Working\Engineers\RLH\Meteotsunami\Data\Sites\ResidualComparisonAll1t.png

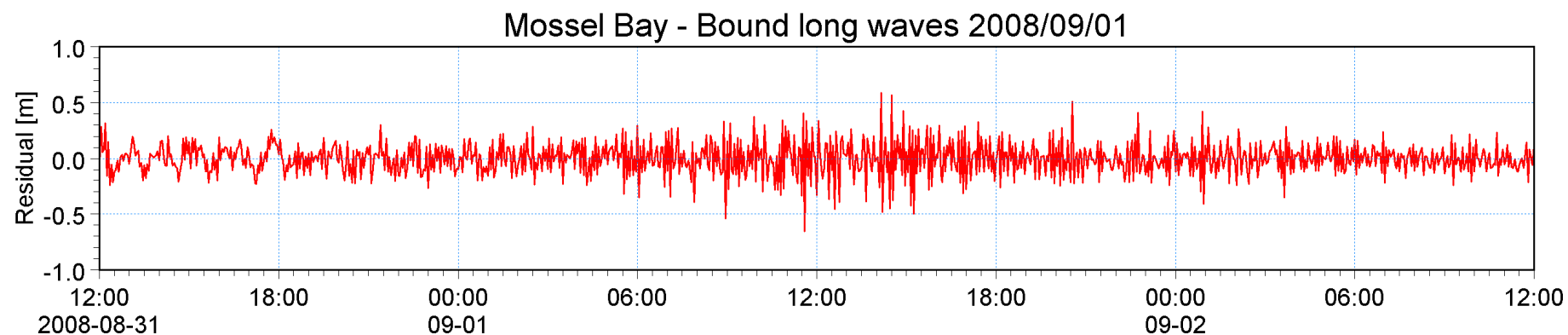
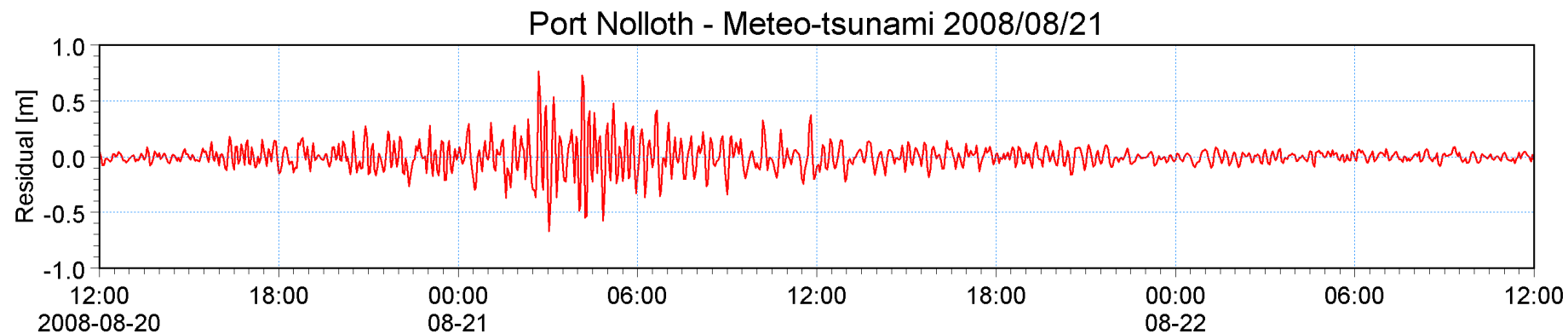


Title:

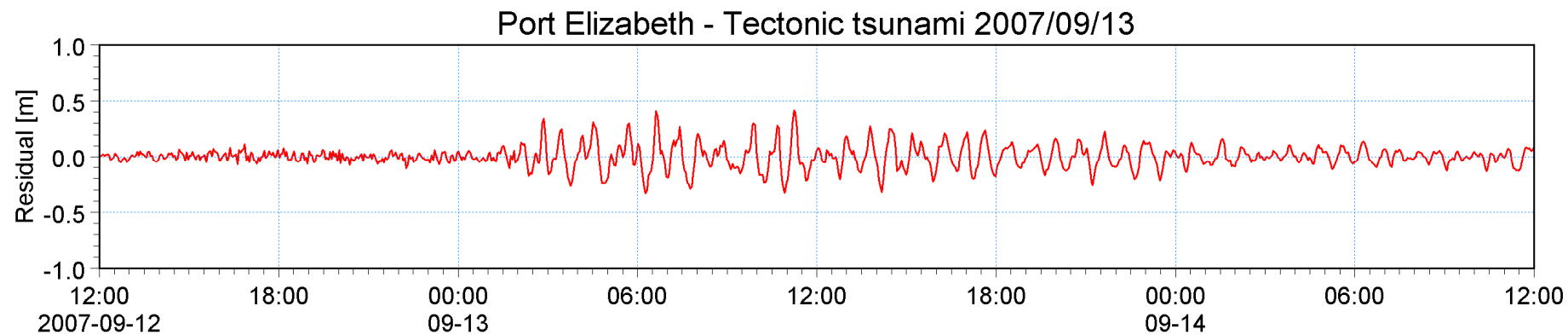
**Complete residuals of three minute data for 5 SANHO
tide gauge locations around South Africa**

Figure No.

4.2



X:\PRDW Projects\Current\SA (1010) Nuclear Sites SSRs\Working\Engineers\RLH\Meteotsunami\Data\Sites\ResidualComparisonEvents.png

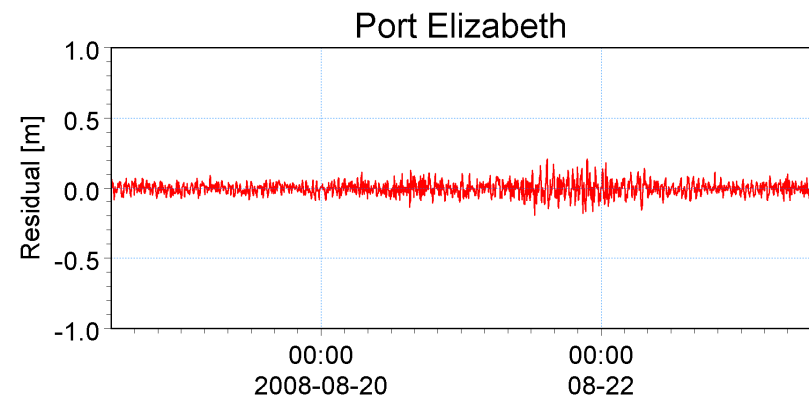
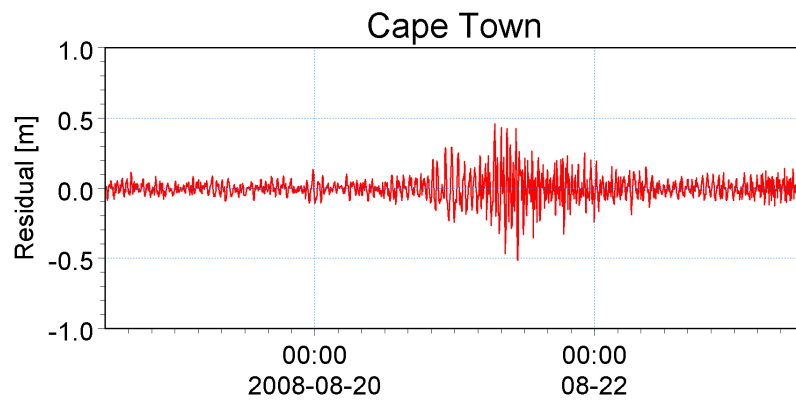
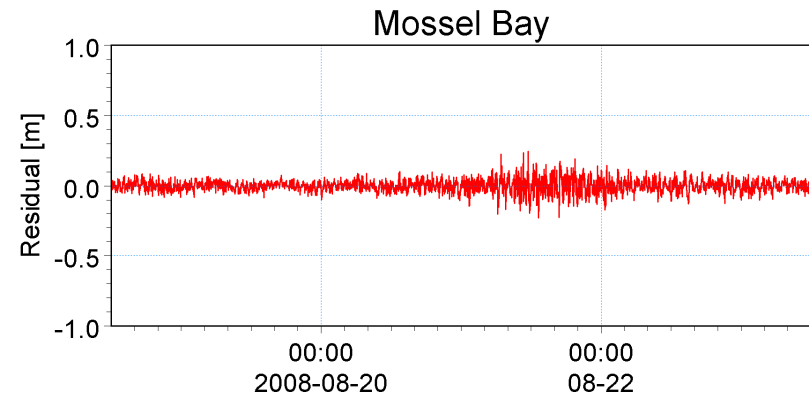
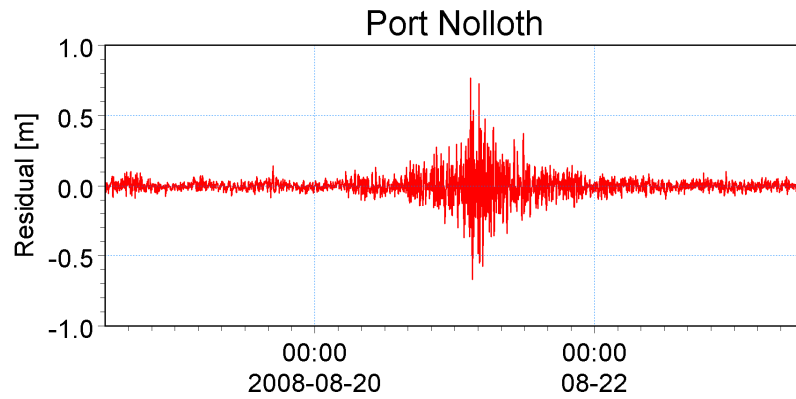


Title:

**Comparison of residual values for three long wave events
for 3 SANHO tide gauge sites around South Africa**

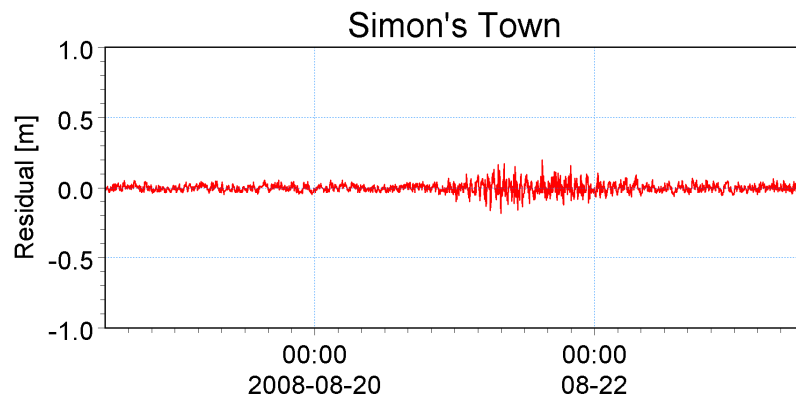
Figure No.

4.3



X:\PRDW Projects\Current\SA (1010) Nuclear Sites
SSRs\Working\Engineers\RLH\Meteotsunami\Data\Sites\ResidualComparison080819rt.png

X:\PRDW Projects\Current\SA (1010) Nuclear Sites
SSRs\Working\Engineers\RLH\Meteotsunami\Data\Sites\ResidualComparison080819rt.png

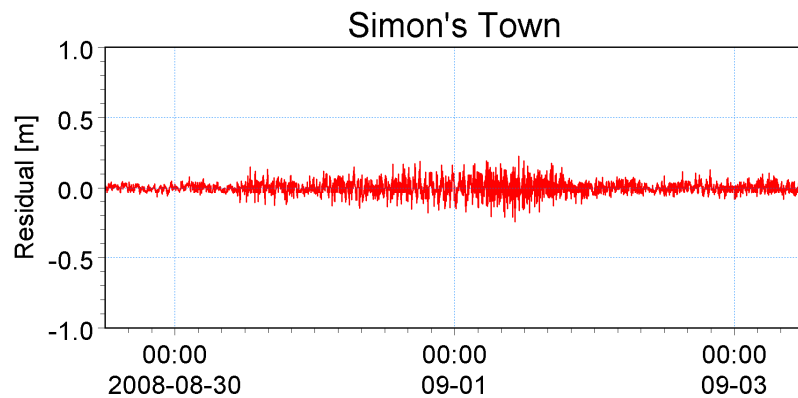
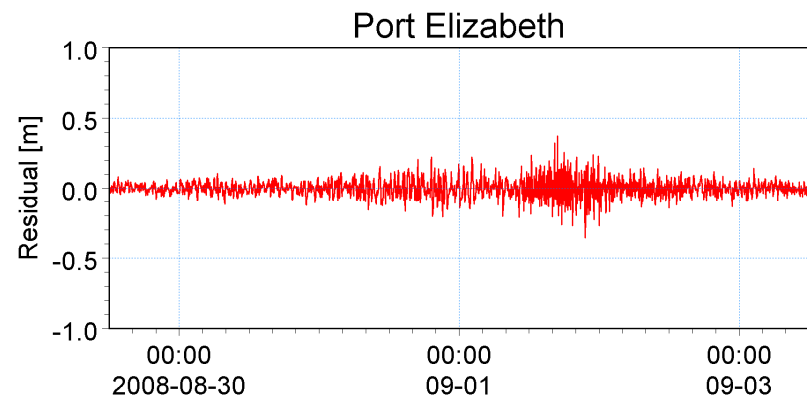
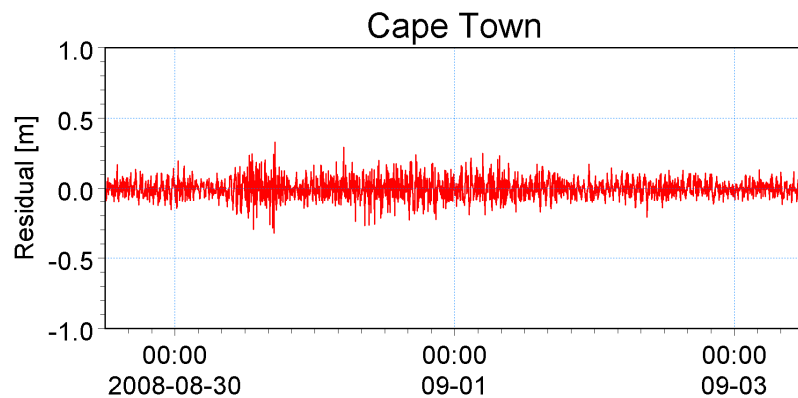
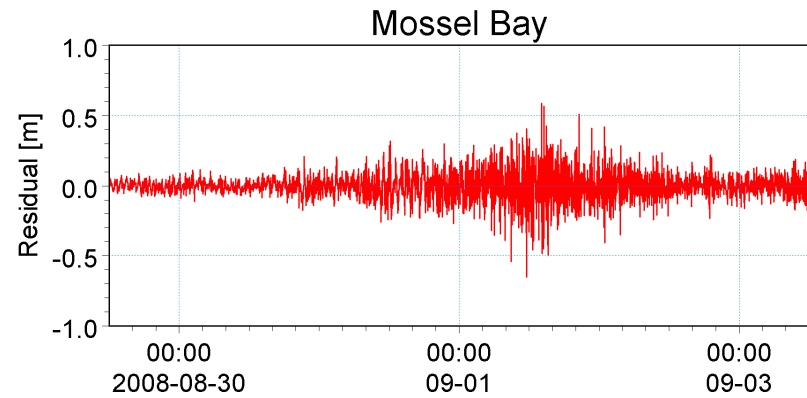
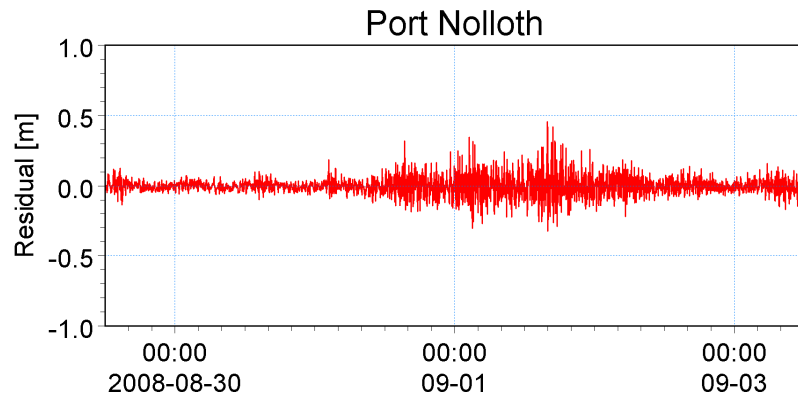


Title:

Comparison of residual values for a meteo-tsunami event
for 5 SANHO tide gauge sites around South Africa

Figure No.

4.4



X:\PRDW Projects\Current\SA (1010) Nuclear Sites
SSRs\Working\Engineers\RLH\Meteotsunami\Data\Sites\ResidualComparison0808311t.png

X:\PRDW Projects\Current\SA (1010) Nuclear Sites
SSRs\Working\Engineers\RLH\Meteotsunami\Data\Sites\ResidualComparison080831rt.png



Title:

Comparison of residual values for a bound long wave event
for 5 SANHO tide gauge sites around South Africa

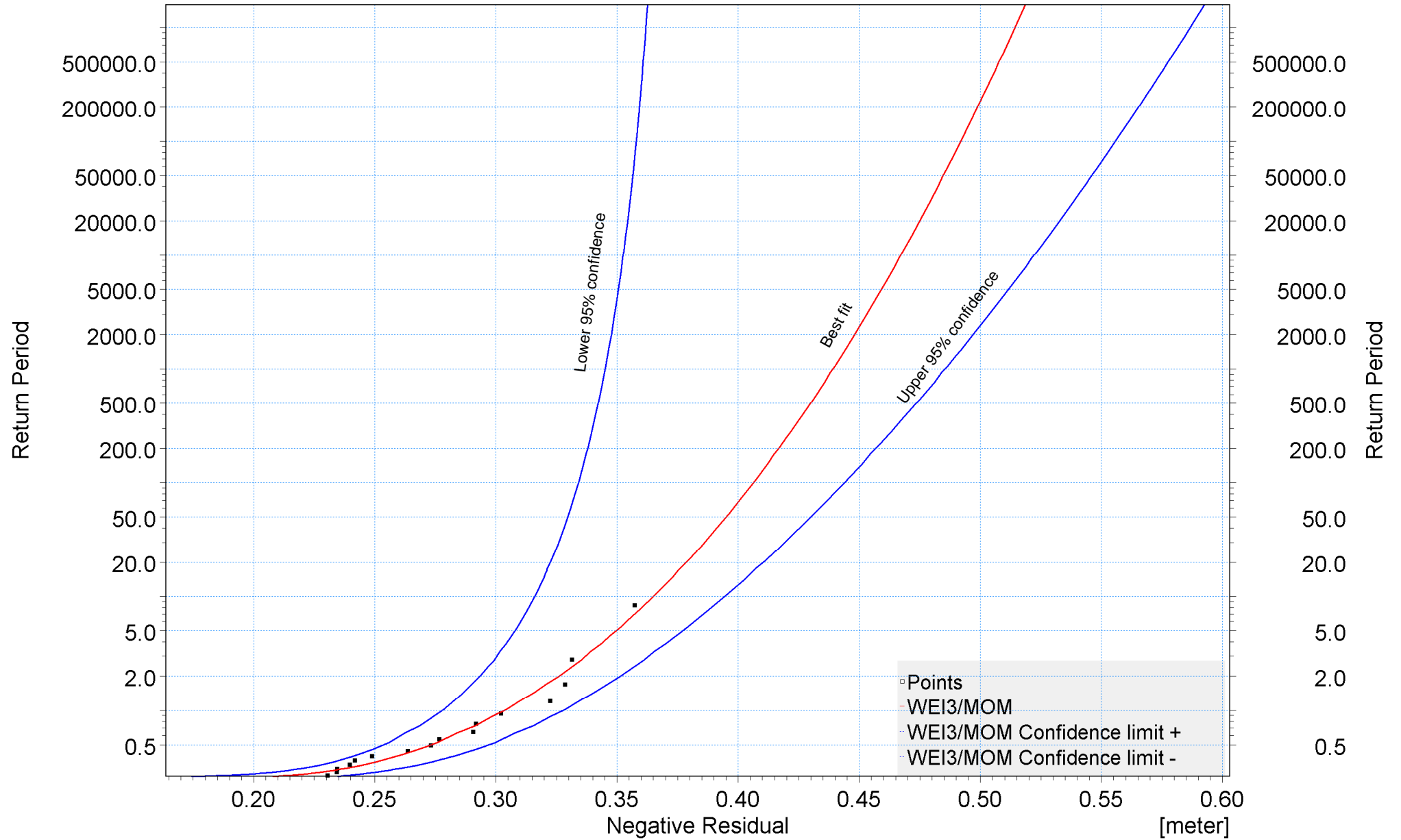
Figure No.

4.5

[Years]

X:\PRDW Projects\Current\SA (1010) Nuclear Sites SSRs\Working\Engineers\RLH\Meteotsunami\Data\Sites\PE\Processed\EVA\EVA02.png

[Years]



Title:

Extreme value analysis of negative long wave residuals at Port Elizabeth

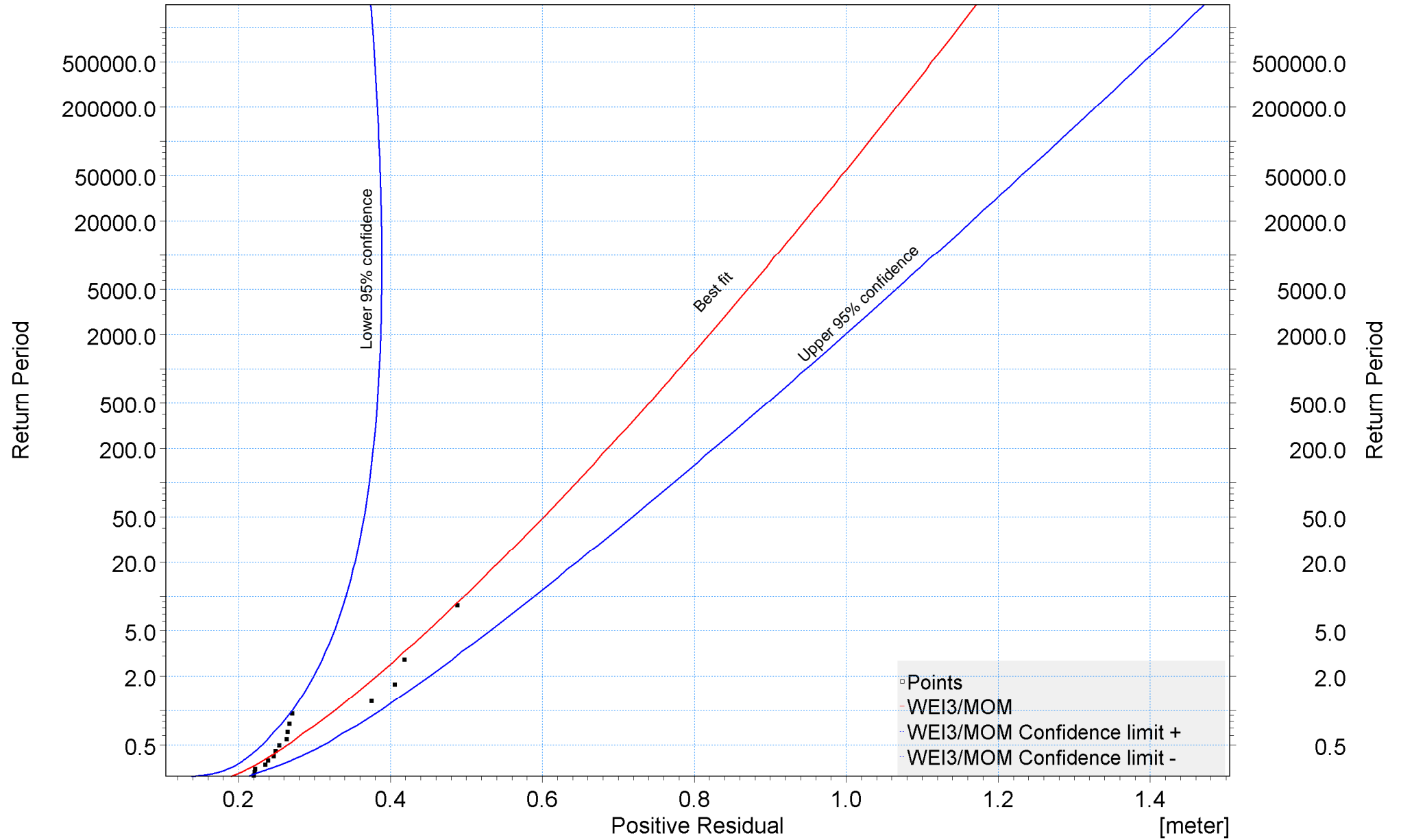
Figure No.

4.6

[Years]

X:\PRDW Projects\Current\SA (1010) Nuclear Sites SSRs\Working\Engineers\RLH\Meteotsunami\Data\Sites\PE\Processed\EVA\EVA01.png

[Years]

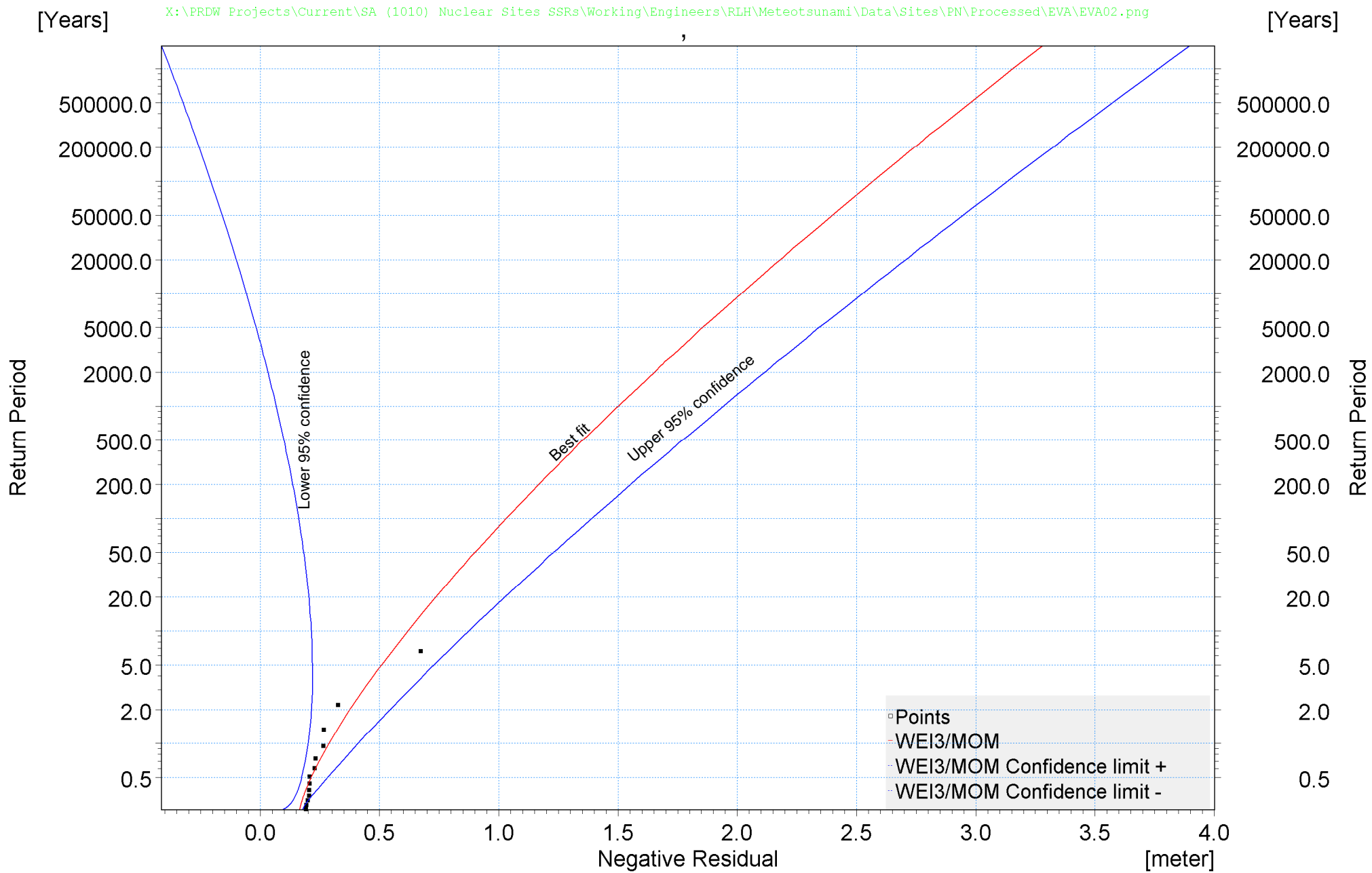


Title:

Extreme value analysis of positive long wave residuals at Port Elizabeth

Figure No.

4.7

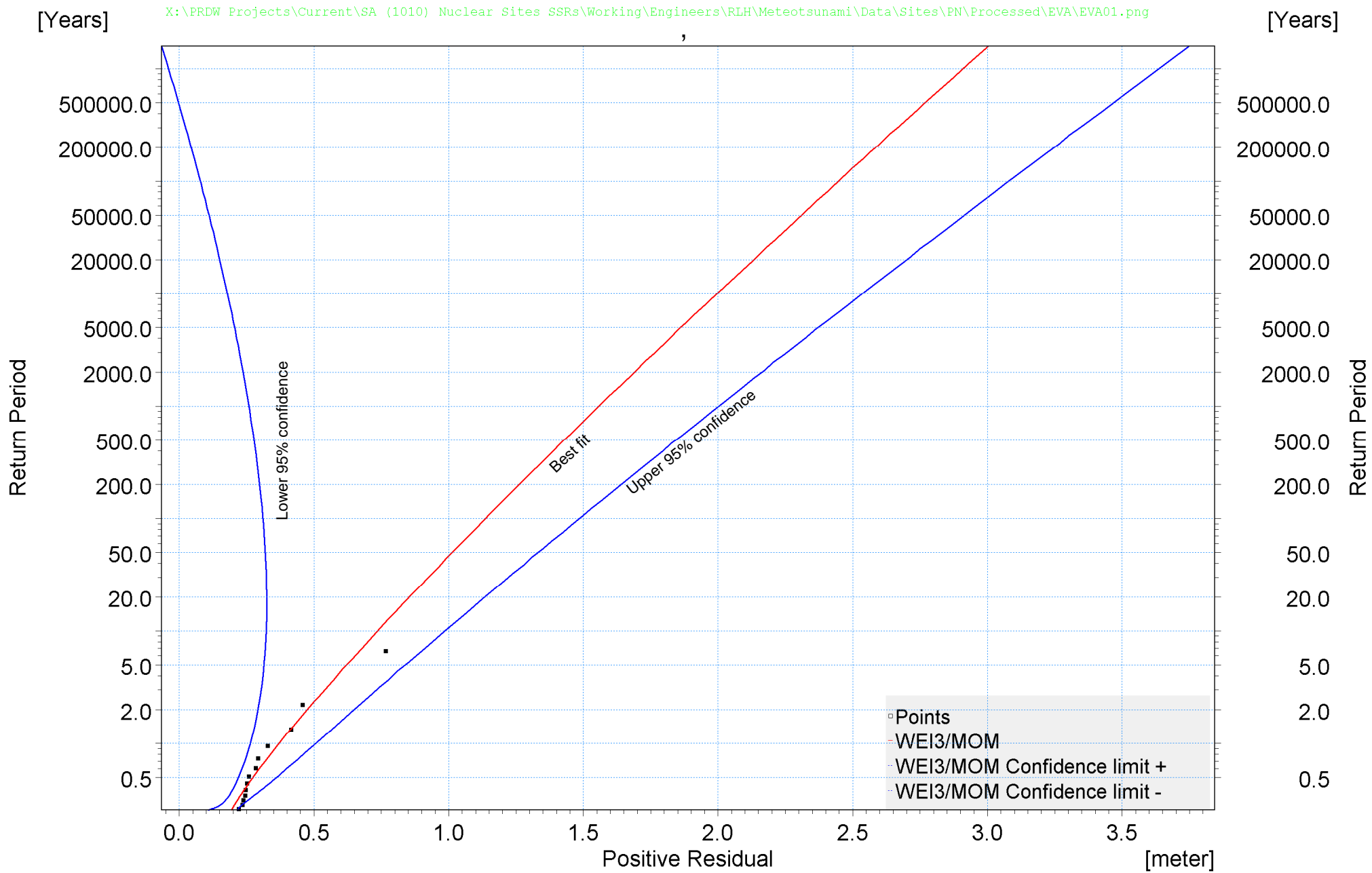


Title:

Extreme value analysis of negative long wave residuals at Port Nolloth

Figure No.

4.8

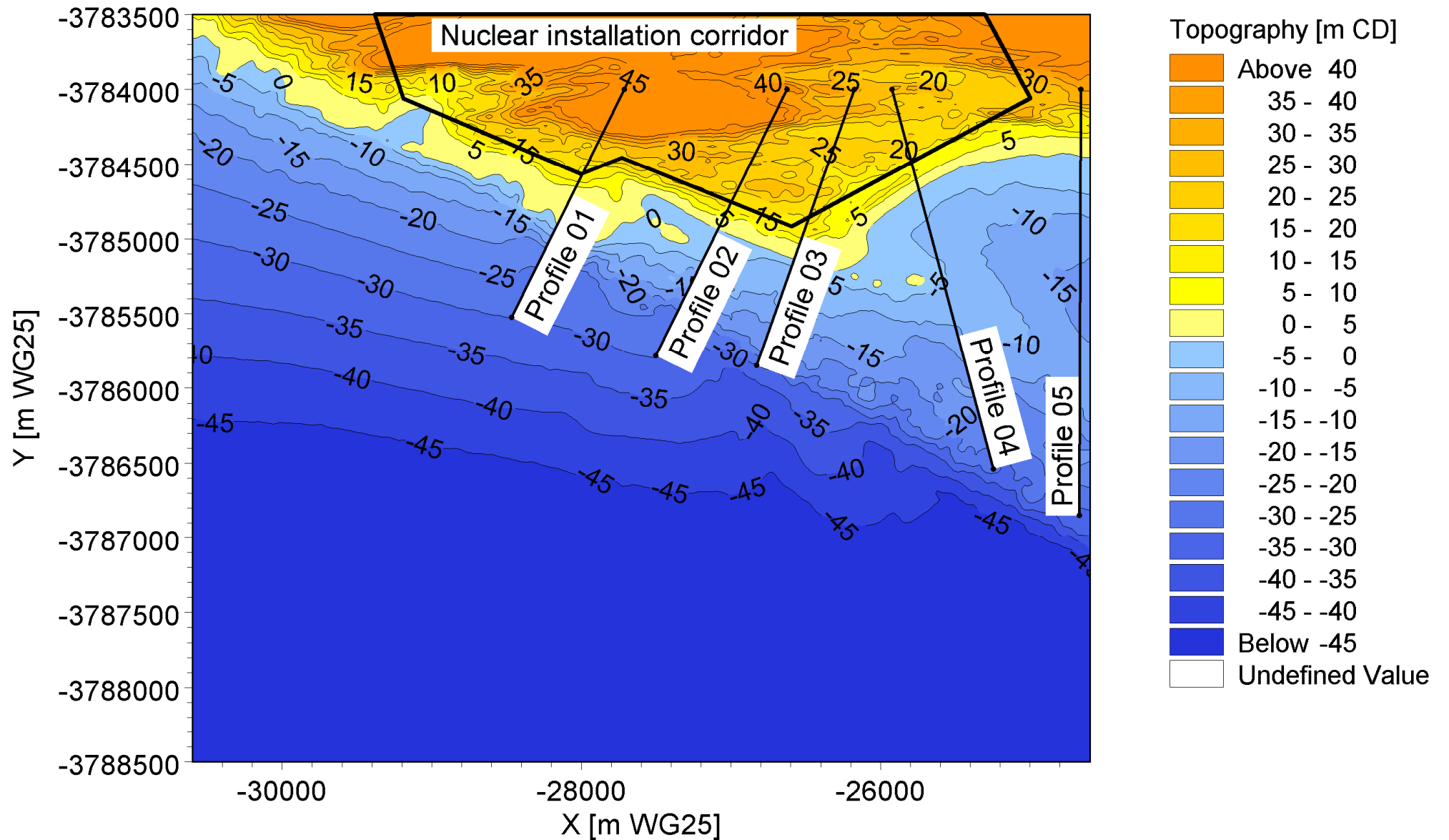


Title:

Extreme value analysis of positive long wave residuals at Port Nolloth

Figure No.

4.9



X:\PRDW Projects\Current\SA (1010) Nuclear Sites
 SSRs\Working\Engineers\RLH\CoastalEngineeringModelling\Thyspunt\Data\Bathy\Thyspunt_WG25_CD_AutoCad_ModelledProfiles.png



Title:

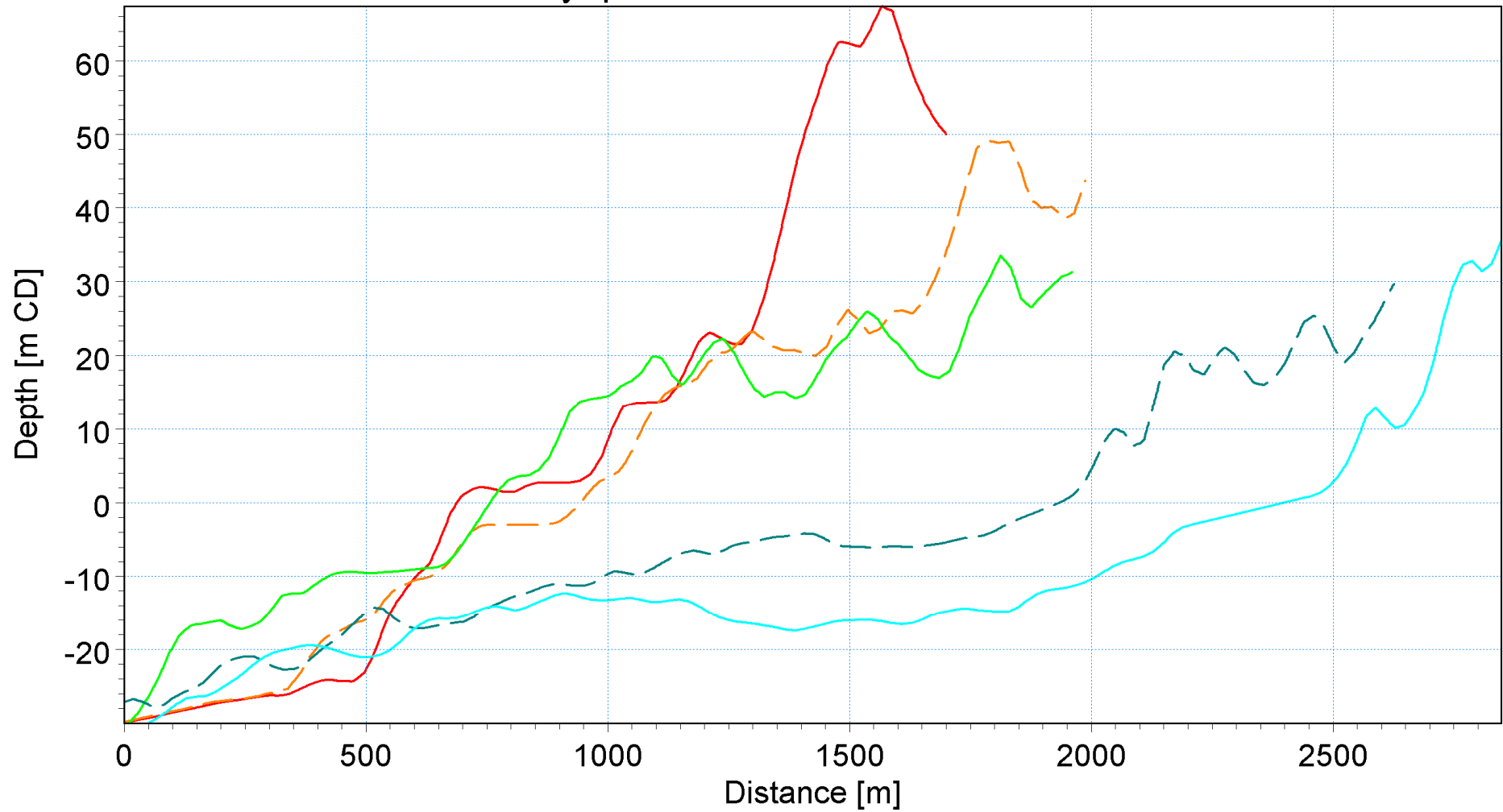
Run-up calculations: Plan view of profiles used

Figure No.

4.10

Profile01 [m] ——— X:\PRDW Projects\Current\SA (1010) Nuclear Sites
 Profile02 [m] - - - - - SSRs\Working\Engineers\RLH\CoastalEngineeringModelling\Thyspunt\Data\RunUpProfiles\Profiles.png
 Profile03 [m] ———
 Profile04 [m] - - - - -
 Profile05 [m] ———

Thyspunt Beach Profile Sections

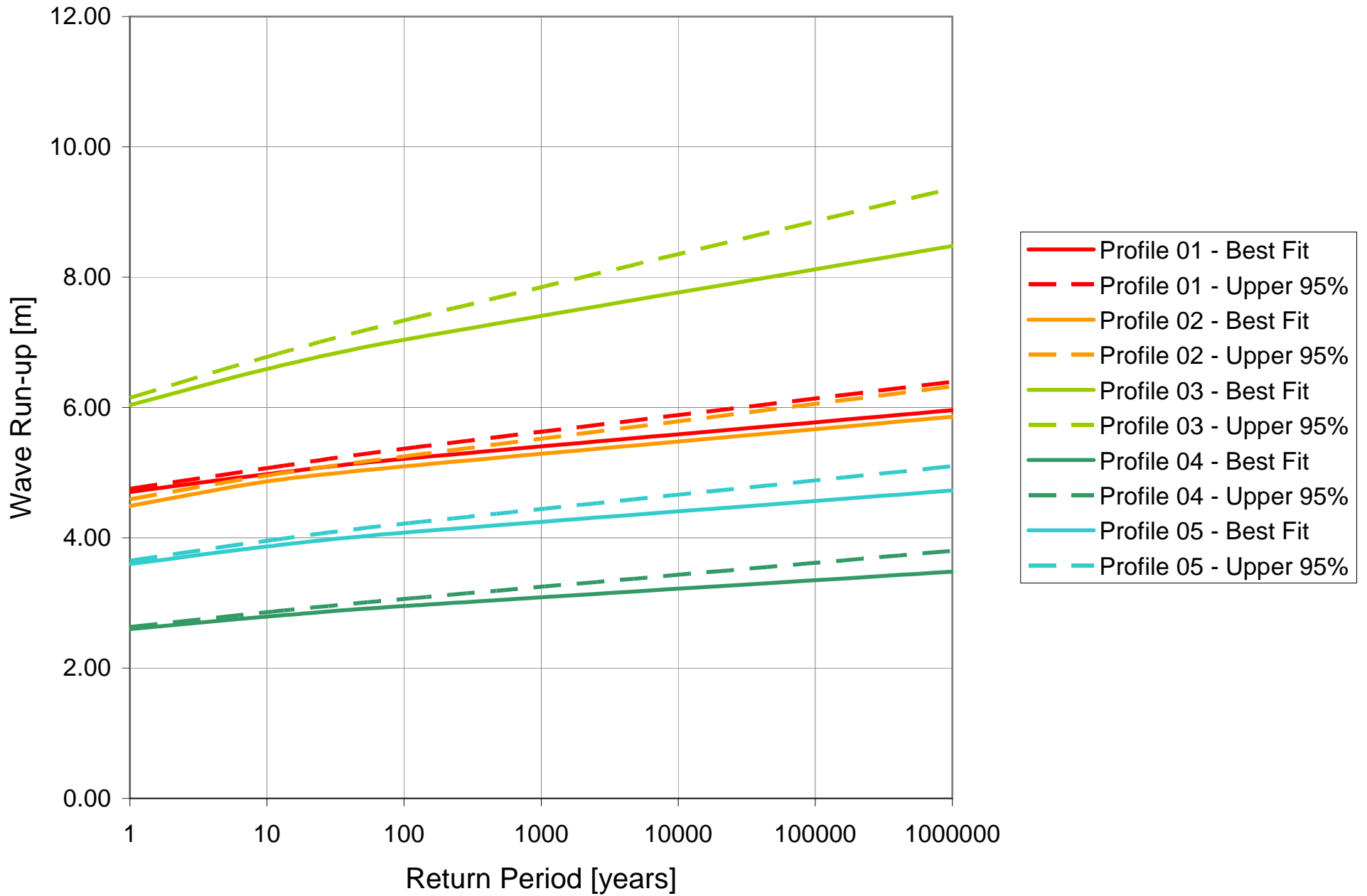


Title:

Selected coastline profiles for run-up calculations

Figure No.

4.11

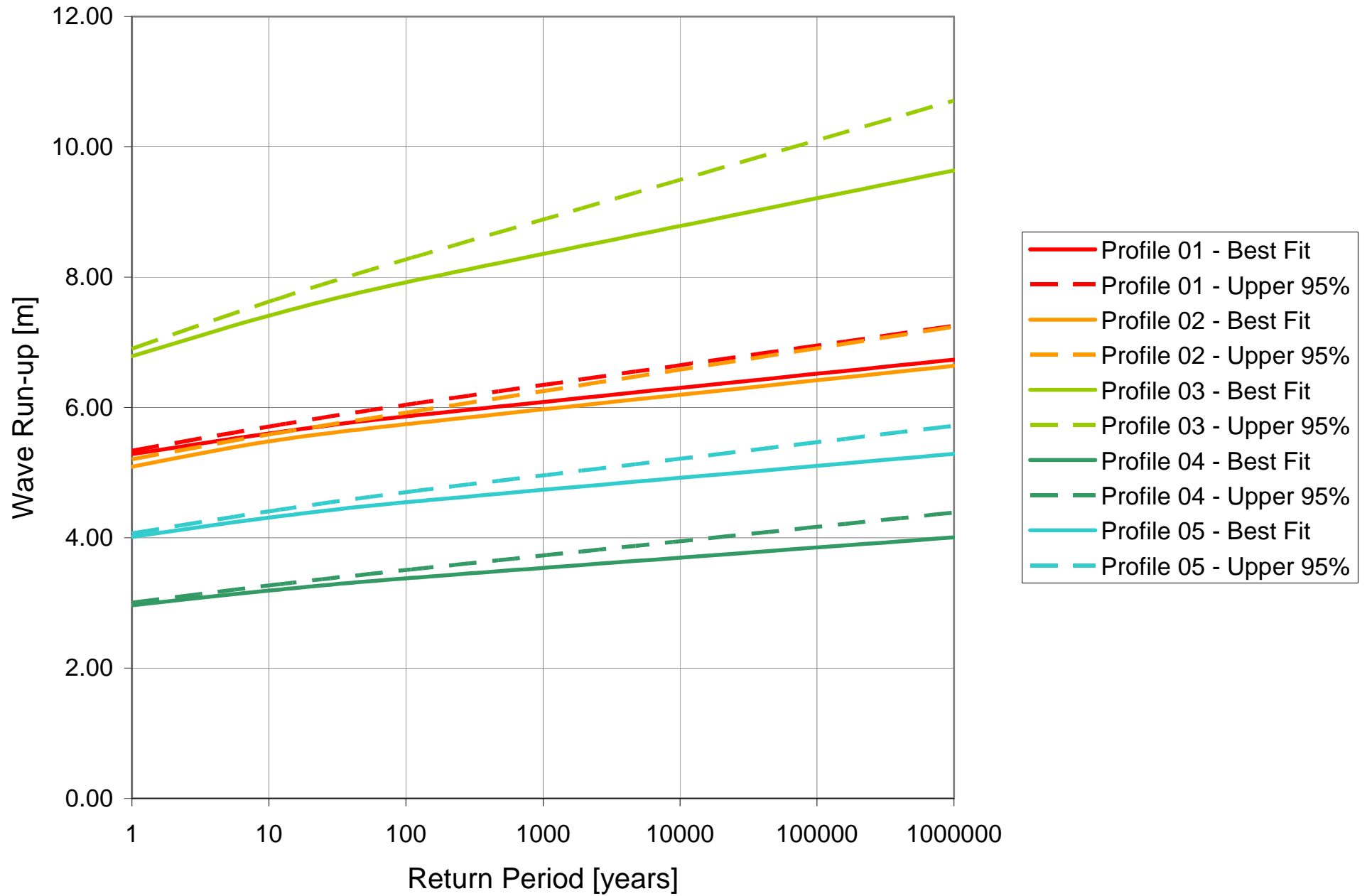


Title:

Extreme high water level beach run-up - Excluding climate change

Figure No.

4.12



Title:

Extreme high water level beach run-up - Including climate change

Figure No.

4.13

Plate deployed 3 m below water surface



Plate deployed 8 m below water surface



Plates are asbestos with dimensions 20 cm x 20 cm.
Water depth is 10 m.

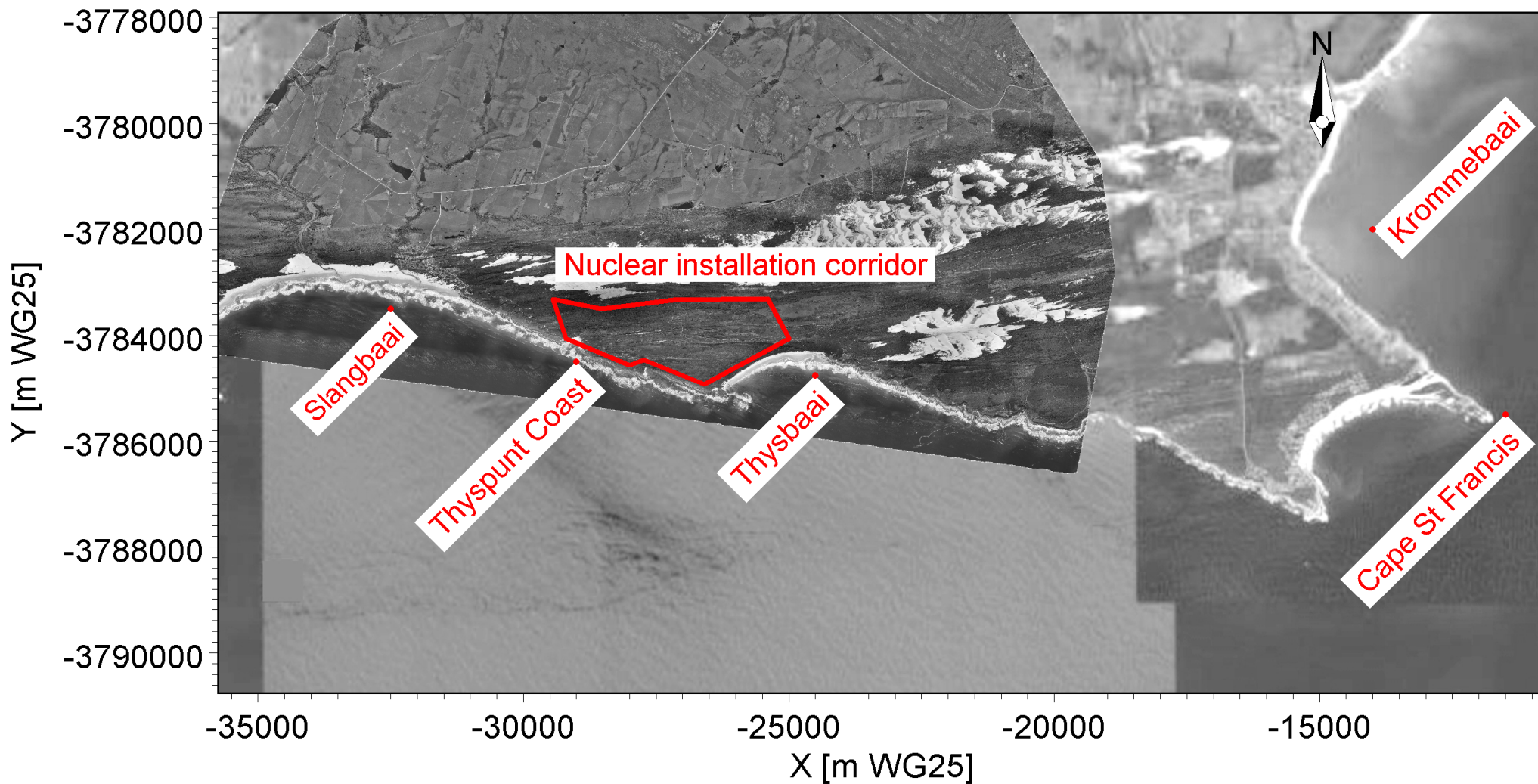


Title:

Biofouling plates recovered from Thyspunt

Figure No.

5.1

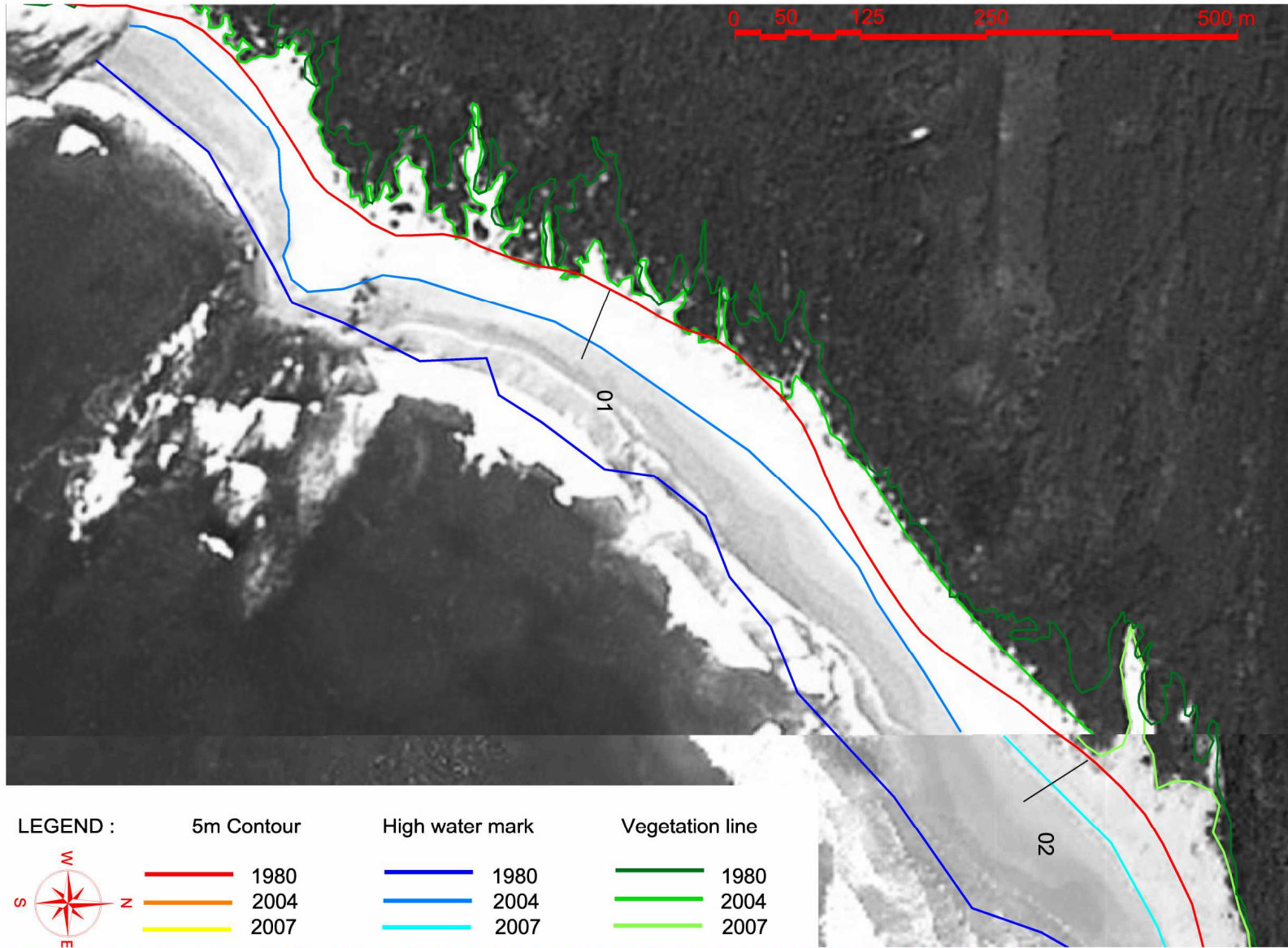


Title:

Combined image of the Thyspunt site showing beach locations used for the coastline study

Figure No.

7.1



X:\PRDW Projects\Current\SA (1010) Nuclear Sites SSRs\Working\Engineers\RLH\Coastline\Thyspunt\Scaled\Coastline_Contours_Comparison_01.png

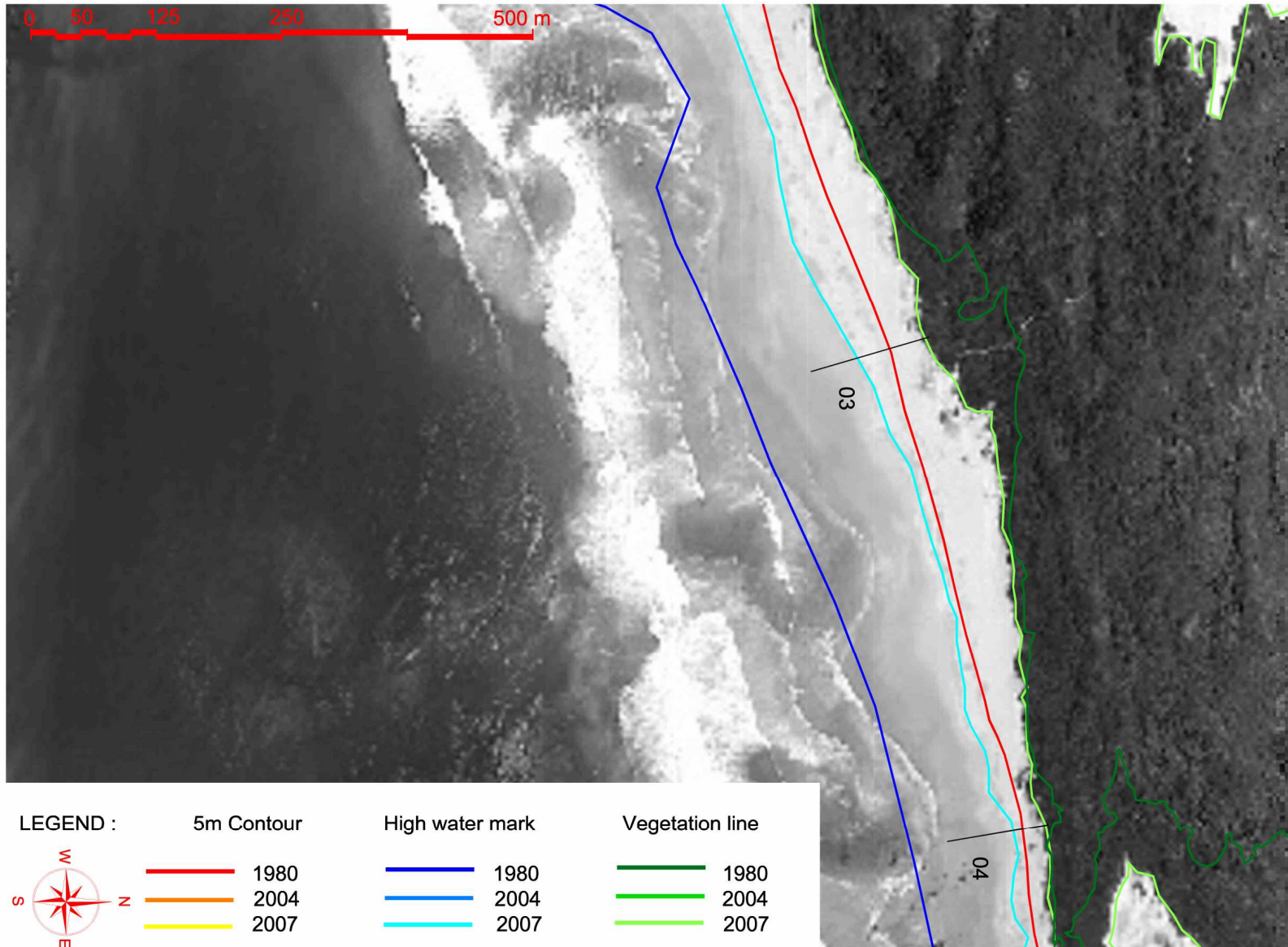


Title:

**Plan view of historical coastline trends from aerial photographs
Slangbaai**

Figure No.

7.2



X:\PRDW Projects\Current\SA (1010) Nuclear Sites SSRs\Working\Engineers\RLH\Coastline\Thyspunt\Scaled\Coastline_Contours_Comparison_02.png

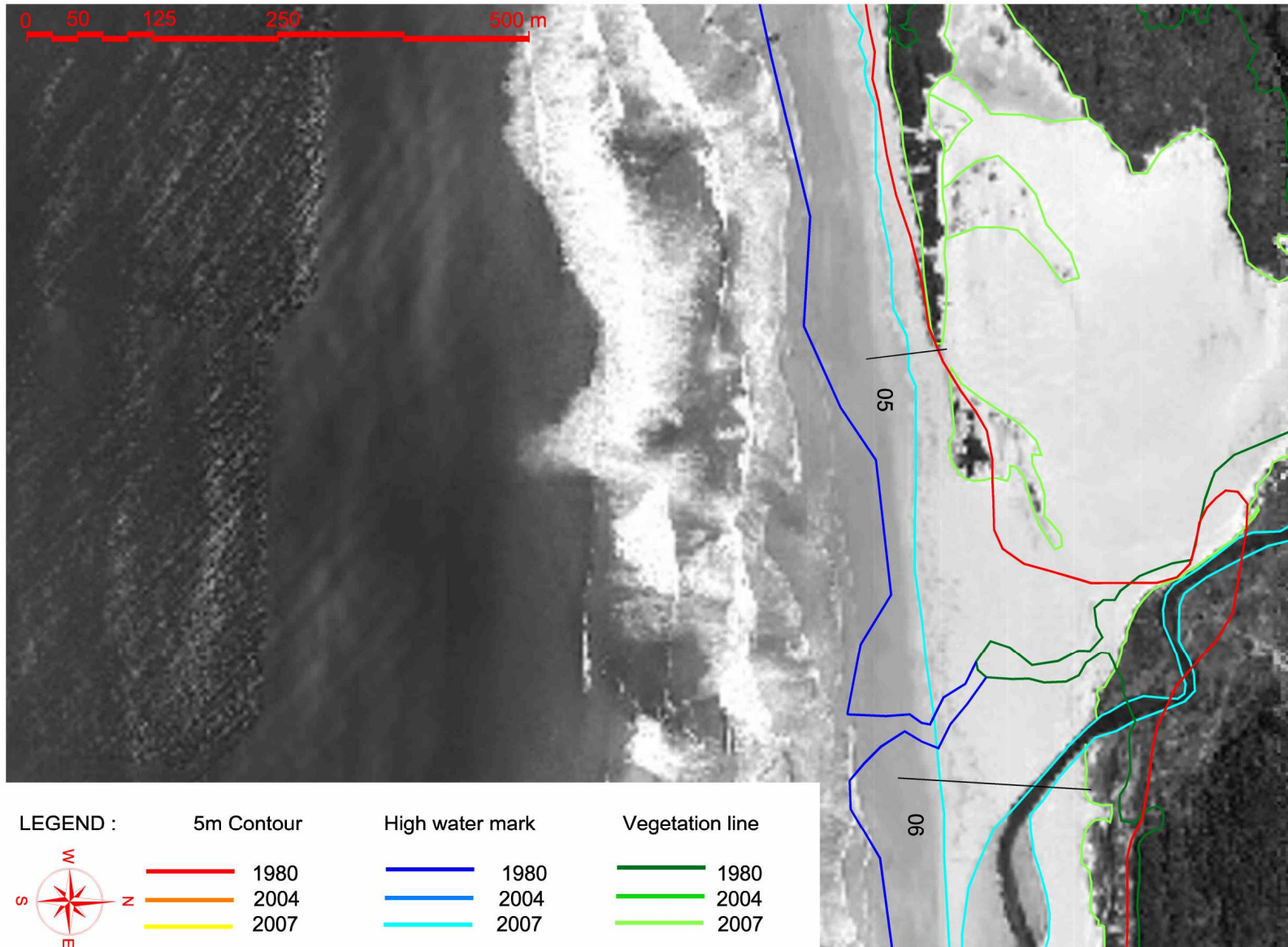


Title:

**Plan view of historical coastline trends from aerial photographs
Slangbaai**

Figure No.

7.3



X:\PRDW Projects\Current\SA (1010) Nuclear Sites SSRs\Working\Engineers\RLH\Coastline\Thyspunt\Scaled\Coastline_Contours_Comparison_03.png

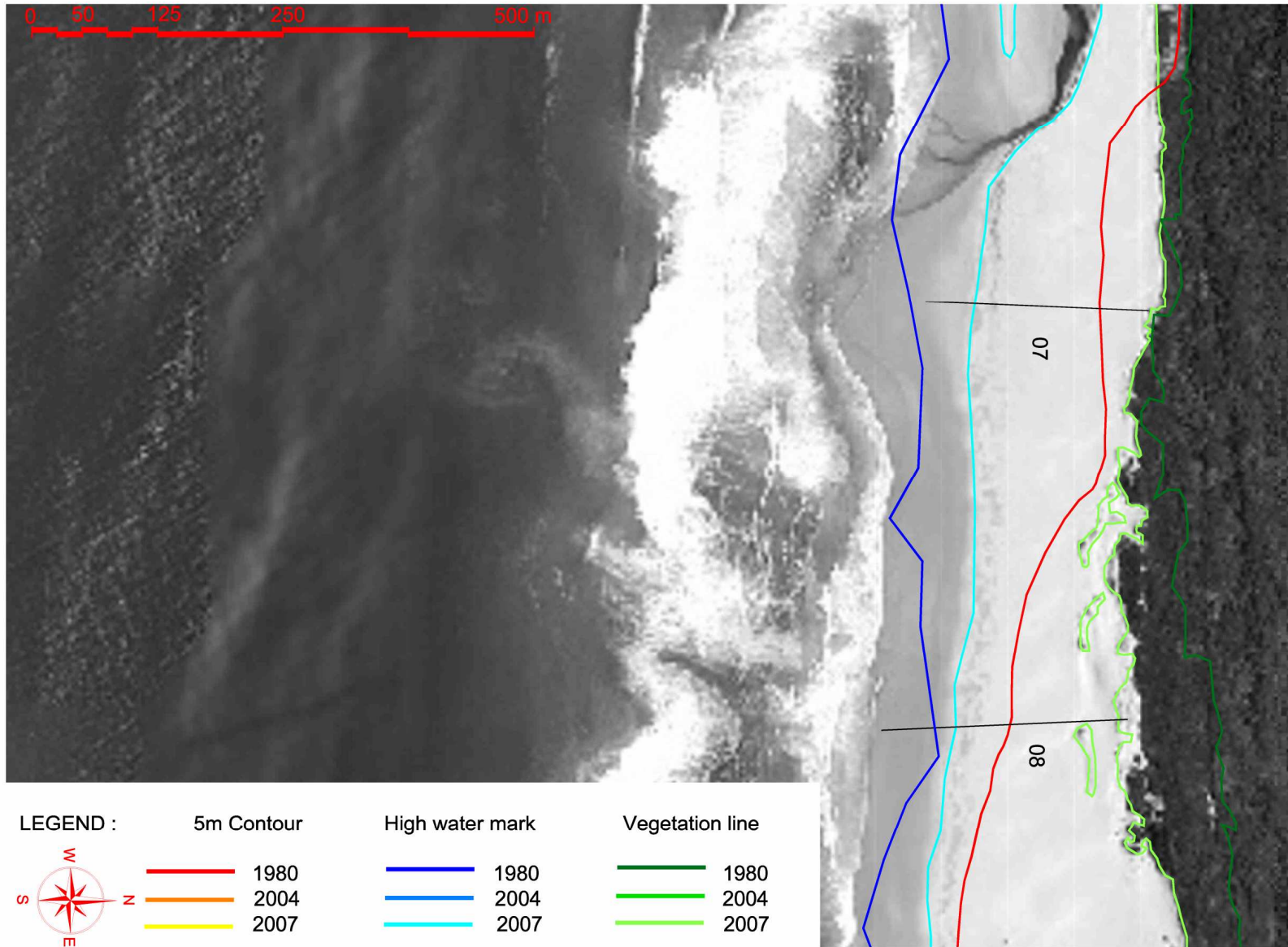


Title:

Plan view of historical coastline trends from aerial photographs
Slangbaai

Figure No.

7.4

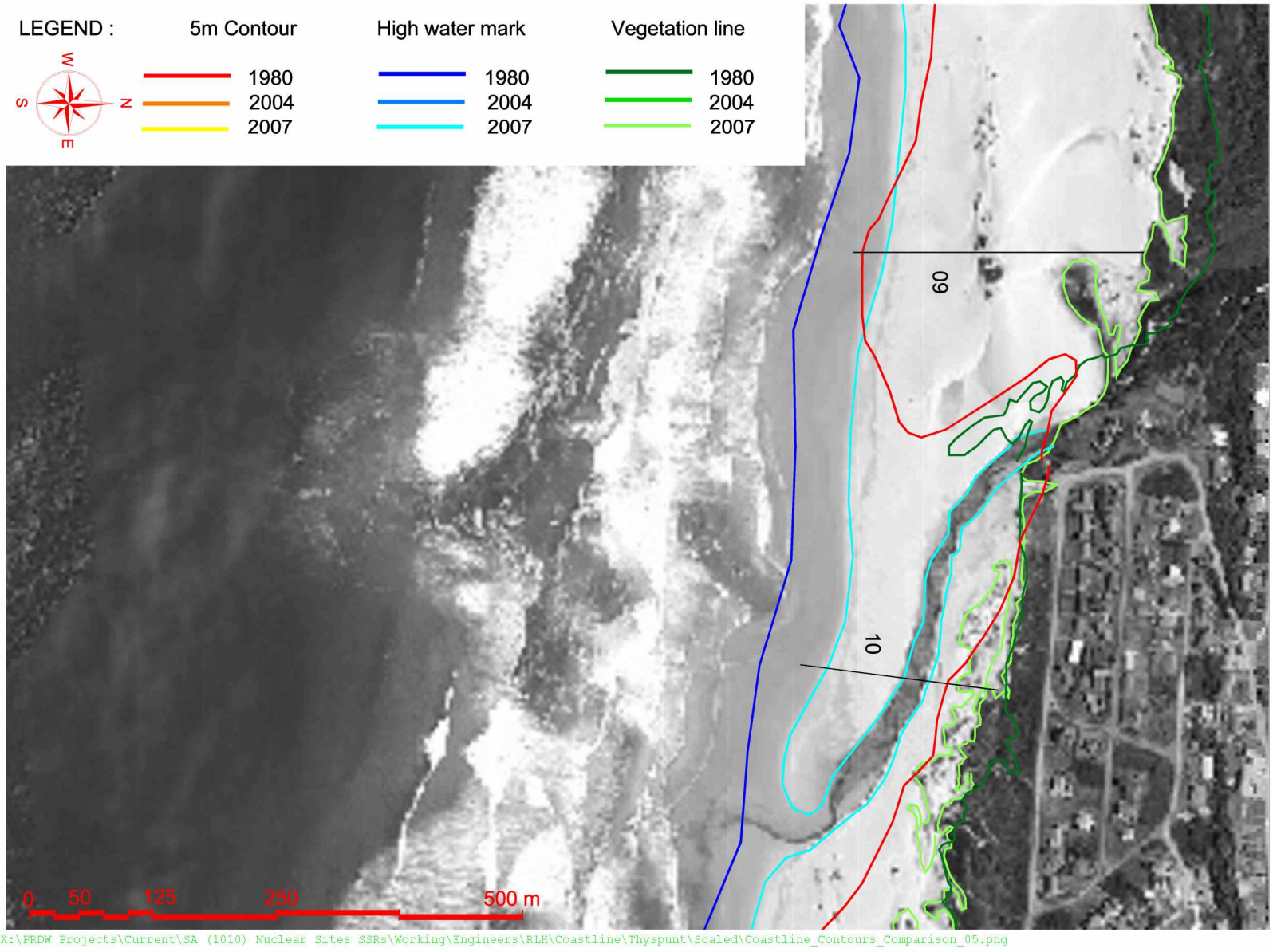


Title:

Plan view of historical coastline trends from aerial photographs
Slangbaai

Figure No.

7.5

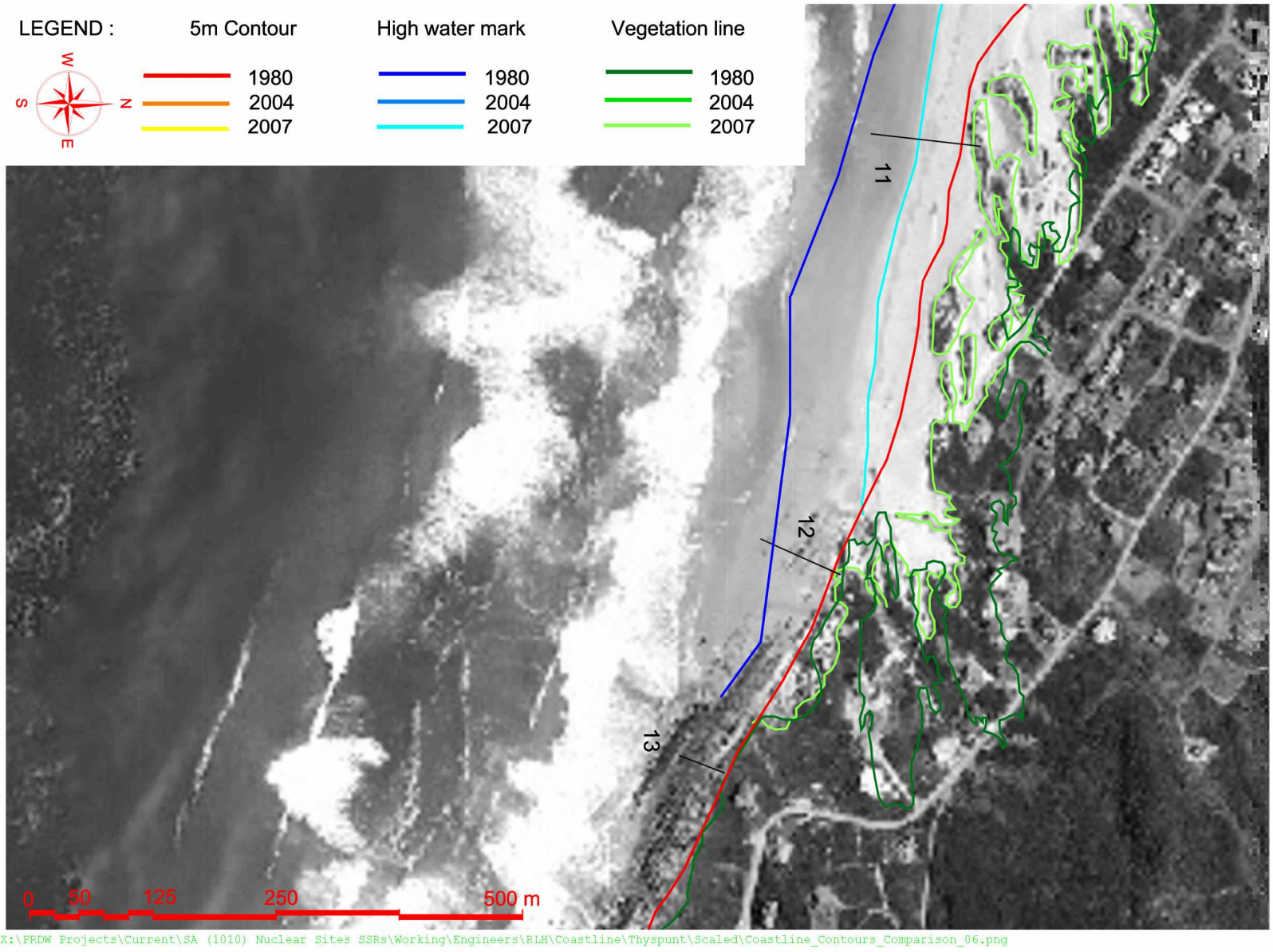


Title:

**Plan view of historical coastline trends from aerial photographs
Slangbaai**

Figure No.

7.6

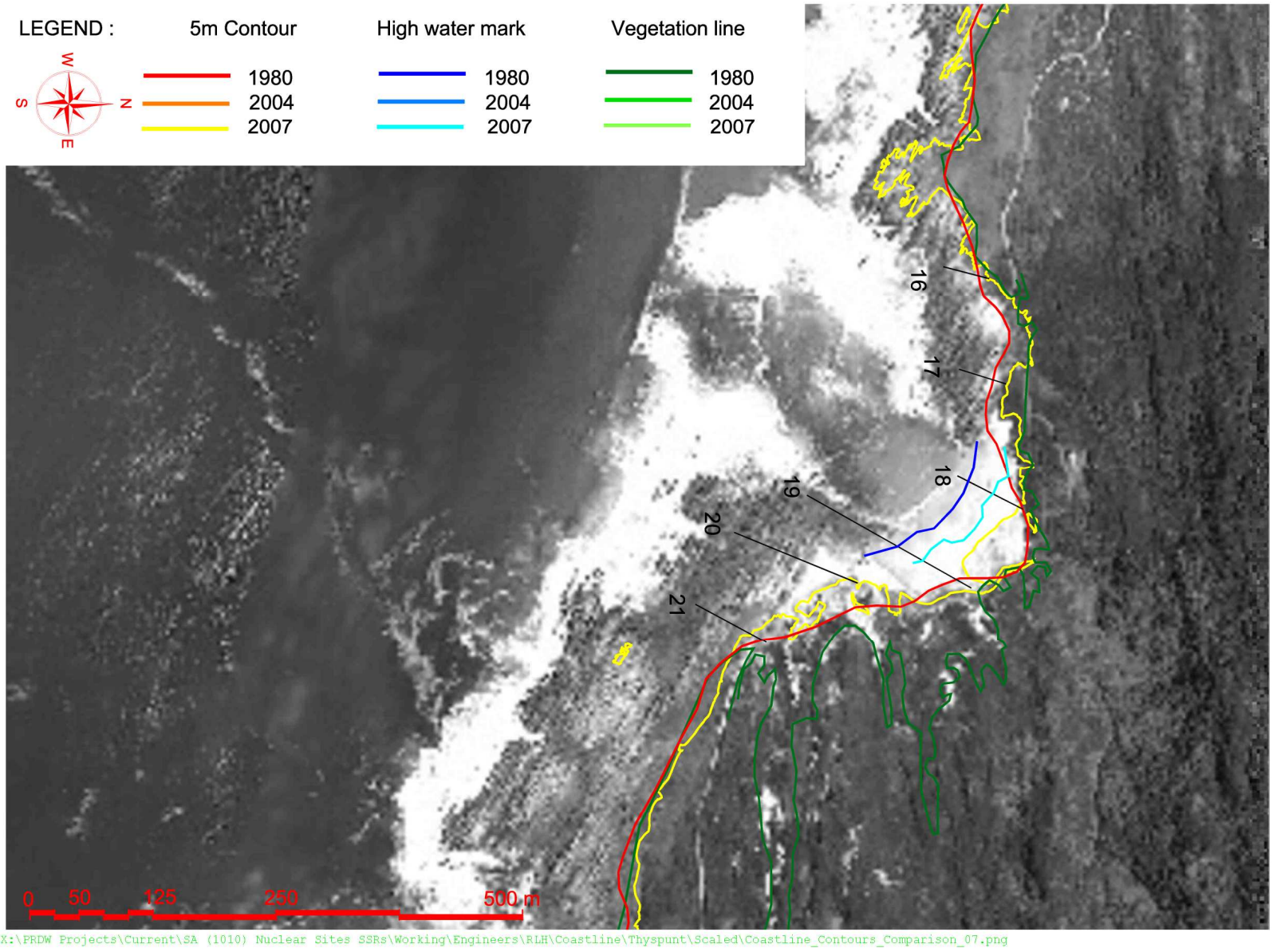


Title:

**Plan view of historical coastline trends from aerial photographs
Slangbaai**

Figure No.

7.7

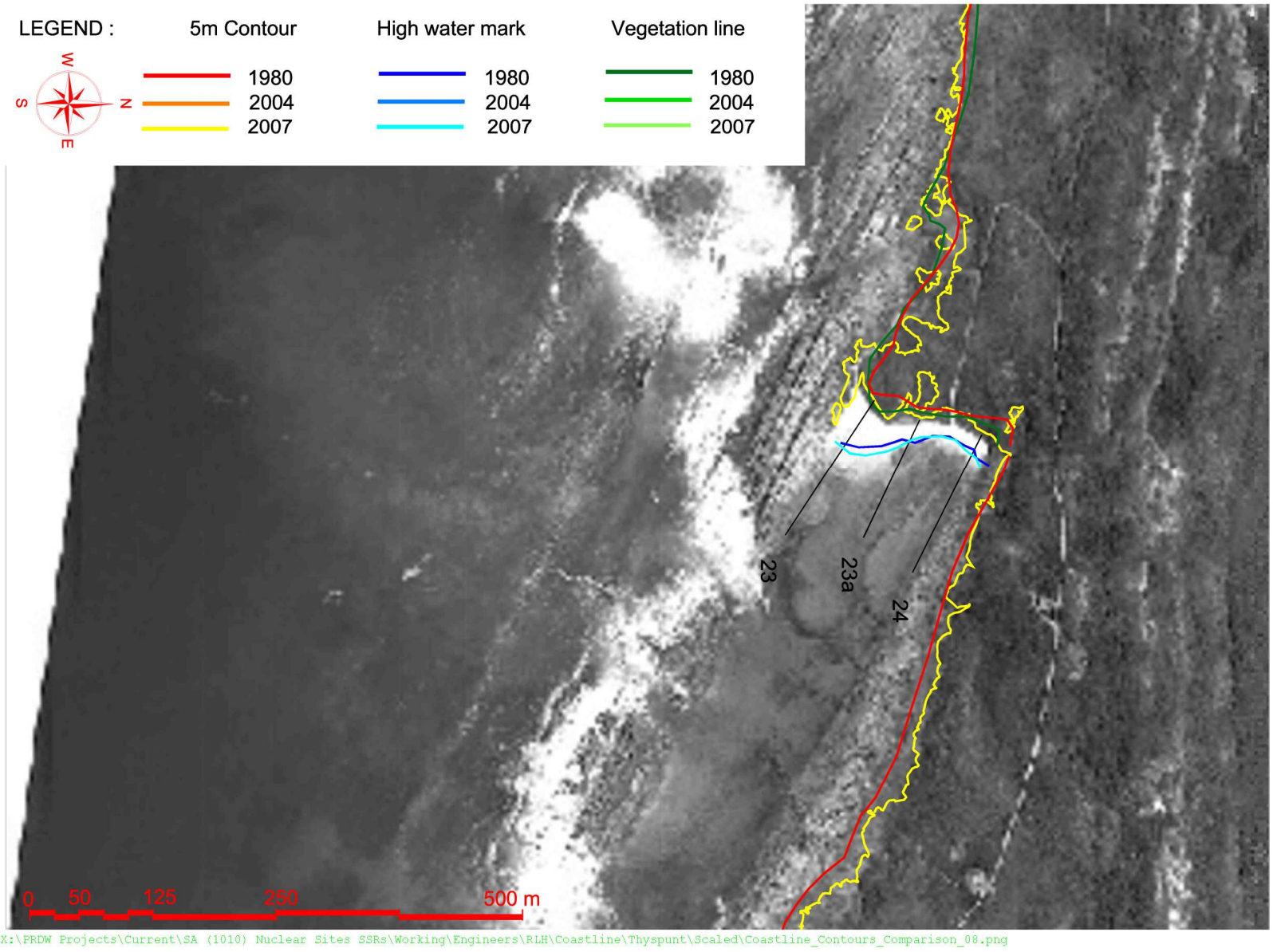


Title:

**Plan view of historical coastline trends from aerial photographs
Thyspunt coast**

Figure No.

7.8

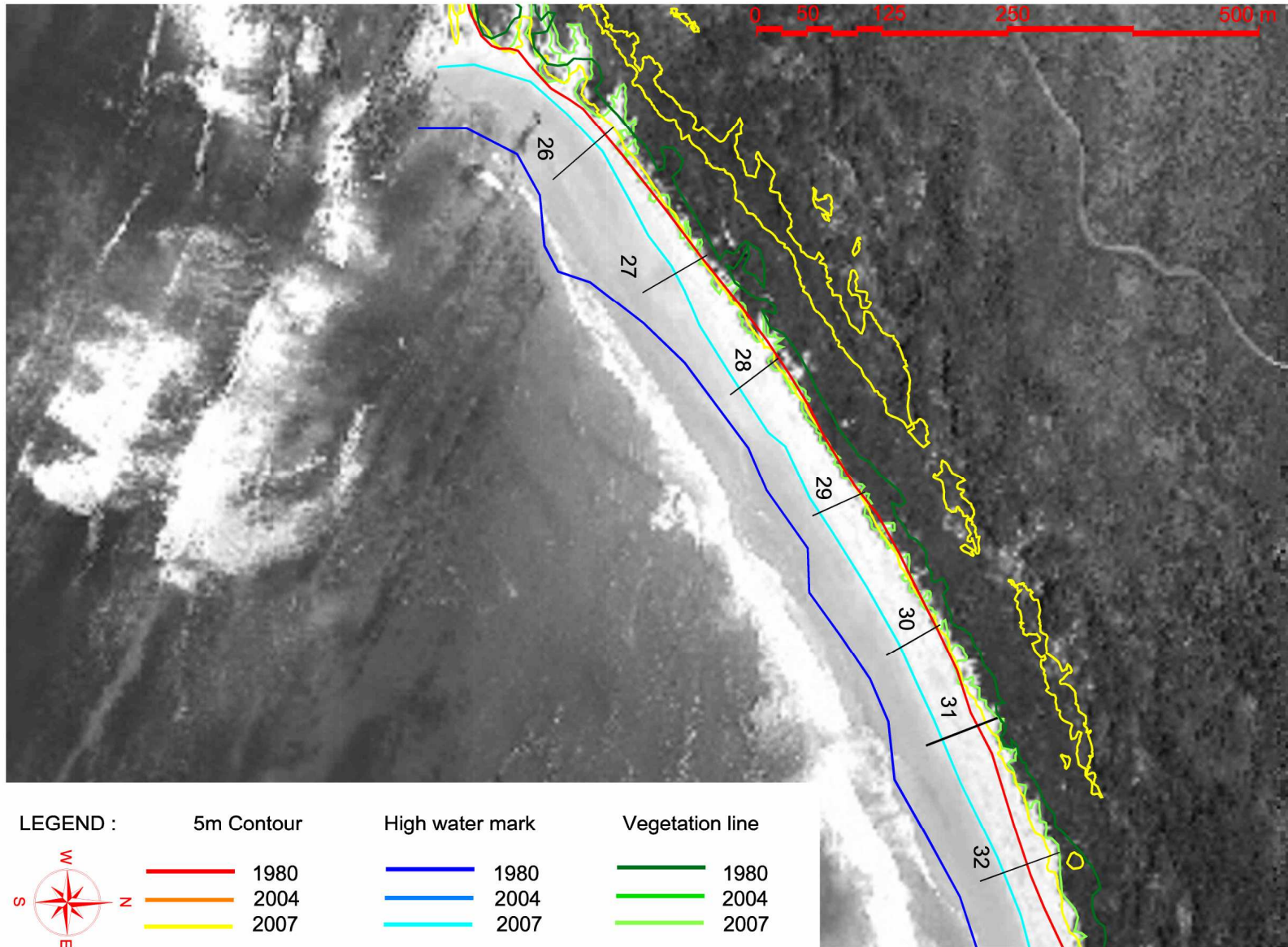


Title:

**Plan view of historical coastline trends from aerial photographs
Thyspunt coast**

Figure No.

7.9

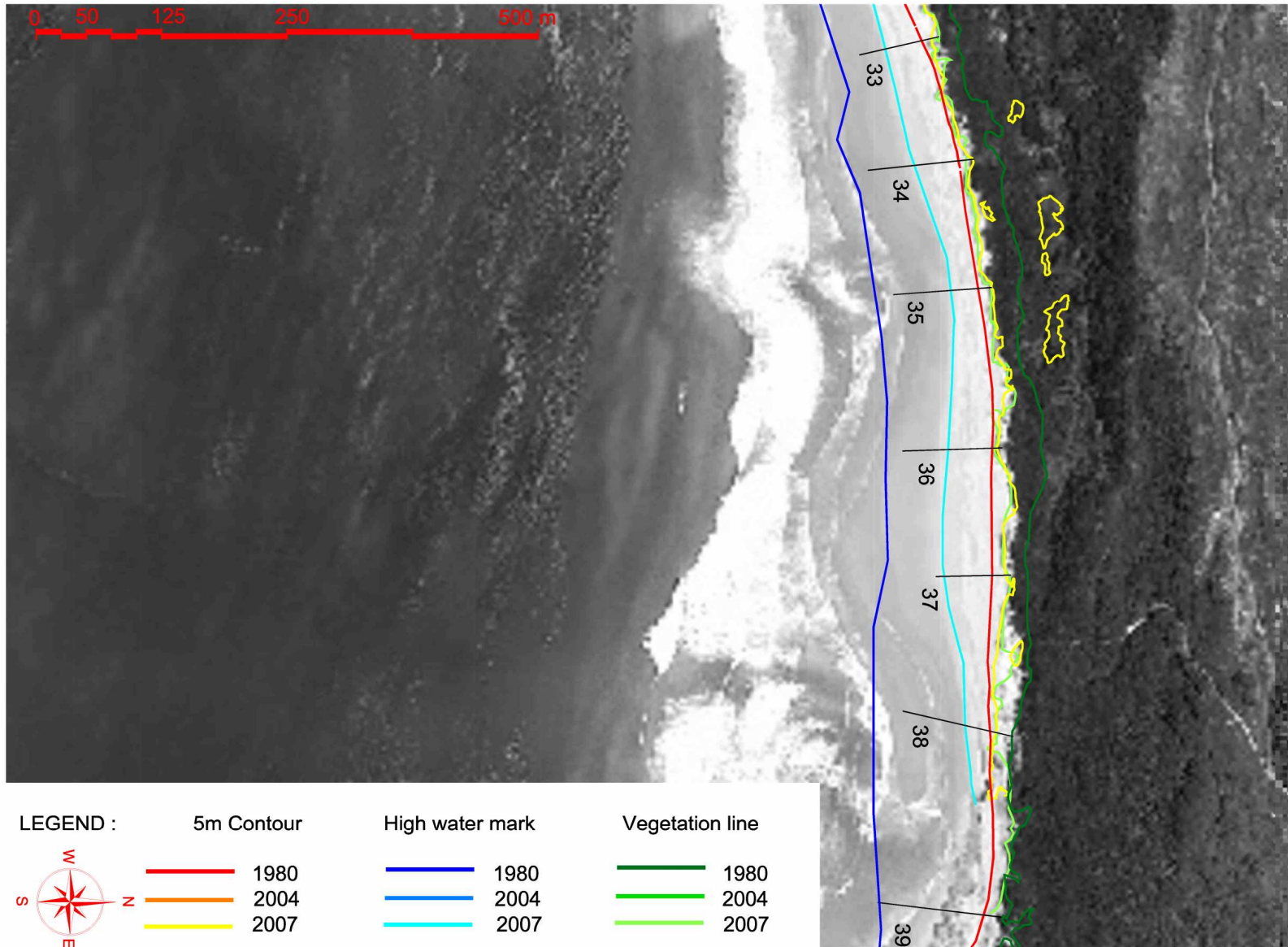


Title:

**Plan view of historical coastline trends from aerial photographs
Thysbaai**

Figure No.

7.10

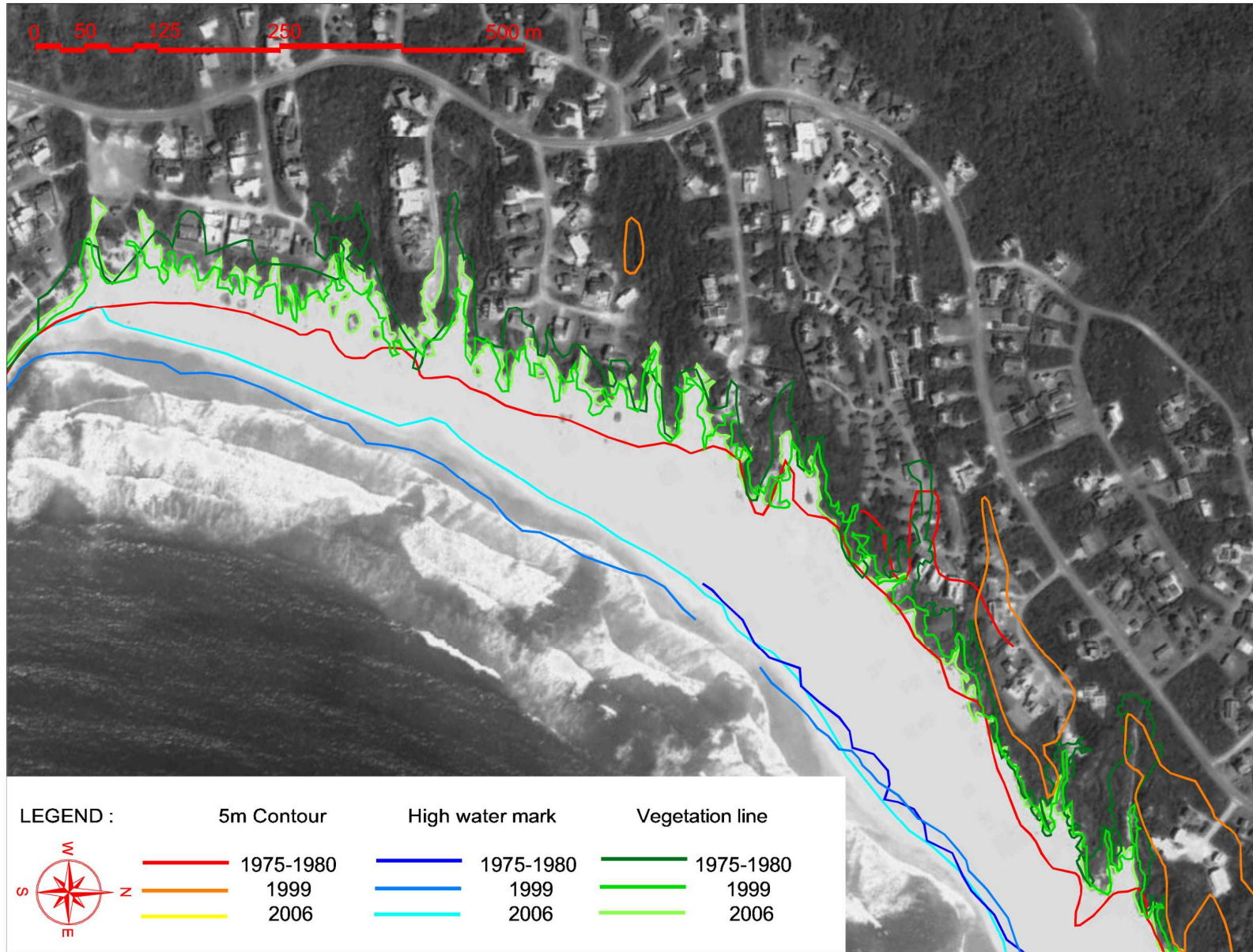


Title:

**Plan view of historical coastline trends from aerial photographs
Thysbaai**

Figure No.

7.11

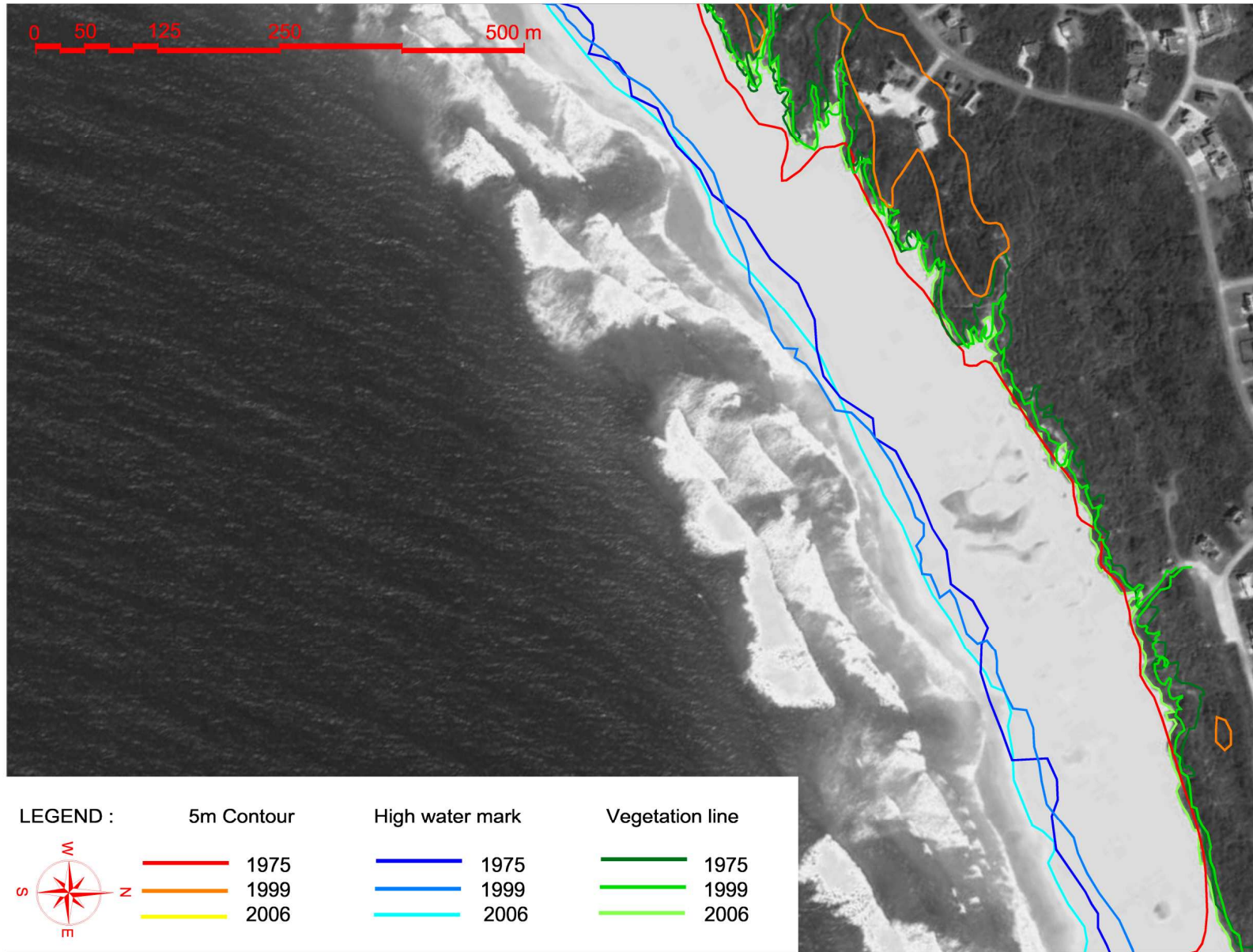


Title:

Plan view of historical coastline trends from aerial photographs
Cape St Francis

Figure No.

7.12

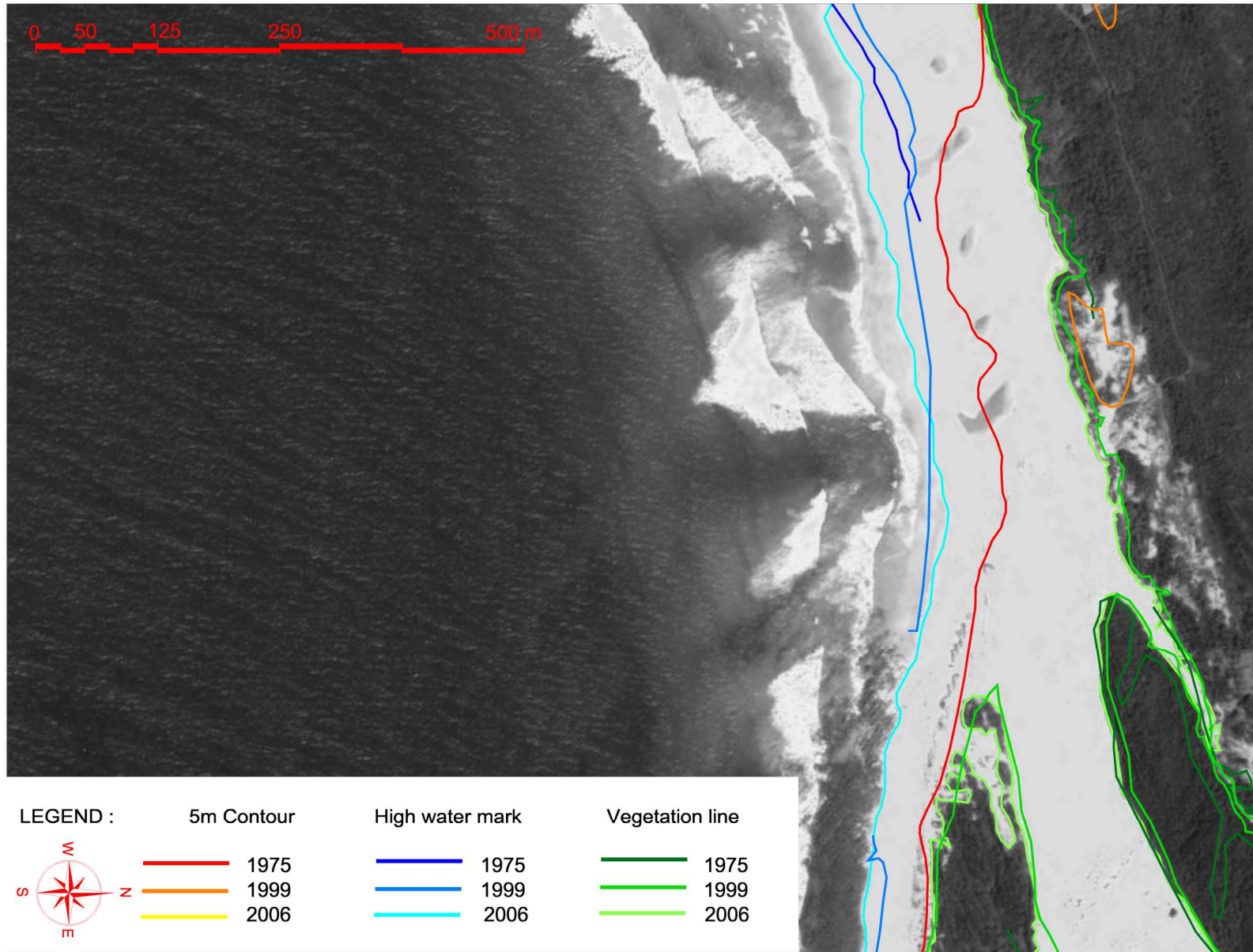


Title:

Plan view of historical coastline trends from aerial photographs
Cape St Francis

Figure No.

7.13

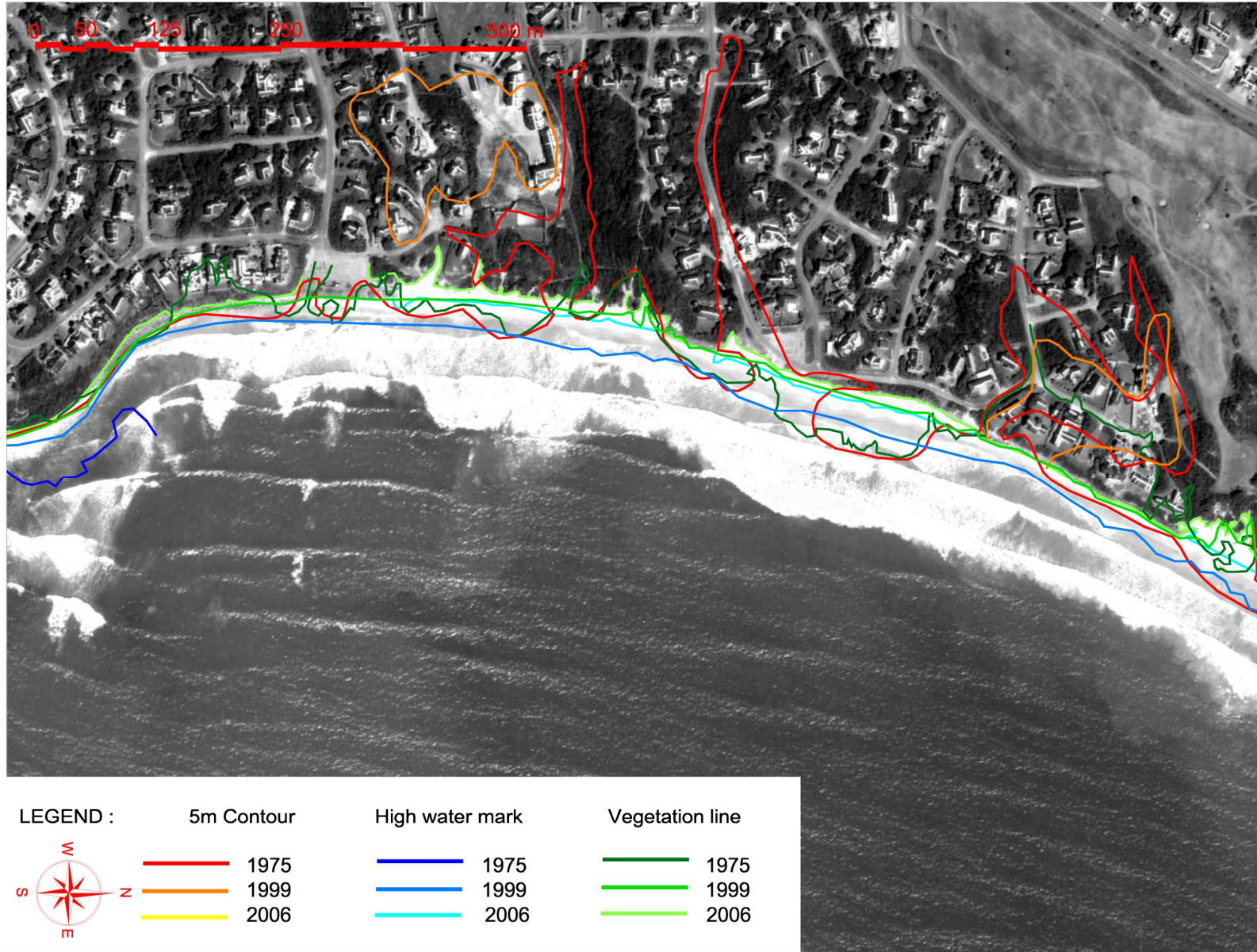


Title:

Plan view of historical coastline trends from aerial photographs
Cape St Francis

Figure No.

7.14



X:\PRDW Projects\Current\SA (1010) Nuclear Sites SSRs\Working\Engineers\RLH\Coastline\Thyspunt\Scaled\Coastline_Contours_Comparison_14.png

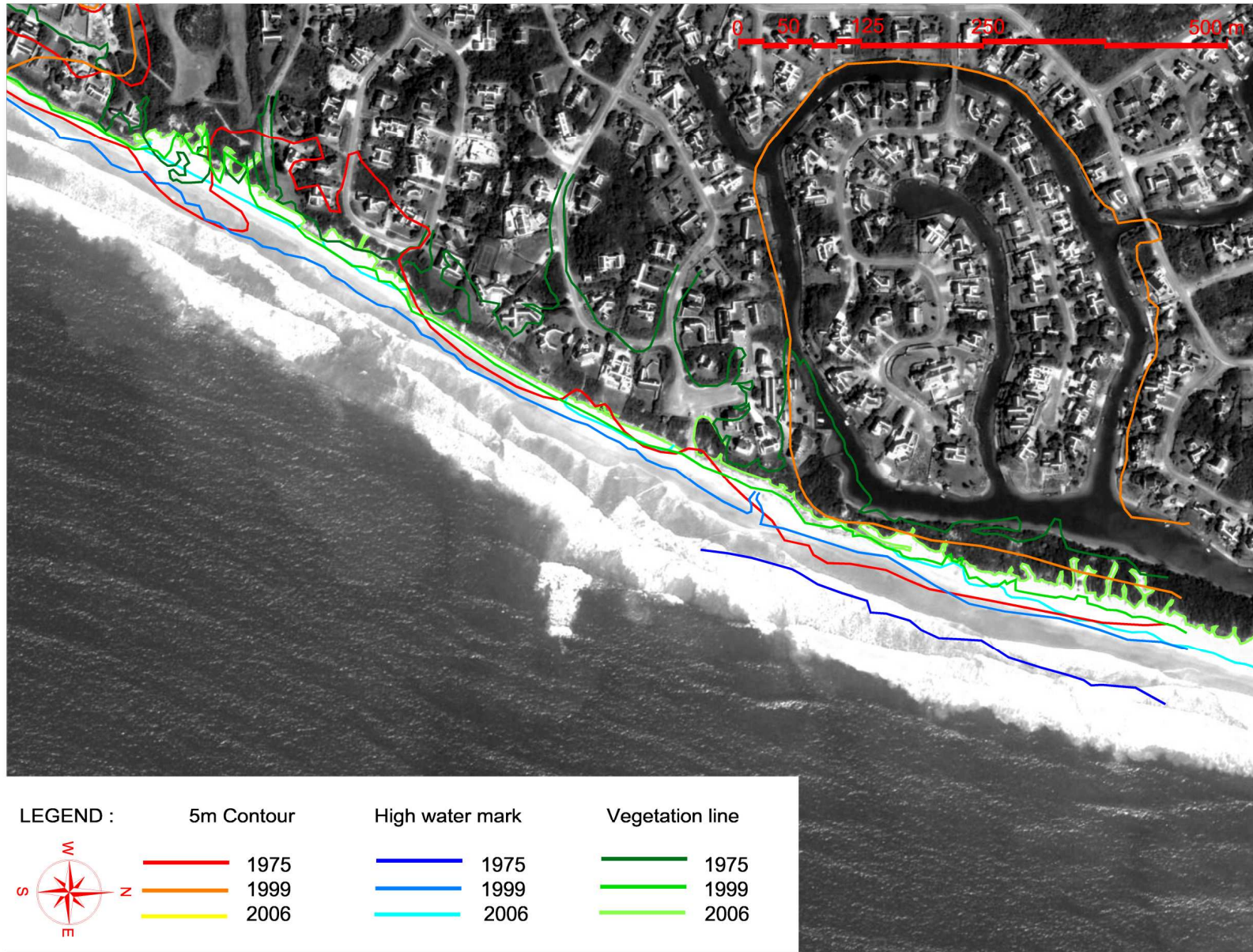


Title:

Plan view of historical coastline trends from aerial photographs
Krommebaai

Figure No.

7.15

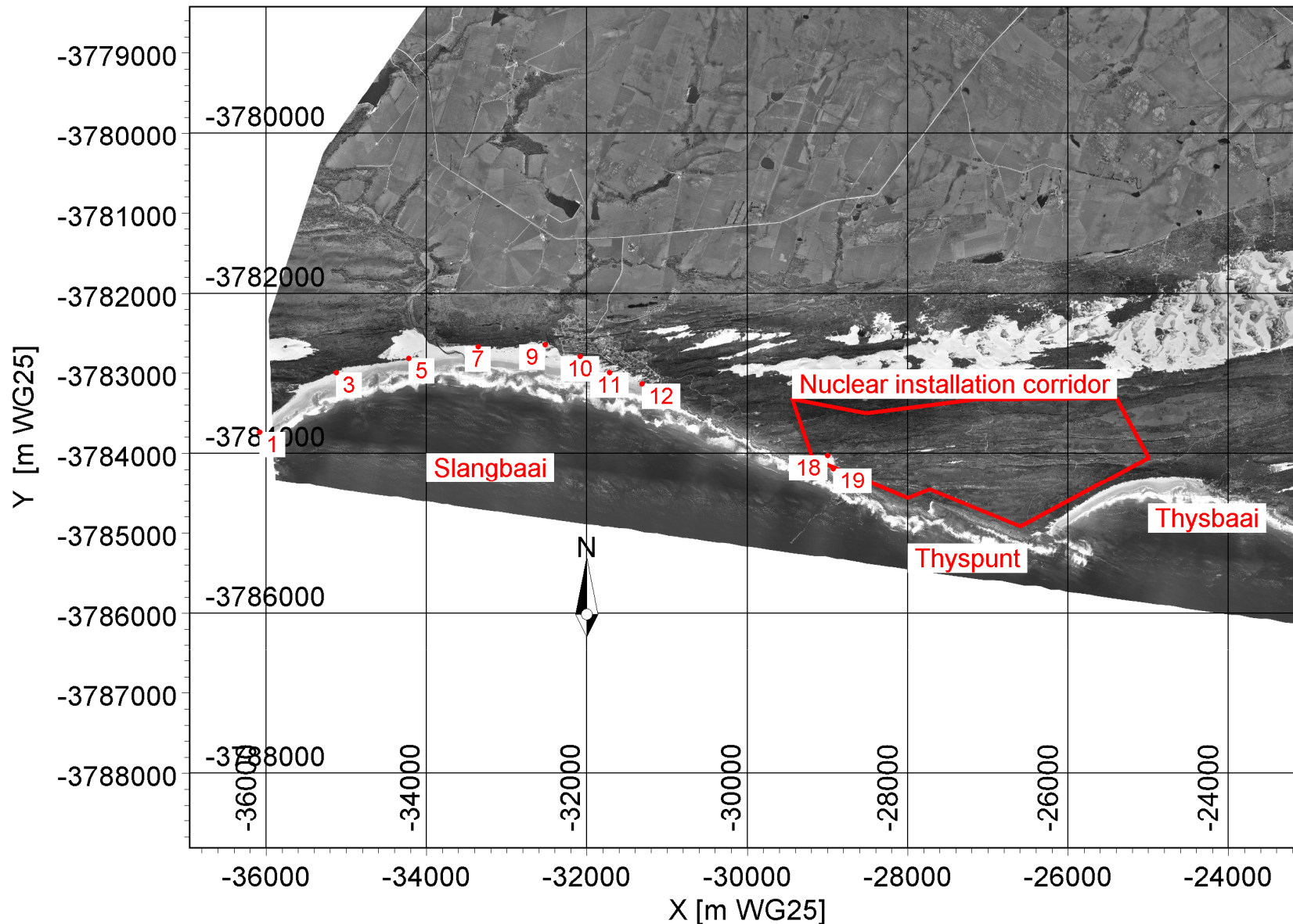


Title:

Plan view of historical coastline trends from aerial photographs
Krommebaai

Figure No.

7.16



X:\PRDW Projects\Current\SA (1010) Nuclear Sites SSRs\Working\Engineers\RLH\CoastalEngineeringModelling\Thyspunt\Data\Profiles locationRLH\Profiles_locationBW_SB.png

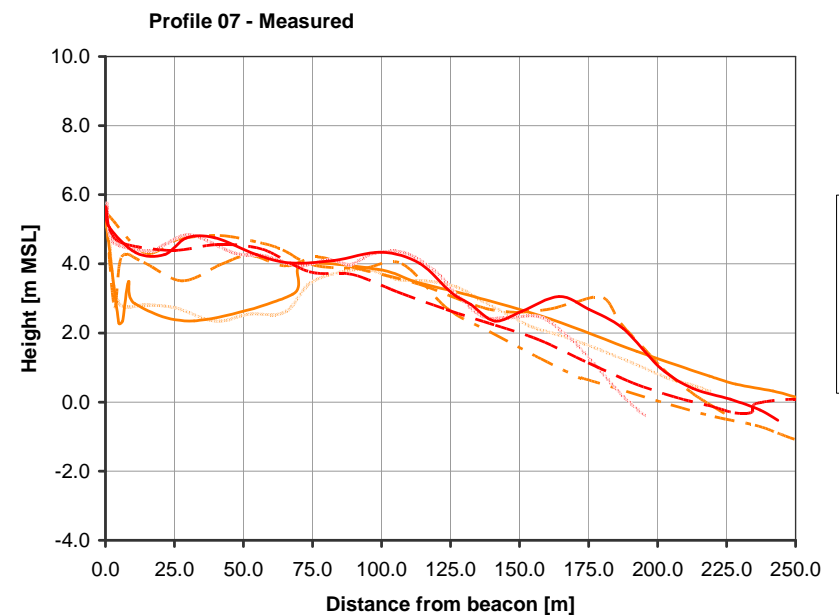
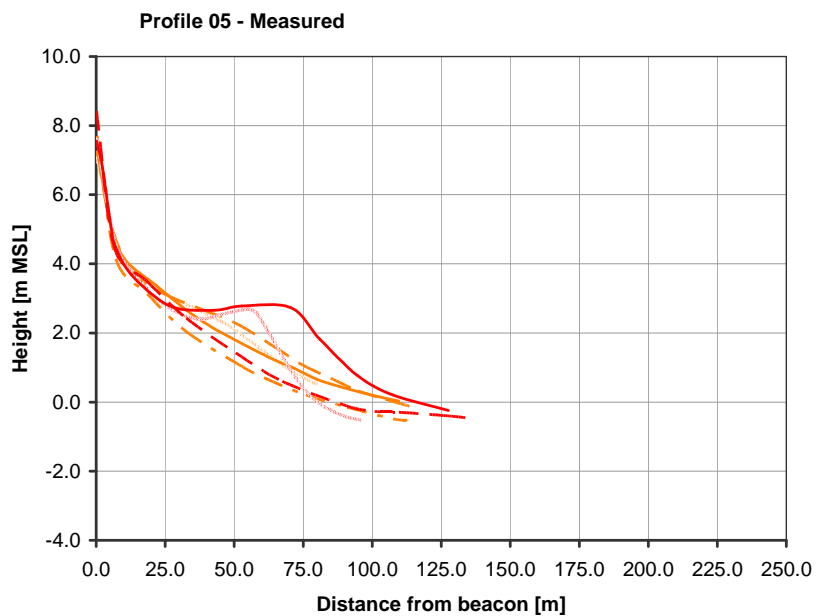
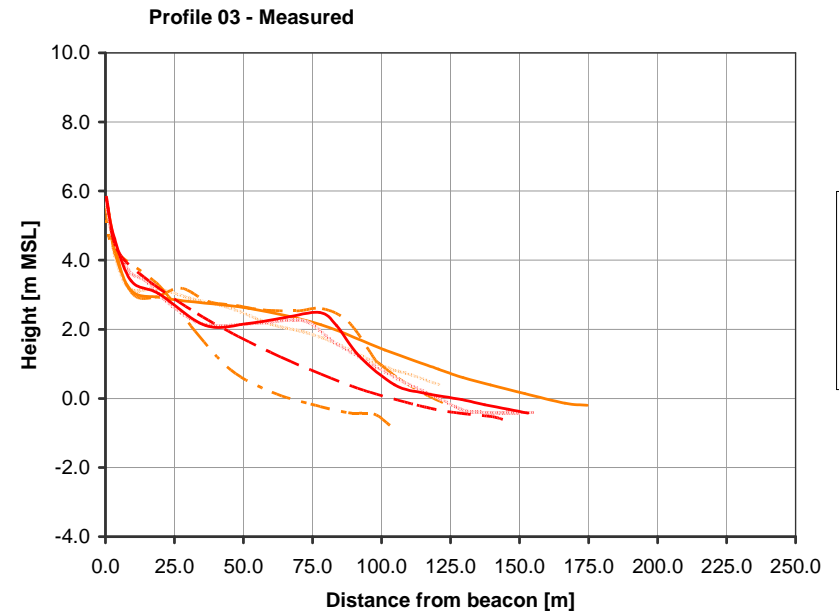
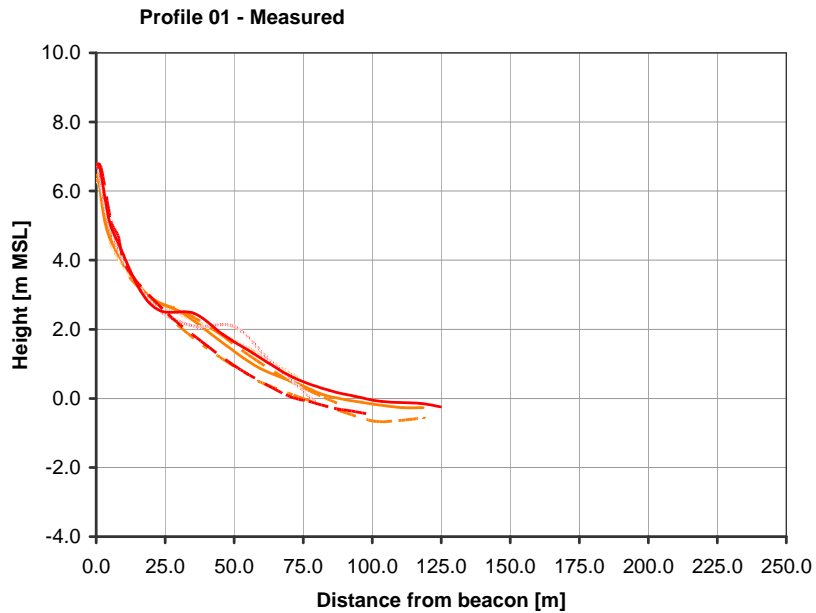


Title:

Satellite image of the Thyspunt site showing profile locations for Slangbaai used for the coastline study

Figure No.

7.17

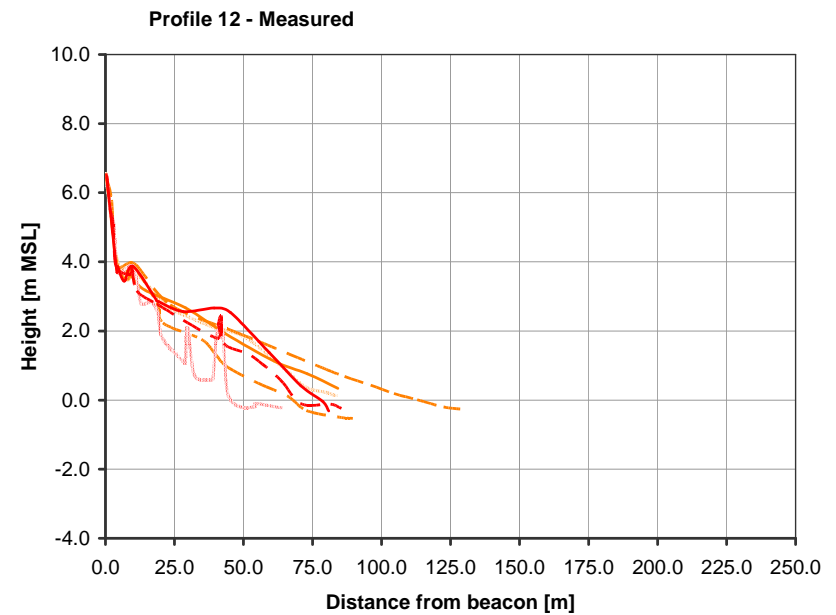
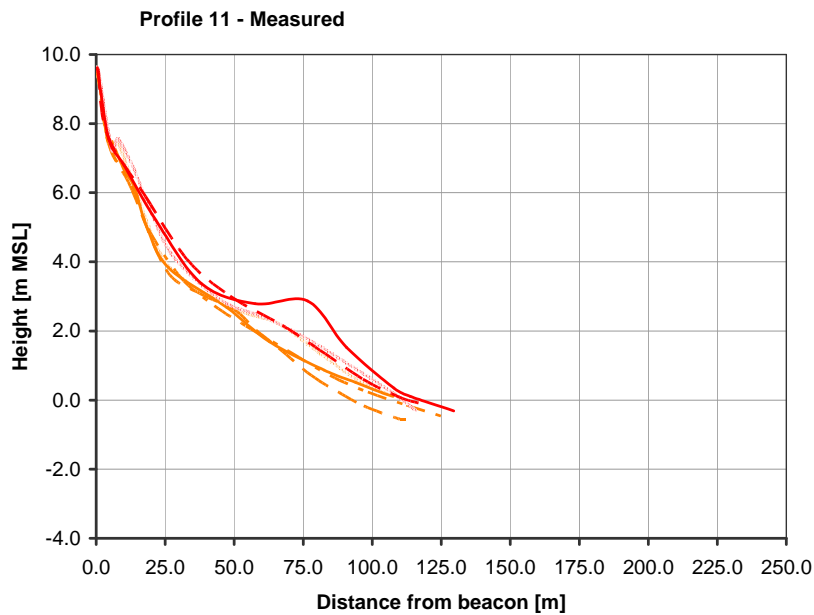
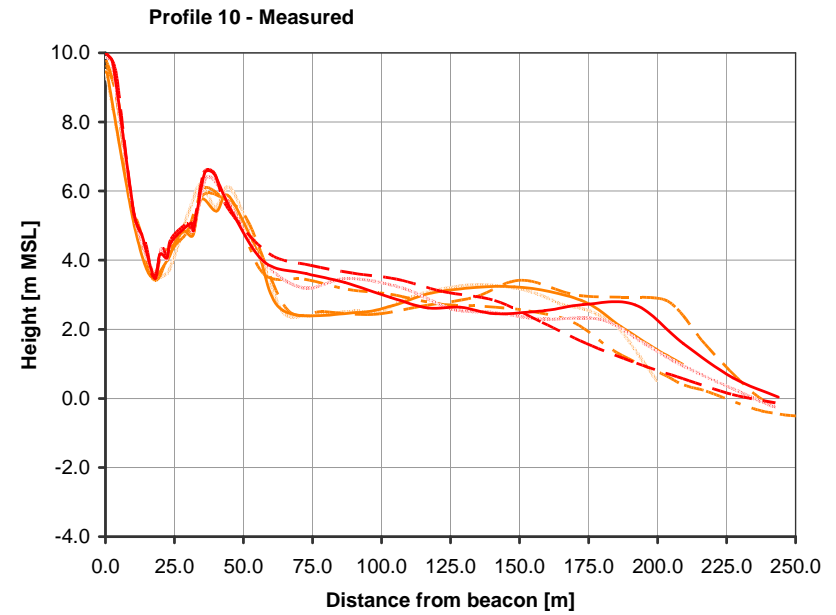
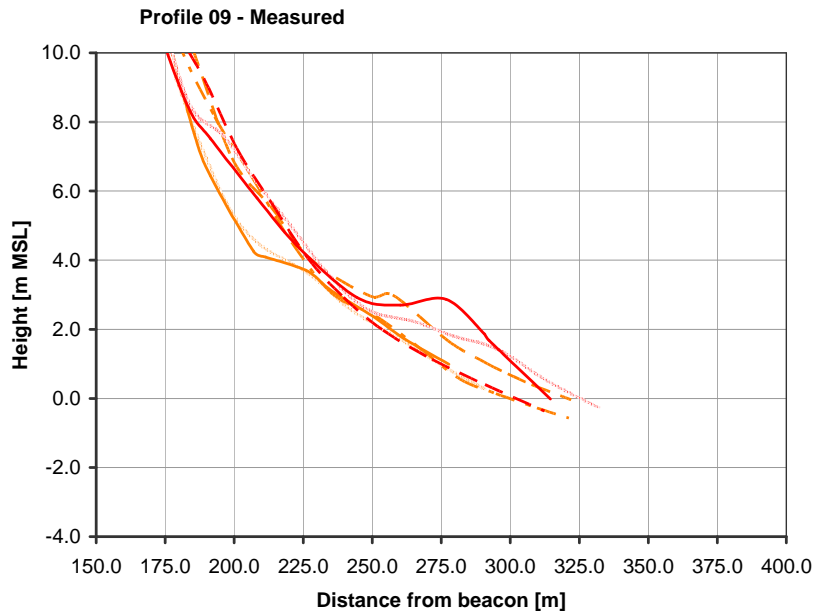


Title:

**Measured beach profiles showing seasonal variations:
Profiles 01, 03, 05, 07 (refer to Figure 7.17 for positions of profiles)**

Figure No.

7.18

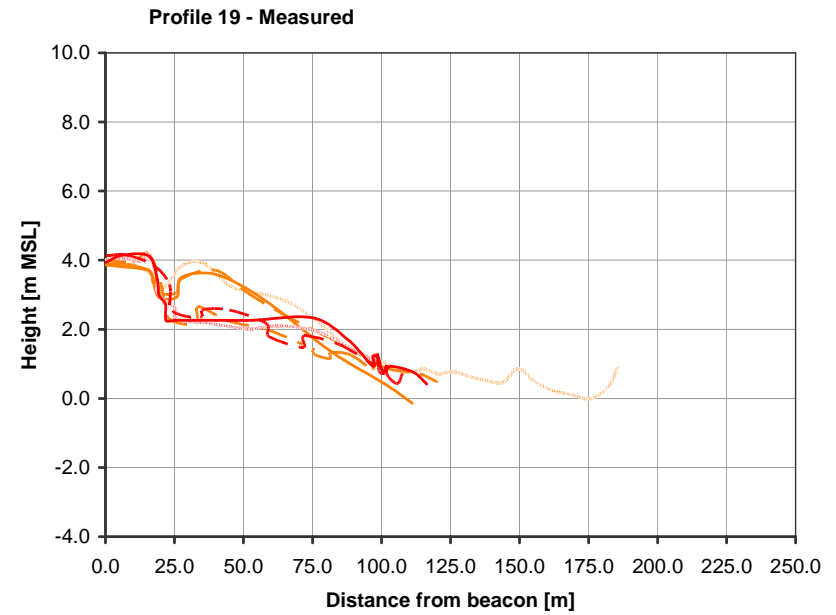
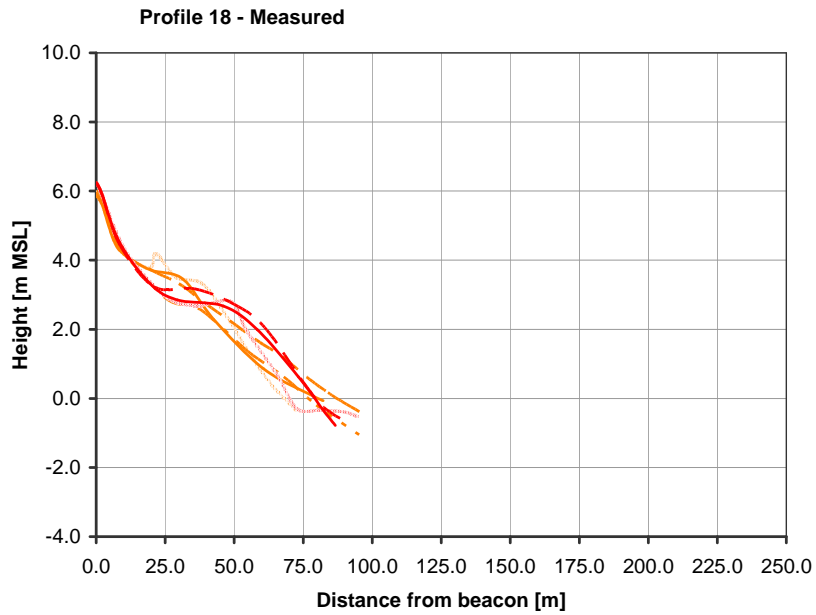


Title:

**Measured beach profiles showing seasonal variations:
Profiles 09 to 12 (refer to Figure 7.17 for positions of profiles)**

Figure No.

7.19

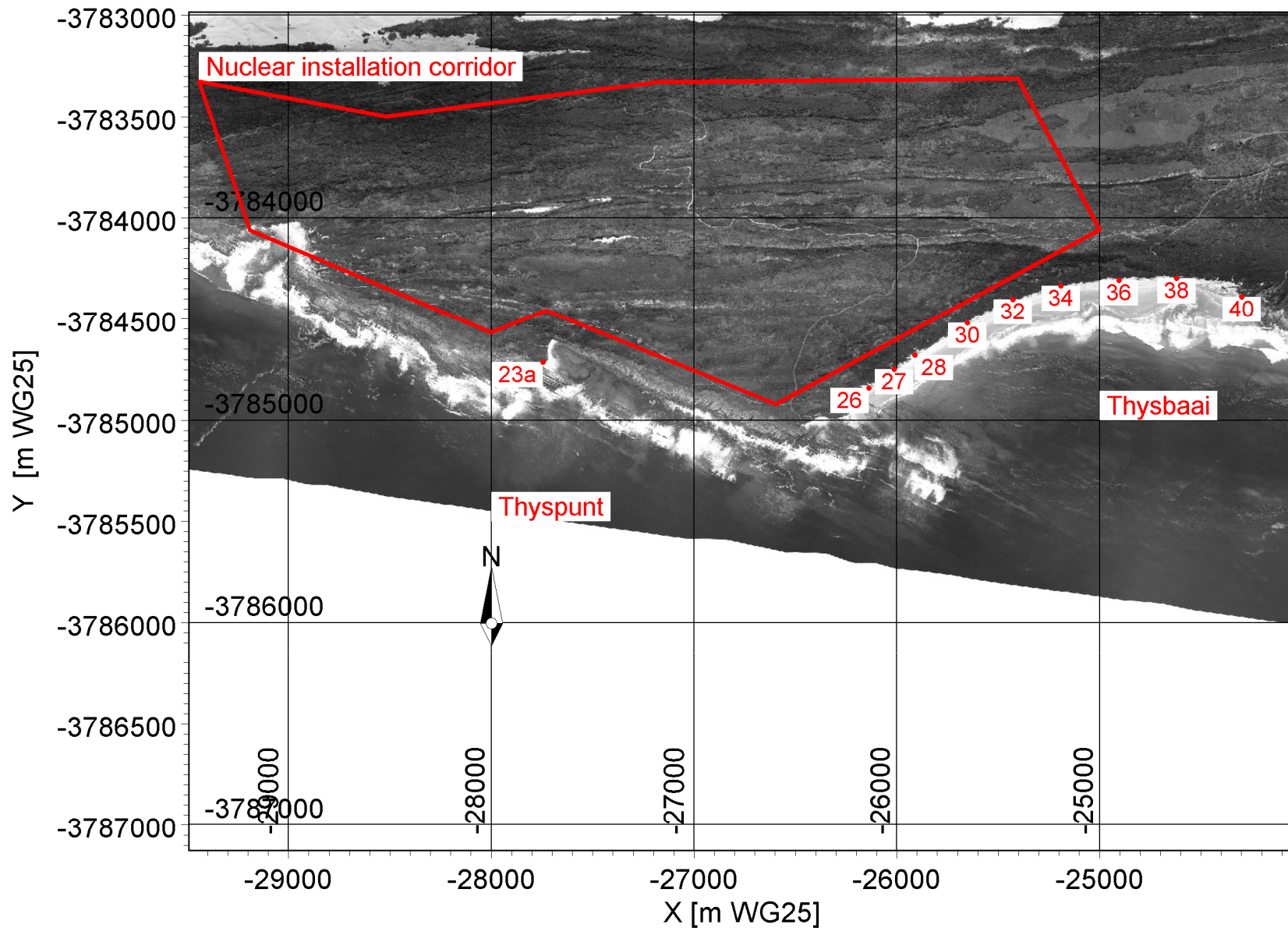


Title:

Measured beach profiles showing seasonal variations:
Profiles 18 to 19 (refer to Figure 7.17 for positions of profiles)

Figure No.

7.20



X:\PRDW Projects\Current\SA (1010) Nuclear Sites SSRs\Working\Engineers\RLH\CoastalEngineeringModelling\Thyspunt\Data\Profiles locationRLH\Profiles_locationBW_TB.png

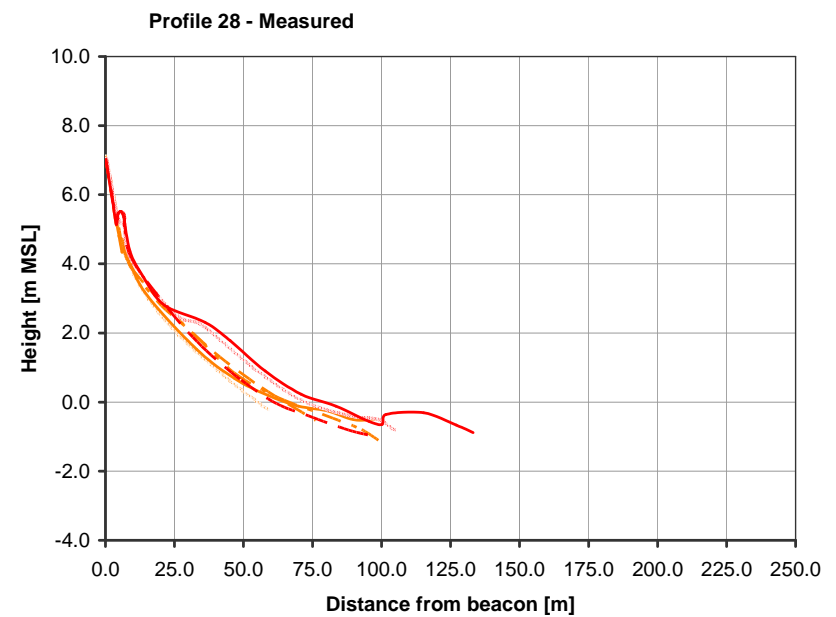
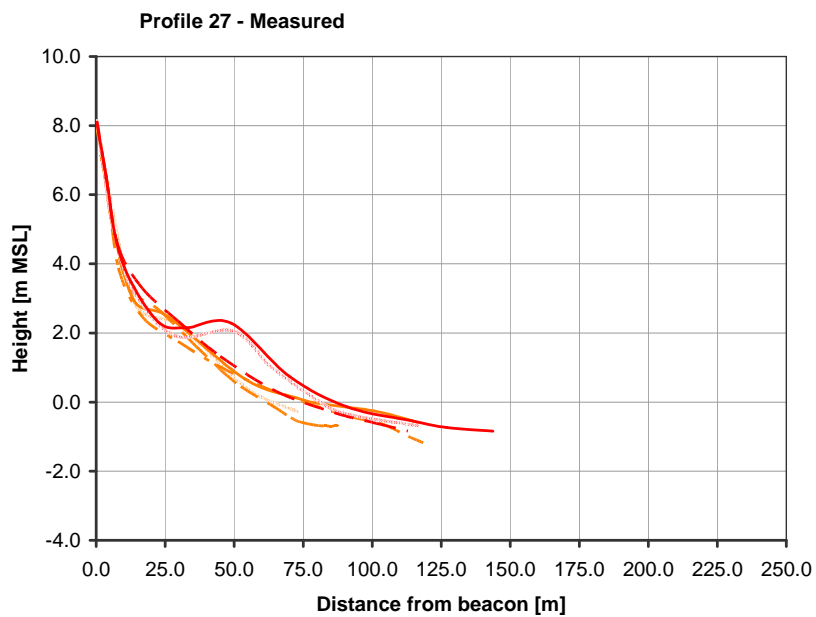
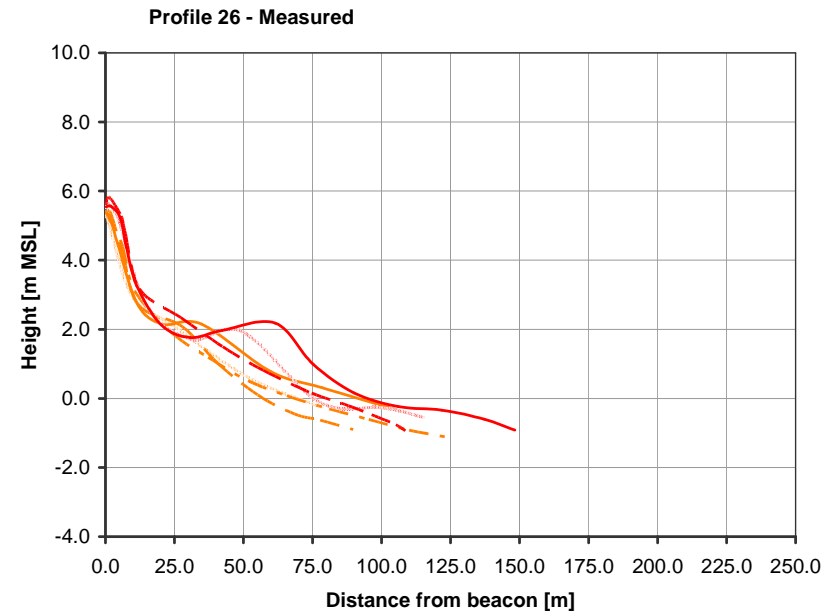
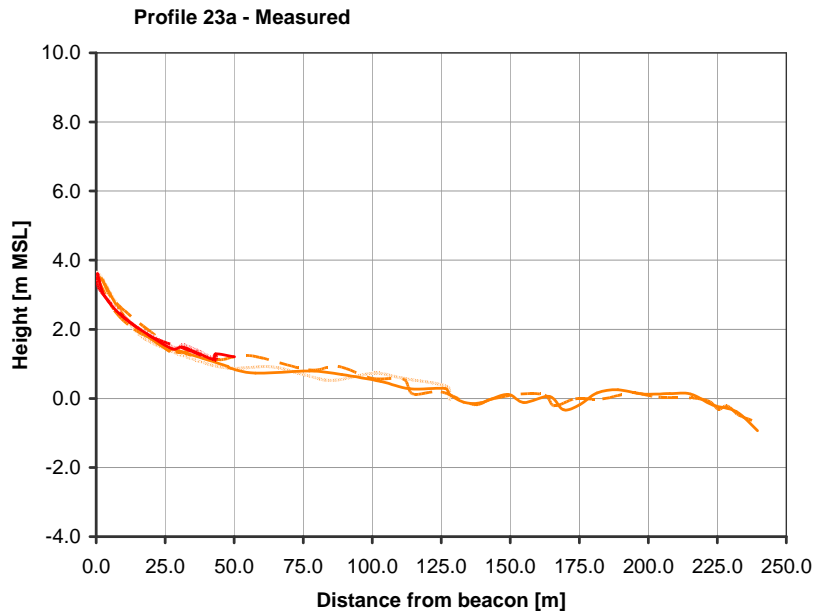


Title:

Satellite image of the Thyspunt site showing profile locations for Thysbaai used for the coastline study

Figure No.

7.21

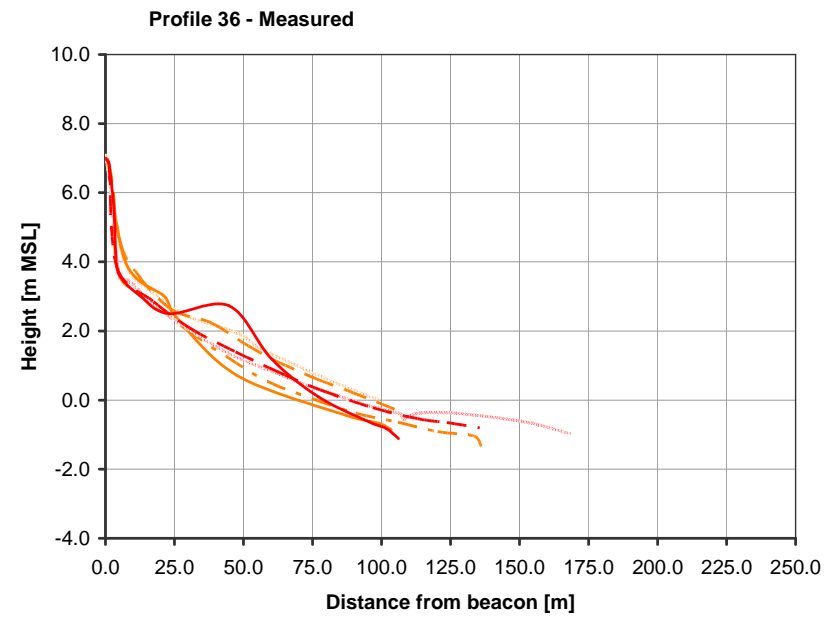
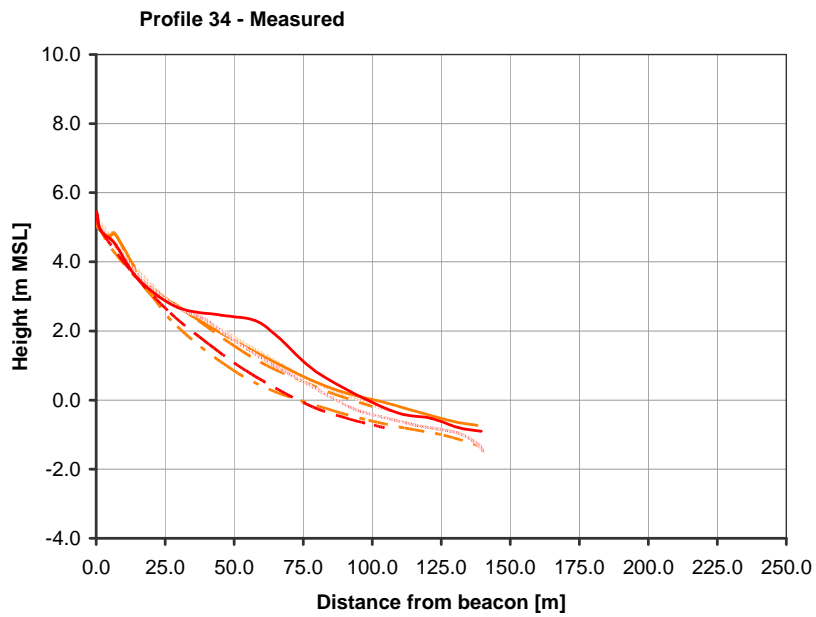
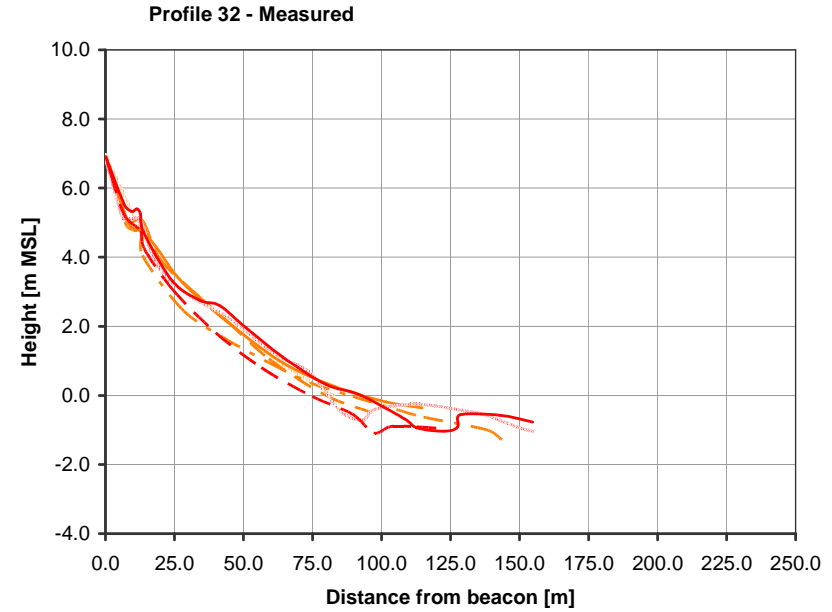
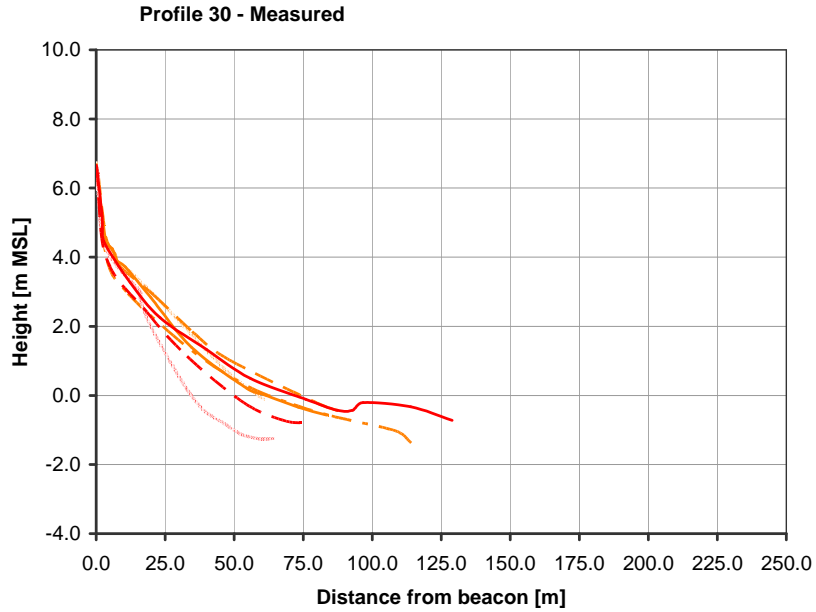


Title:

**Measured beach profiles showing seasonal variations:
Profiles 23a, 26 to 28 (refer to Figure 7.21 for positions of profiles)**

Figure No.

7.22

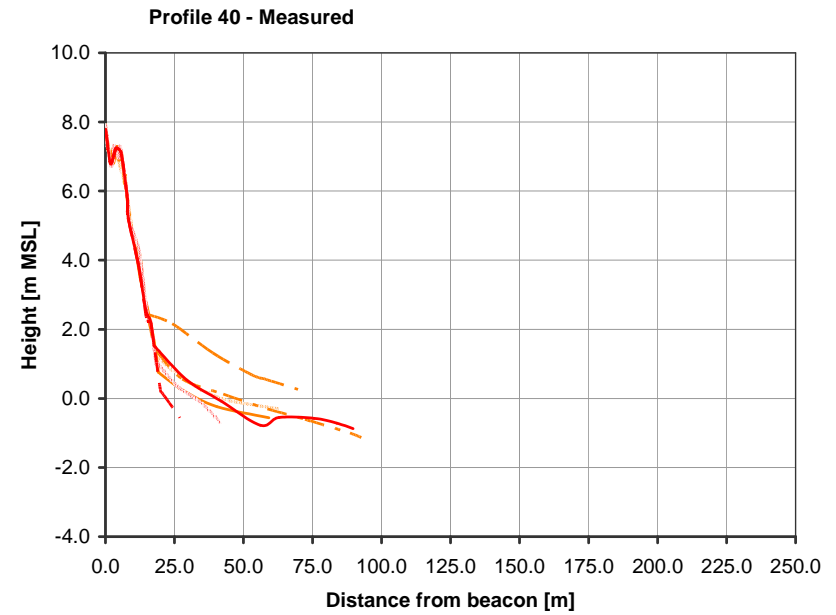
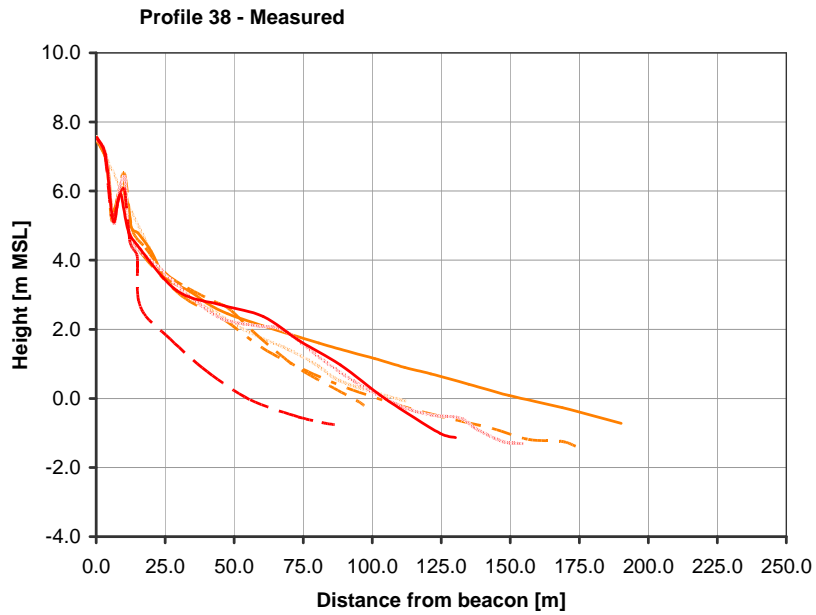


Title:

**Measured beach profiles showing seasonal variations:
Profiles 30, 32, 34, 36 (refer to Figure 7.21 for positions of profiles)**

Figure No.

7.23

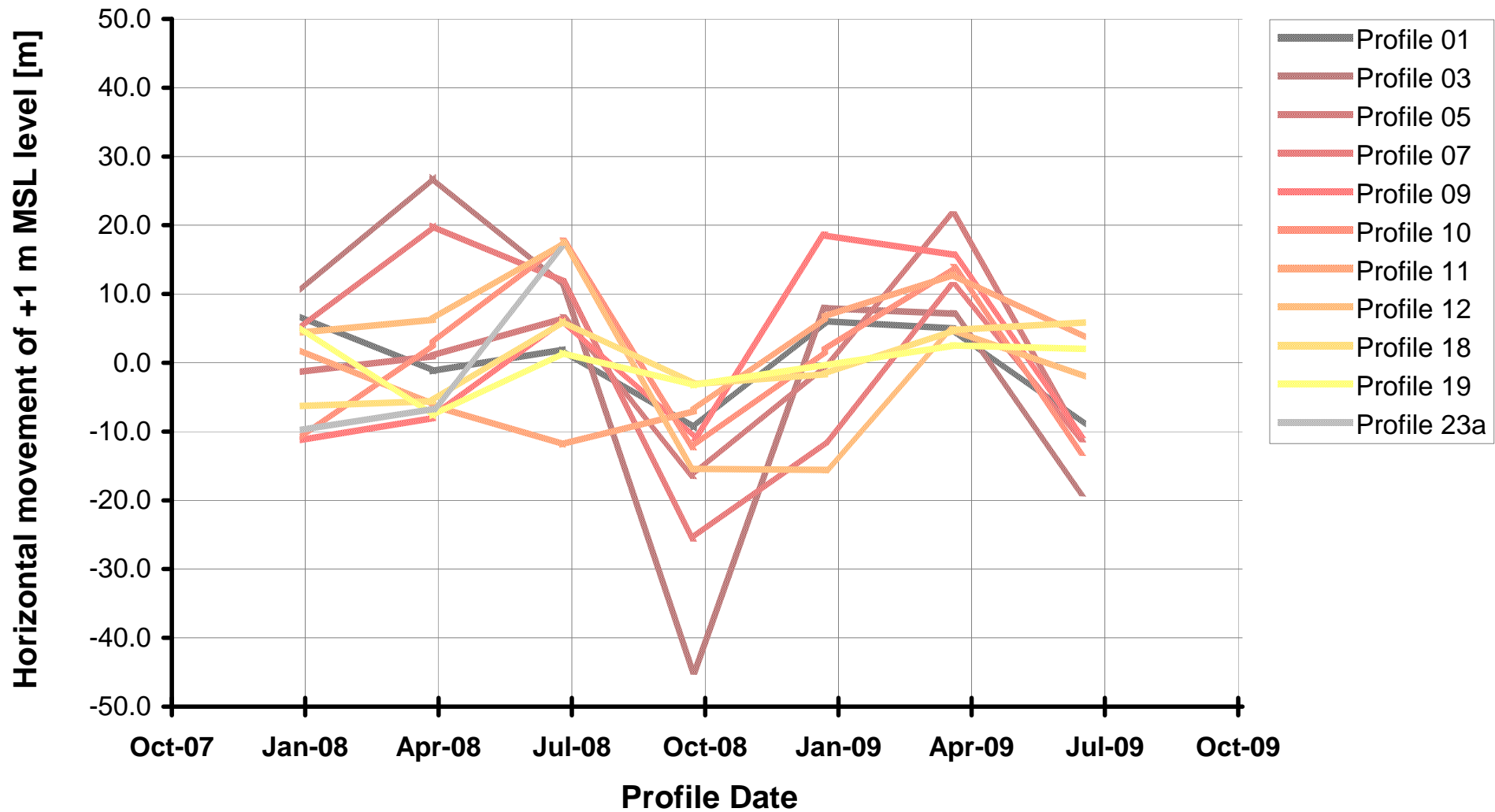


Title:

**Measured beach profiles showing seasonal variations:
Profiles 38, 40 (refer to Figure 7.21 for positions of profiles)**

Figure No.

7.24



+ Values indicate accretion, -ve values indicate erosion

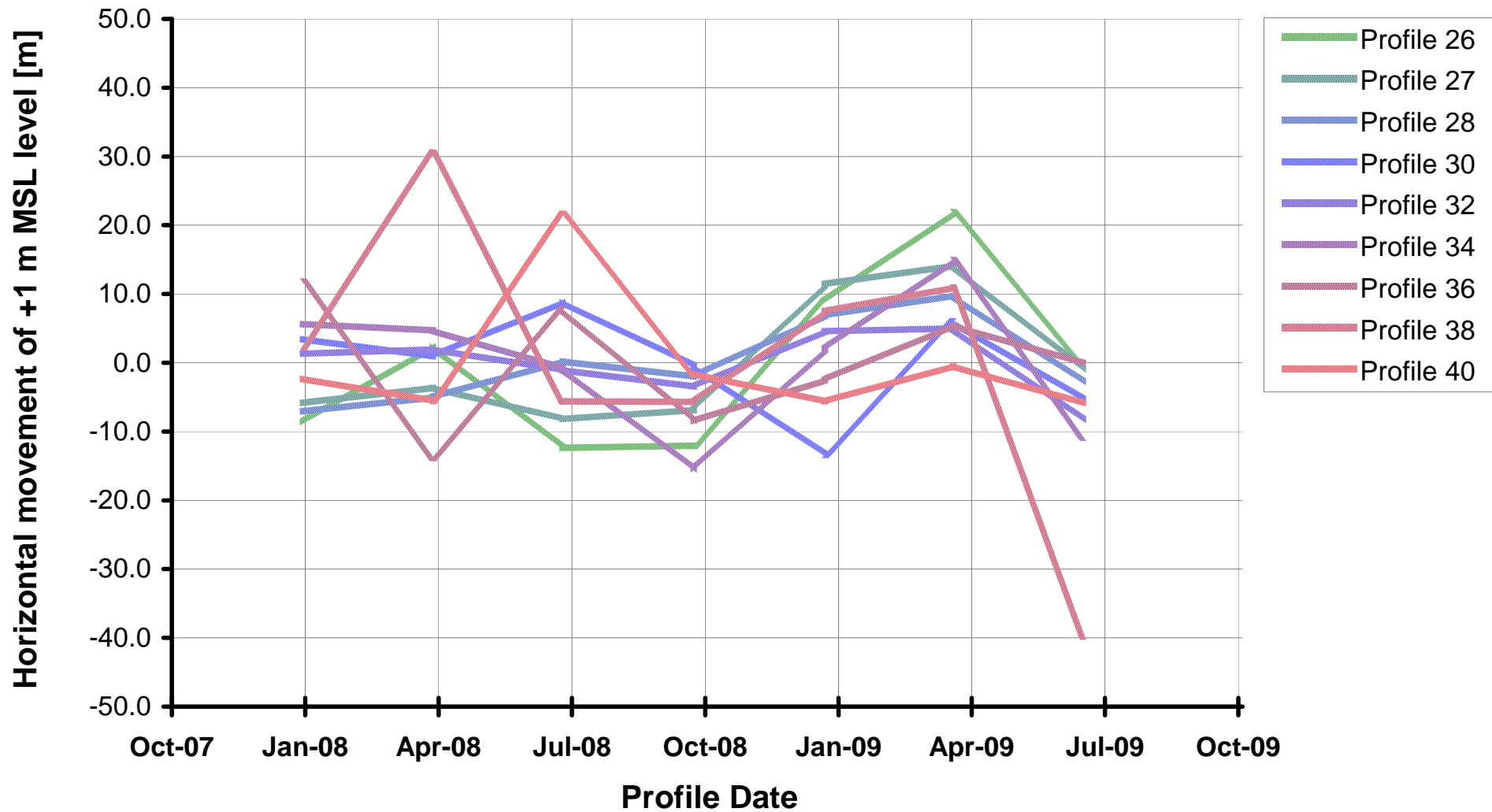


Title:

**Seasonal erosion/accretion variation from mean: 2008 - 2009
Distance from beacon at +1 m MSL (Slangbaai)**

Figure No.

7.25



+ Values indicate accretion, -ve values indicate erosion

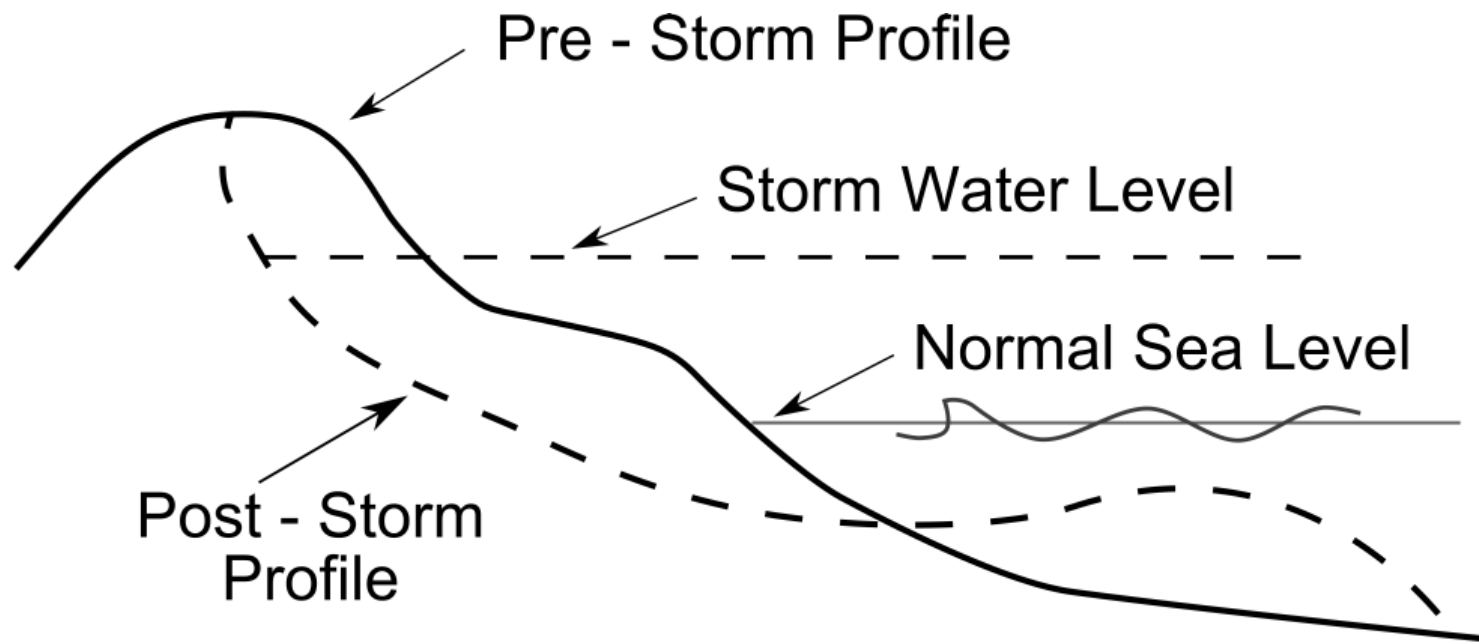


Title:

**Seasonal erosion/accretion variation from mean: 2008 - 2009
Distance from beacon at +1 m MSL (Thysbaai)**

Figure No.

7.26

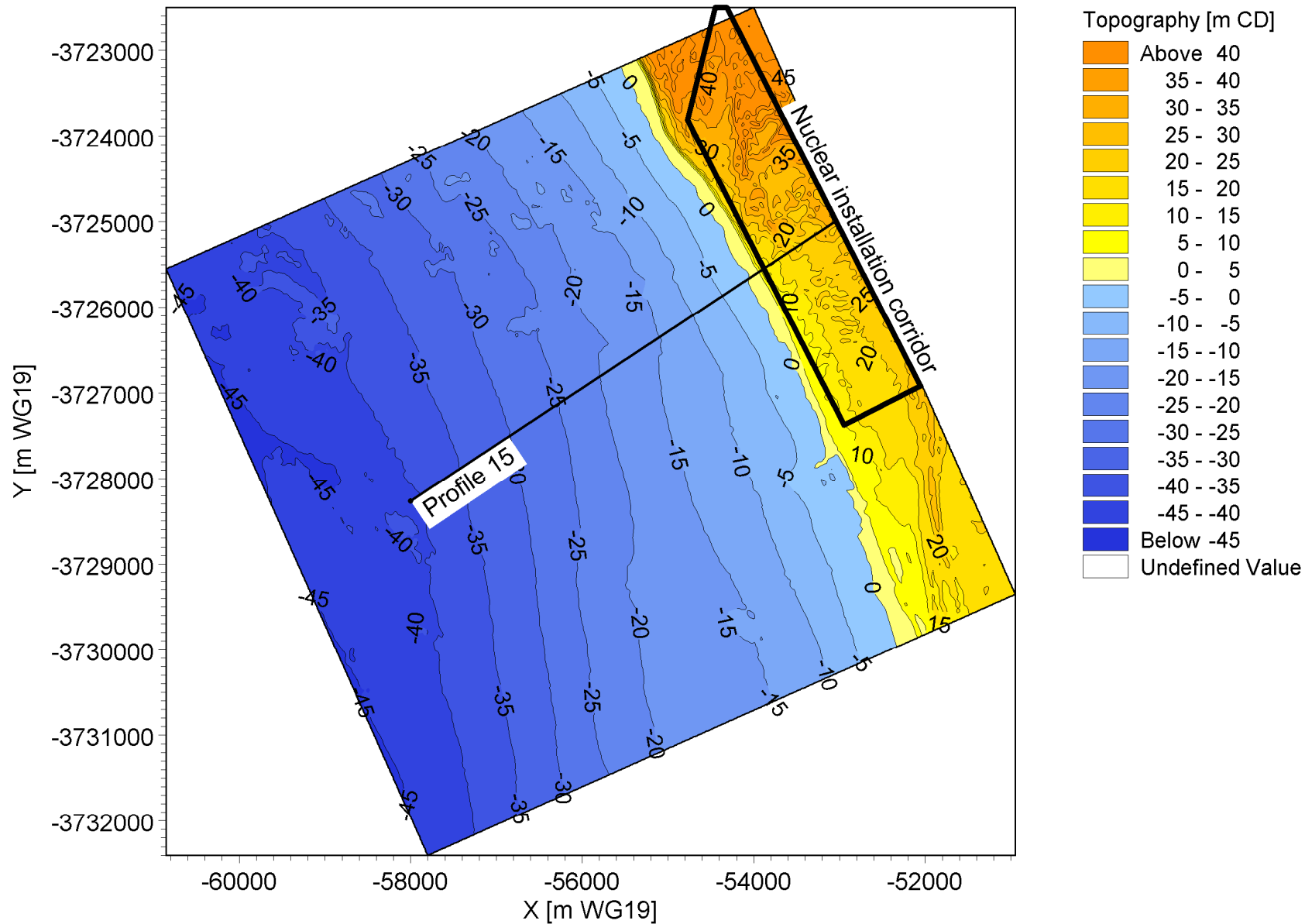


Title:

Beach profile instability due to extreme storm events

Figure No.

7.27



X:\PRDW Projects\Current\SA (1010) Nuclear Sites
 SSRs\Working\Engineers\RLH\CoastalEngineeringModelling\Duynefontein\Data\Bathy\Koeberg_WG19_CD_AutoCad_CalibrationP15.png

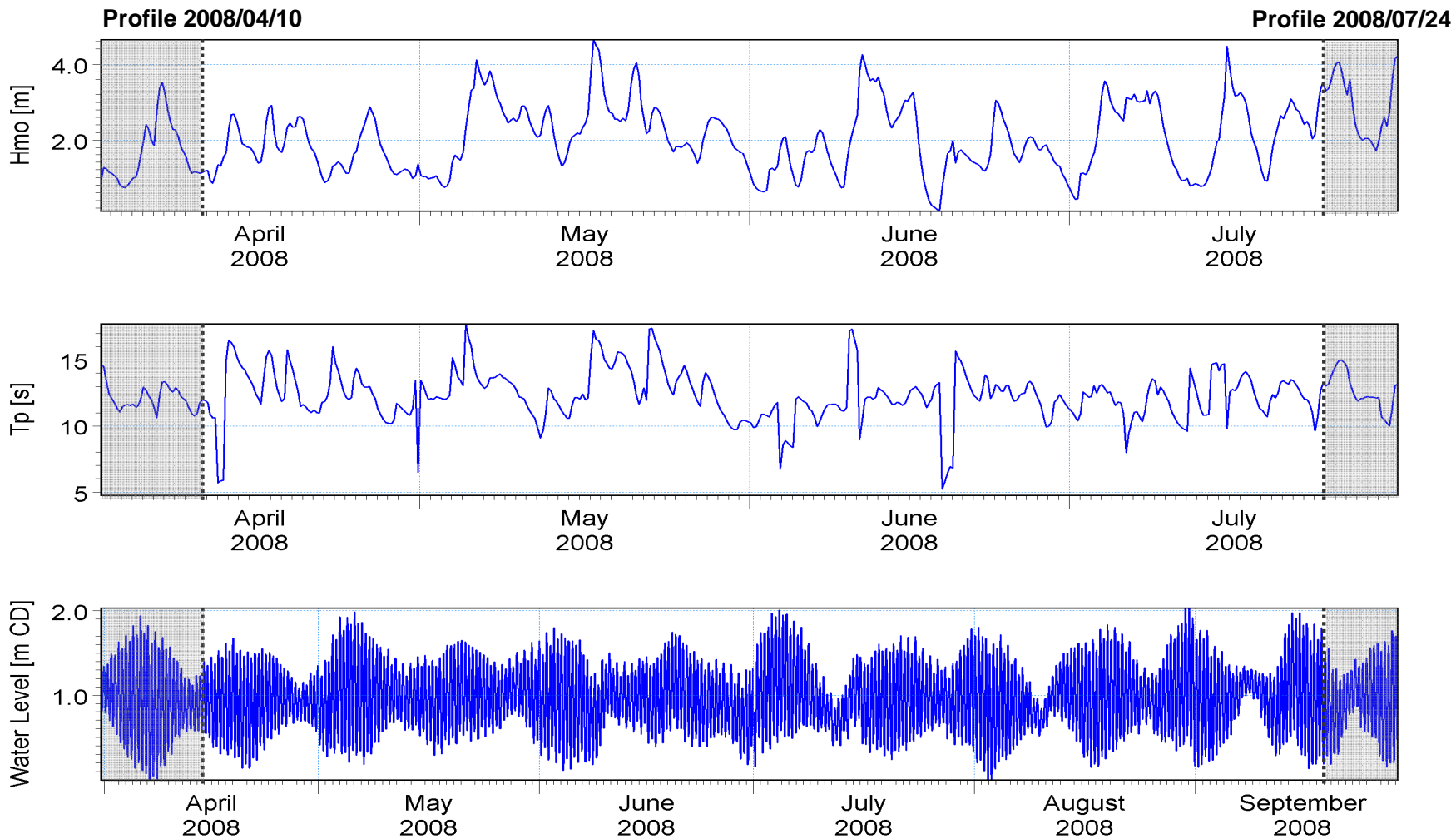


Title:

**Duynefontein storm erosion model verification:
 Extrapolation of measured beach Profile 15 from available bathymetric data - Plan view**

Figure No.

7.28

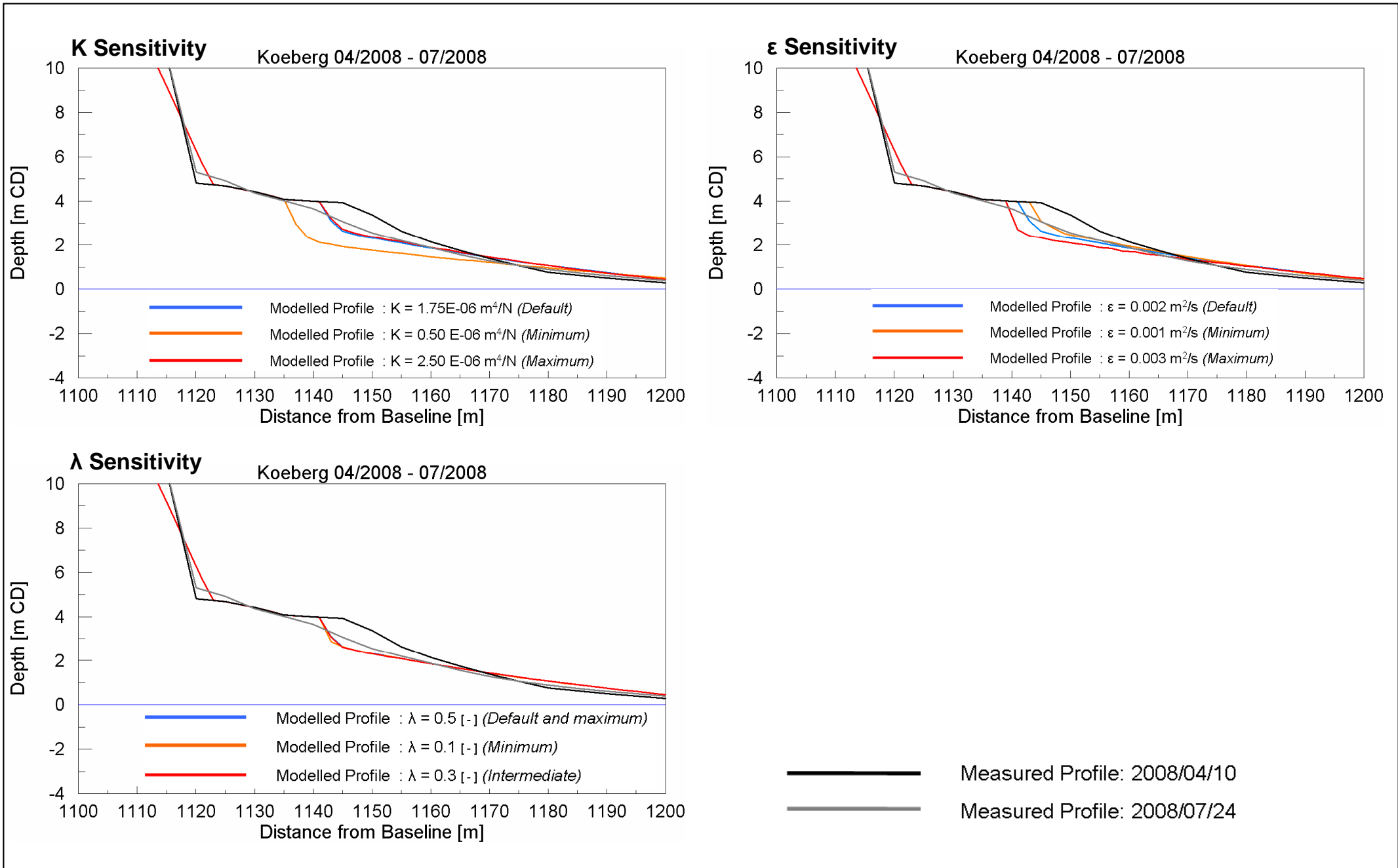


Title:

**Duynfontein storm erosion model verification:
Measured wave and water levels April 2008 - July 2008**

Figure No.

7.29

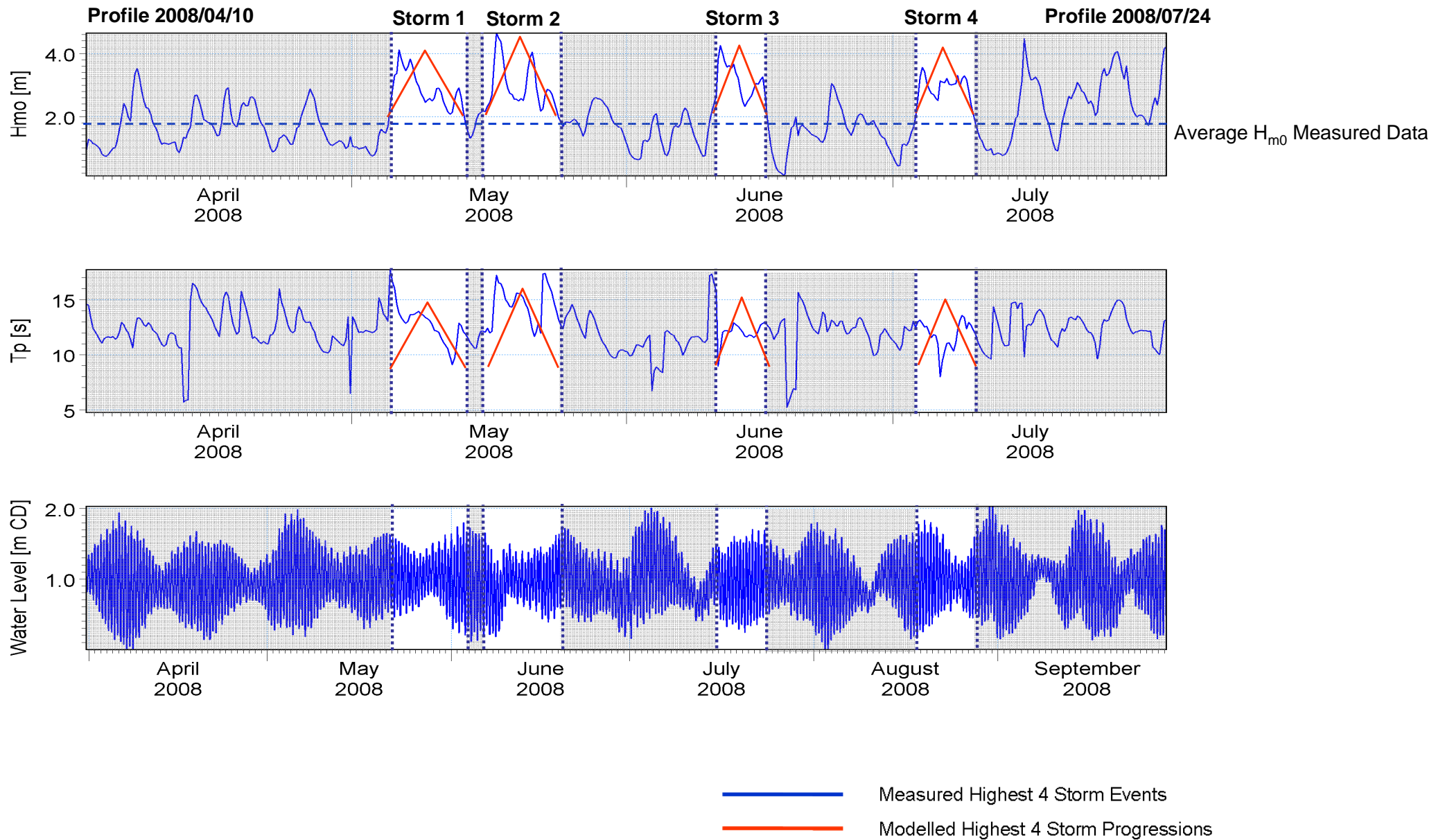


Title:

**Duynfontein storm erosion model verification:
Comparison of modelled profile response of SBEACH
calibration parameters against measured profile data**

Figure No.

7.30

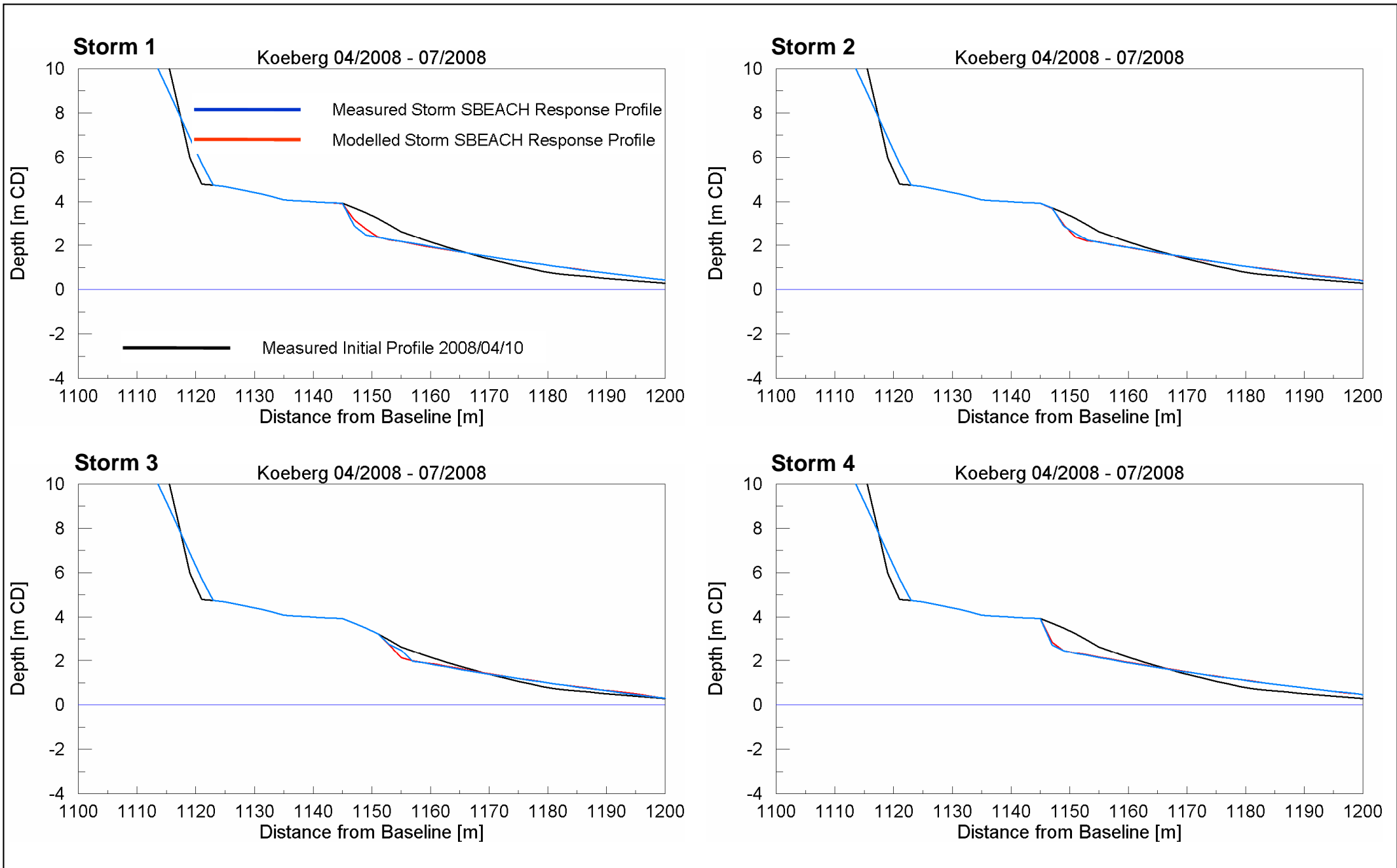


Title:

**Duynfontein storm erosion model verification:
Comparison of measured storm events and modelled storm progressions**

Figure No.

7.31

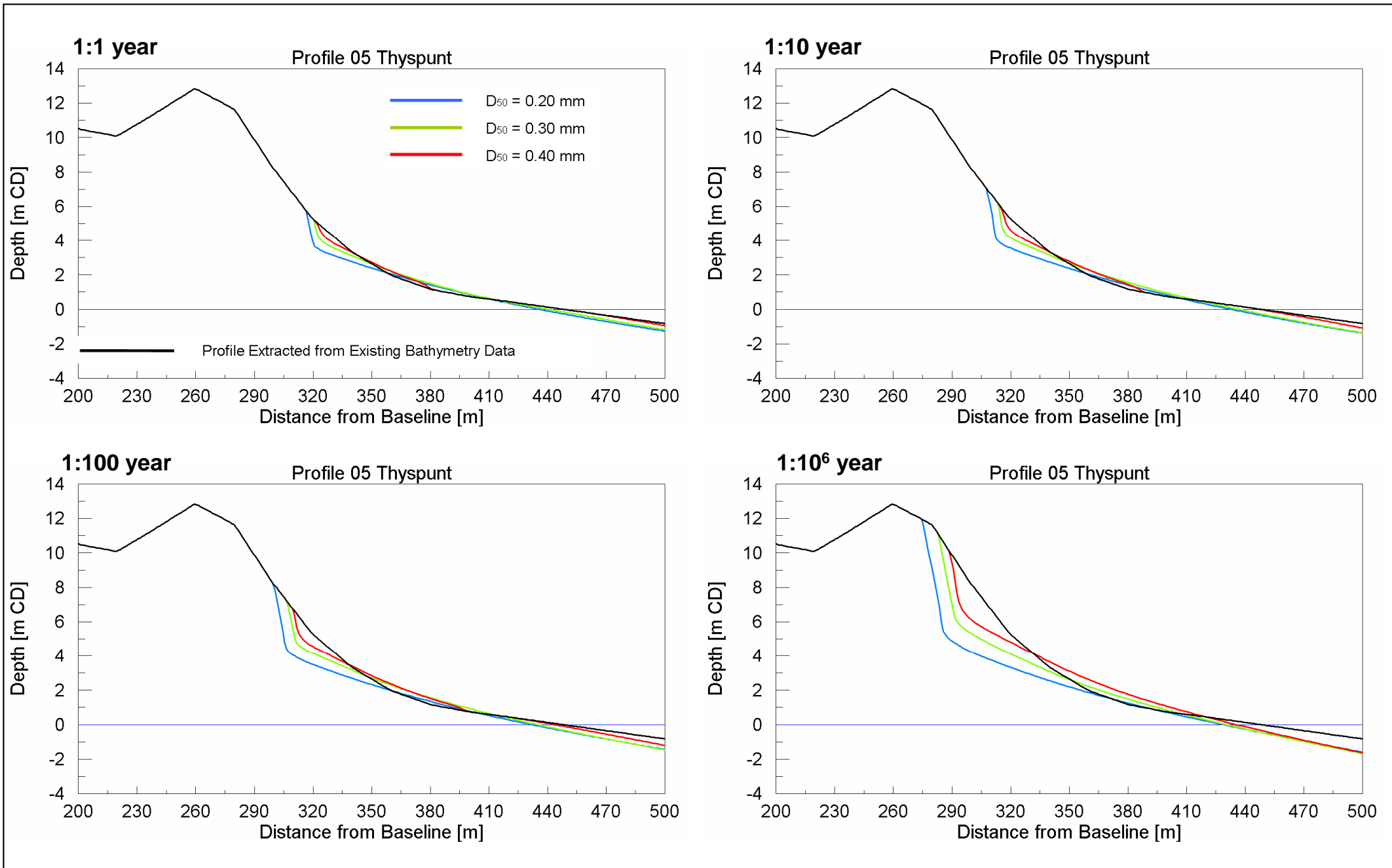


Title:

**Duynfontein storm erosion model verification:
SBEACH modelled beach response profiles for measured storms and modelled storms**

Figure No.

7.32

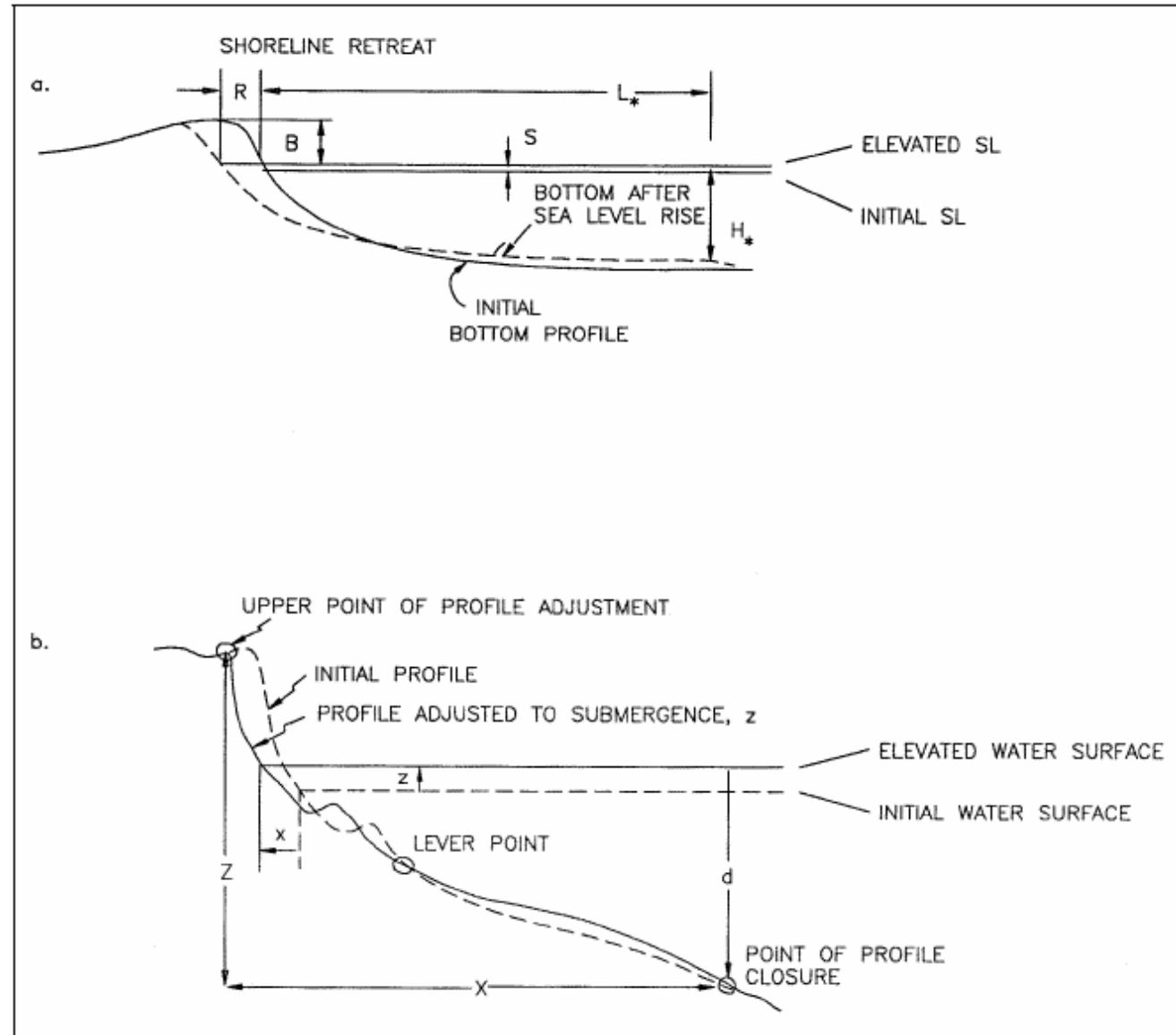


Title:

**Thyspunt beach storm erosion Profile 05 - excluding climate change:
Comparison of SBEACH response profiles using varying D_{50} values**

Figure No.

7.33



Original Bruun's Rule

Implemented Modification

Ref: CEM (2003)



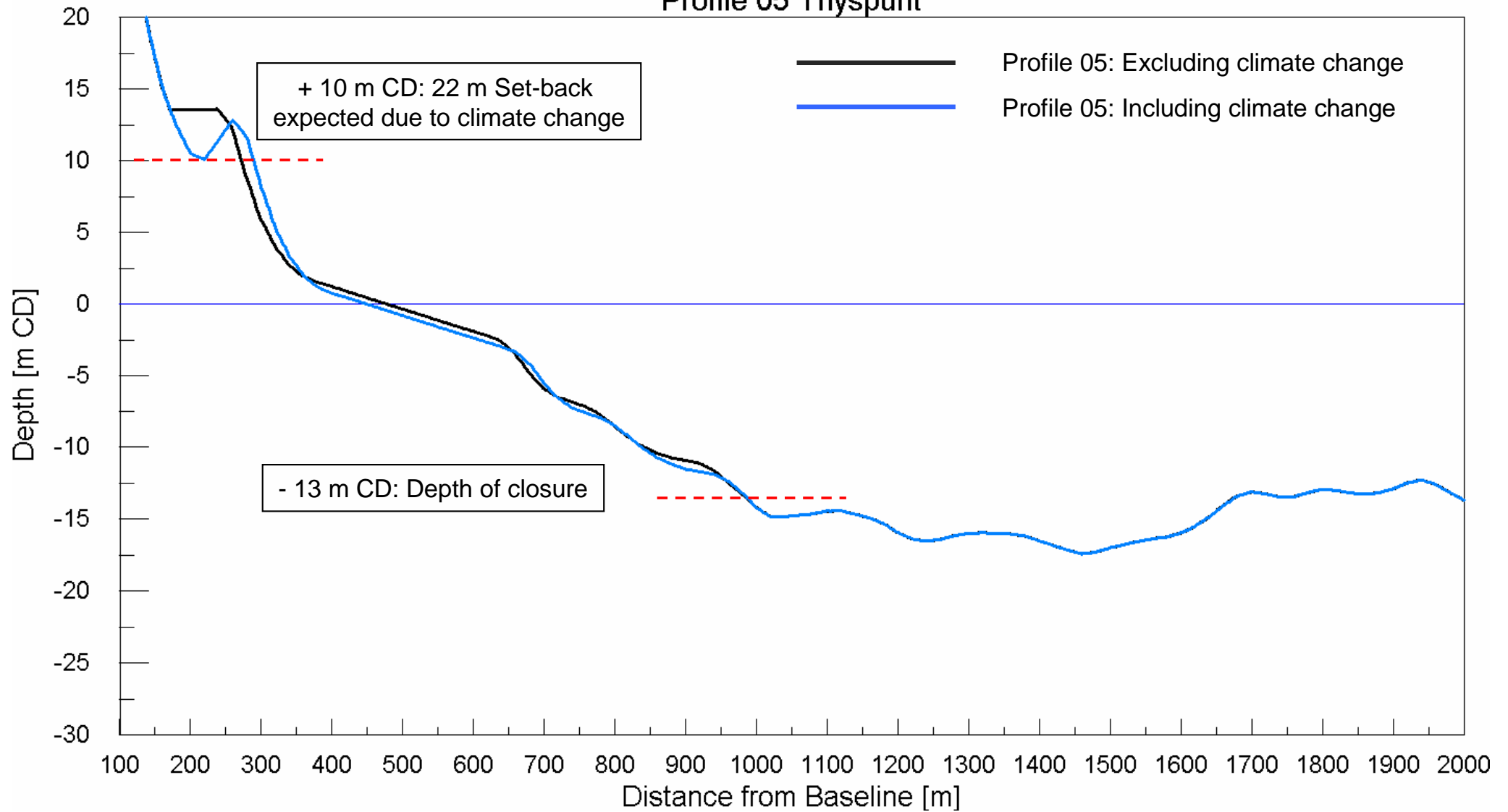
Title:

Schematic diagrams of original Bruun's rule and implemented modification

Figure No.

7.34

Profile 05 Thyspunt

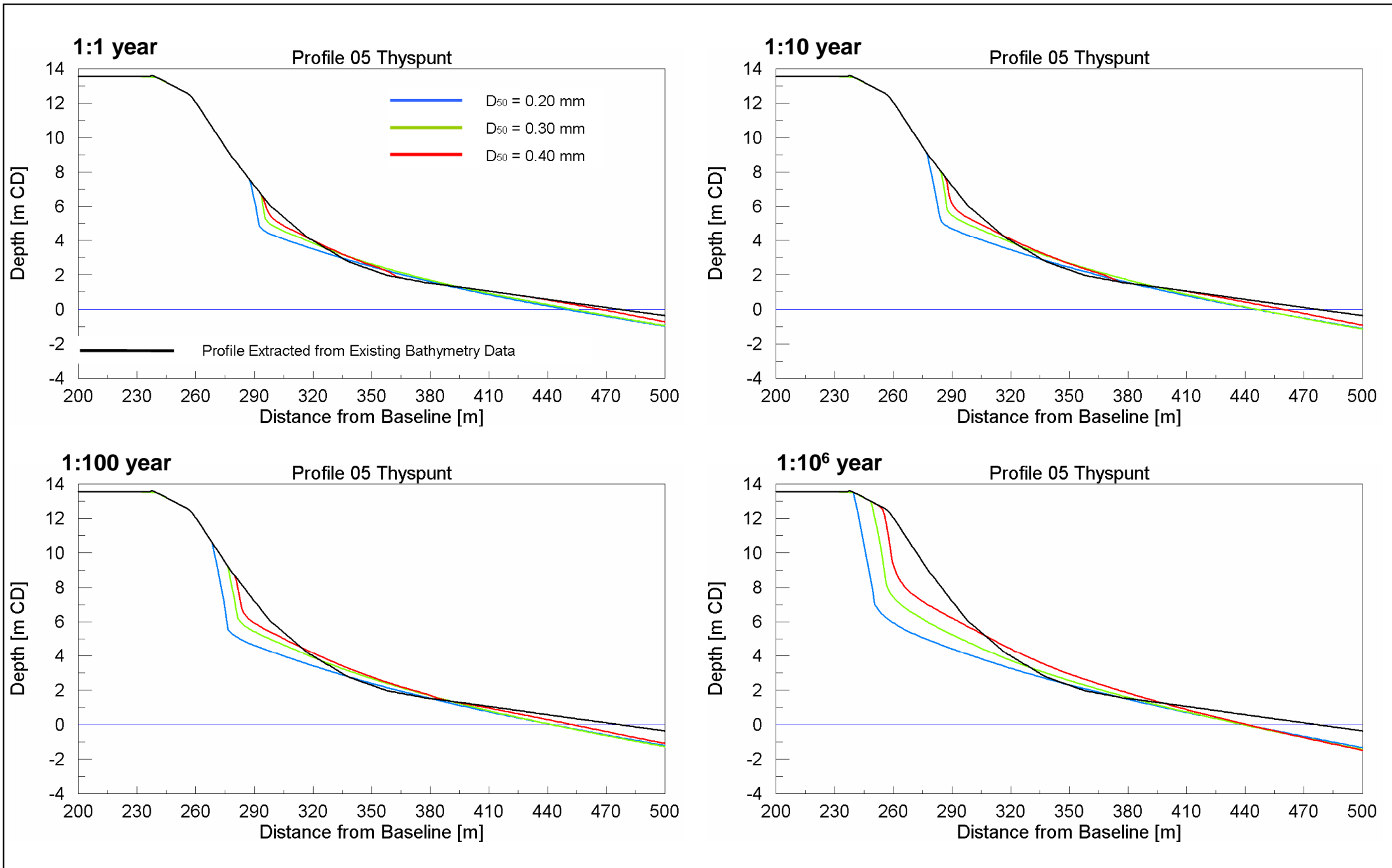


Title:

Coastal morphology: Application of Bruun's rule to Profile 05 from existing bathymetric data

Figure No.

7.35



Title:

**Thyspunt beach storm erosion Profile 05 - including climate change:
Comparison of SBEACH response profiles using varying D_{50} values**

Figure No.

7.36

ESKOM

**NUCLEAR SITES
SITE SAFETY REPORTS**

**COASTAL ENGINEERING
INVESTIGATIONS**

THYSPUNT

Report No. 1010/2/102

APPENDICES

APPENDIX A: Global Climate Change: Consequences for Coastal Engineering Design

APPENDIX A:
Global Climate Change: Consequences for Coastal Engineering Design

**GLOBAL CLIMATE CHANGE:
CONSEQUENCES FOR COASTAL
ENGINEERING DESIGN**

POSITION PAPER

REPORT NO. 939/1/001

SEPTEMBER 2009



**PRESTEDGE RETIEF DRESNER WIJNBERG (PTY) LTD
CONSULTING PORT AND COASTAL ENGINEERS**

Global Climate Change: Consequences for Coastal Engineering Design Report No. 939/1/001					
Revision	Date	Author	Checked	Status	Approved
01	September 2009	SAL	ARW	For Use	

Keywords: Climate change, coastal engineering design

GLOBAL CLIMATE CHANGE: CONSEQUENCES FOR COASTAL ENGINEERING DESIGN

POSITION PAPER

TABLE OF CONTENTS

	PAGE NO.
1. SCOPE.....	1
2. SEA LEVEL RISE	1
3. WIND.....	6
4. STORM SURGE.....	7
5. WAVES	7
6. CURRENTS	9
7. SEAWATER TEMPERATURE	9
8. RECOMMENDED DESIGN APPROACH	10
REFERENCES	12

APPENDIX A: ADAPTIVE VERSUS PRECAUTIONARY APPROACH

LIST OF TABLES

Table 1: Projected sea level rise during this century (2000 - 2100)	3
Table 2: Recommended increase in design parameters due to climate change	10

LIST OF FIGURES

Figure 1: Historical and projected future sea level rise for emissions scenario A1B (IPCC, 2007).....	2
Figure 2: Projections and uncertainties (5 to 95% ranges) of global average sea level rise and its components in 2090 to 2099 (relative to 1980 to 1999) for the six emissions scenarios (Meehl <i>et al</i> , 2007).	2
Figure 3: Estimated UK absolute sea level (ASL) rise time-series for the 21 st century. High emissions scenario. Central estimates (thick lines) are shown together with range given by 5 th and 95 th percentiles (thin Lines). (Lowe <i>et al</i> , 2009).	5
Figure 4: Estimates of linear trends in significant wave height for regions along the major ship routes for 1950 to 2002. Trends are shown only for locations where they are significant at the 5% level. (Trenberth <i>et al</i> , 2007).....	8

1. SCOPE

The purpose of this document is to summarize PRDW's position on the effects of climate change on coastal engineering design. The consequences of climate change are the subject of ongoing research work which will require that this paper be reviewed on an annual basis. Specific parameters to be reviewed include sea level rise and wind-generated waves.

The following parameters relevant to coastal engineering design are expected to be affected by climate change and are assessed in this position paper:

- Sea level rise
- Wind
- Storm surge
- Waves
- Currents
- Seawater temperature.

Since sediment transport is a function of water level, waves and currents, any climate-induced changes to sediment transport will require a site-specific analysis based on changes to the primary forcing parameters listed above.

This position paper considers climate changes to the end of this century only. Due to a lack of local data the changes described here are generally global changes rather than local changes.

2. SEA LEVEL RISE

There has been approximately 0.17 m of sea level rise in the 20th century and an accelerating trend is predicted in the 21st century (see Figure 1). The rise is mainly due to thermal expansion of the ocean, decreases in glaciers and ice caps and losses from the polar ice sheets (see Figure 2). The main source of uncertainty is the melting of the Greenland and Antarctic ice sheets (IPCC, 2007).

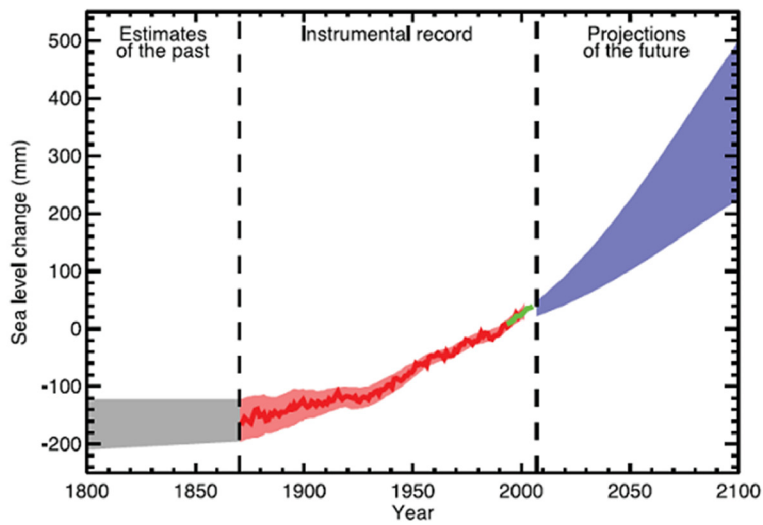


FIGURE 1: HISTORICAL AND PROJECTED FUTURE SEA LEVEL RISE FOR EMISSIONS SCENARIO A1B (IPCC, 2007).

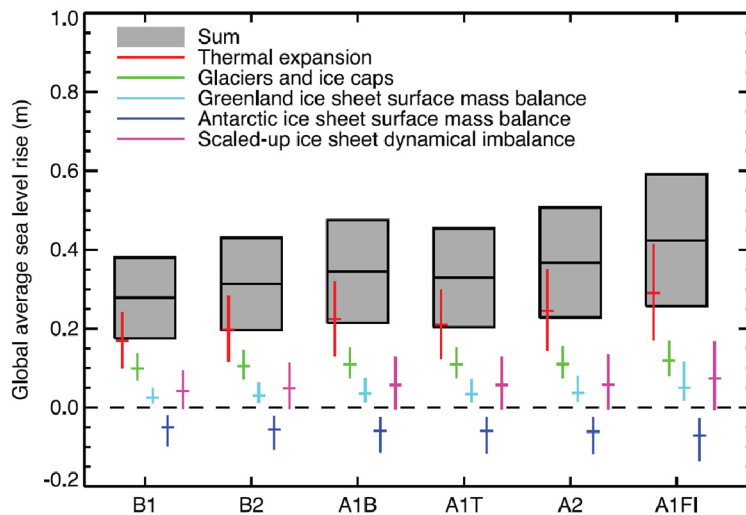


FIGURE 2: PROJECTIONS AND UNCERTAINTIES (5 TO 95% RANGES) OF GLOBAL AVERAGE SEA LEVEL RISE AND ITS COMPONENTS IN 2090 TO 2099 (RELATIVE TO 1980 TO 1999) FOR THE SIX EMISSIONS SCENARIOS (MEEHL *ET AL*, 2007).

Table 1 summarises the projected sea level rise for this century extracted from a number of recent sources and arranged chronologically.

TABLE 1: PROJECTED SEA LEVEL RISE DURING THIS CENTURY (2000 - 2100)*

Sea Level Rise [m]	Source	Comment
0.35 - 0.85	IAEA (2003)	<ul style="list-style-type: none"> Recommended values for 100 year lifetime of a nuclear power plant by the International Atomic Energy Agency. Estimate from 2003.
0.86	Defra (2006)	<ul style="list-style-type: none"> Guidelines from Department for Environment, Food and Rural Affairs, UK Government. Values given exclude local land subsidence.
0.26 - 0.59	IPCC (2007)	<ul style="list-style-type: none"> Predictions from the Fourth Assessment Report of the Intergovernmental Panel on Climate Change. These are model predicted ranges for the worst case future emissions scenario A1F1. Does not address uncertainties in climate-carbon cycle feedbacks nor include the full effects of changes in ice sheet flow, because a basis in published literature is lacking. Therefore the upper values given are not to be considered upper bounds for sea level rise.
0.79	IPCC (2007)	<ul style="list-style-type: none"> The IPCC projections given above include a contribution due to increased ice flow from Greenland and Antarctica at the rates observed for 1993-2003, but these flow rates could increase or decrease in the future. If this contribution were to grow linearly with global average temperature change, the upper ranges of sea level rise would increase by 0.1 - 0.2 m. Adding 0.2 m to 0.59 m increases the upper range to 0.79 m.
0.5 - 1.4	Rahmstorf (2007)	<ul style="list-style-type: none"> A semi-empirical relation is presented that connects global sea-level rise to global mean surface temperature. When applied to future warming scenarios of the IPCC, this relationship results in a projected sea-level rise in 2100 of 0.5 to 1.4 m above the 1990 level. Concludes that a rise of over 1 m by 2100 for strong warming scenarios cannot be ruled out.
1.6	Rohling <i>et al</i> (2008)	<ul style="list-style-type: none"> Based on average rise each century during the interglacial period ~120 000 years ago during which sea levels reached 6 m above where they are now. Data from the Red Sea indicates a rise of 1.6 ± 0.8 m per century.
0.79	Pfeffer <i>et al</i> (2008)	<ul style="list-style-type: none"> The study addresses the plausibility of very rapid sea level rise from land ice occurring this century by considering kinematic constraints on glacier contributions. “Low 1” scenario: a low range estimate based on specific adjustments to dynamic discharge in certain potentially vulnerable locations.
0.83	Pfeffer <i>et al</i> (2008)	<ul style="list-style-type: none"> “Low 2” scenario: in addition to the assumptions made in Low 1, the authors integrated presently observed rates of change in dynamic discharge forward in time.
2.0	Pfeffer <i>et al</i> (2008)	<ul style="list-style-type: none"> “High 1” scenario: combines all eustatic sources taken as high but reasonable values. No firm upper limit can be established so the values chosen represent judged upper limits of likely behaviour on the century timescale. The Greenland and Antarctic Glacier velocities required for very large increases in sea level (2-5 m) are found to be far beyond the range of observations, and while no physical proof is offered that these velocities cannot be reached, the authors recommend that they should not be adopted as a central working hypothesis.
0.5	PIANC (2008)	<ul style="list-style-type: none"> Recommendation by The International Navigation Association (PIANC), based on average values in IPCC (2007).

0.55 - 1.2	Deltacommissie (2008)	<ul style="list-style-type: none"> ▪ Commission set up by Dutch government to recommend how to protect the Dutch coast and the low-lying hinterland against the consequences of climate change. ▪ Based on research conducted by 20 leading national and international climate experts, including several IPCC authors. ▪ Supplements the scenarios for 2100 produced by the IPCC (2007). ▪ Regarded as <i>plausible upper limit scenarios</i>, which are regarded as possible by the group of sea level experts consulted, based on current scientific knowledge. ▪ Note that the values given exclude land subsidence, which will increase the relative sea level rise locally in the Netherlands by 0.1 m.
2.0	Ananthaswamy (2009)	<ul style="list-style-type: none"> ▪ With climate change modelling being so uncertain, with many ice dynamics not included due to lack of knowledge of those systems, this article states that climate scientists are looking for other ways to predict sea level rise. Some approaches being explored may take a more black box approach, where the rate of sea level rise is proportional to the increase in temperature: the warmer Earth gets, the faster ice melts and the oceans expand. This held true for the last 120 years at least. ▪ A worst case scenario indicated in this article would present up to 2 m sea level rise by 2100.
0.15 - 0.76	Lowe <i>et al</i> (2009)	<ul style="list-style-type: none"> ▪ This is from the recent UK Climate Projections Report of June 2009. ▪ Based on a UK regionalisation of the IPCC (2007) projections. ▪ Based on the high emissions scenario including ice melt. ▪ Range represents 5th – 95th confidence intervals (see Figure 3).
0.93 - 1.9	Lowe <i>et al</i> (2009)	<ul style="list-style-type: none"> ▪ This is the so-called “High-plus-plus” (H++) scenario from the UK Climate Projections Report of June 2009. ▪ The top of the H++ scenario range is derived from indirect observations of sea level rise in the last interglacial period, at which time the climate bore some similarities to the present day, and from estimates of maximum glacial flow rate. ▪ This is a UK regionalisation of an upper limit global rise from Rohling <i>et al</i> (2008) of 2.5 m \approx 1.6+0.8 m, taking glacial-isostatic adjustment (GIA) of the earth’s crust into account. ▪ This value might be used for contingency planning and to help users thinking about the limits to adaptation. It is very unlikely that the upper limit of this scenario will occur during the 21st century, but it cannot yet be ruled out completely given past climate proxy observations and current model limitations.

* The IPCC projections are from 1980-1999 until 2090-2099.

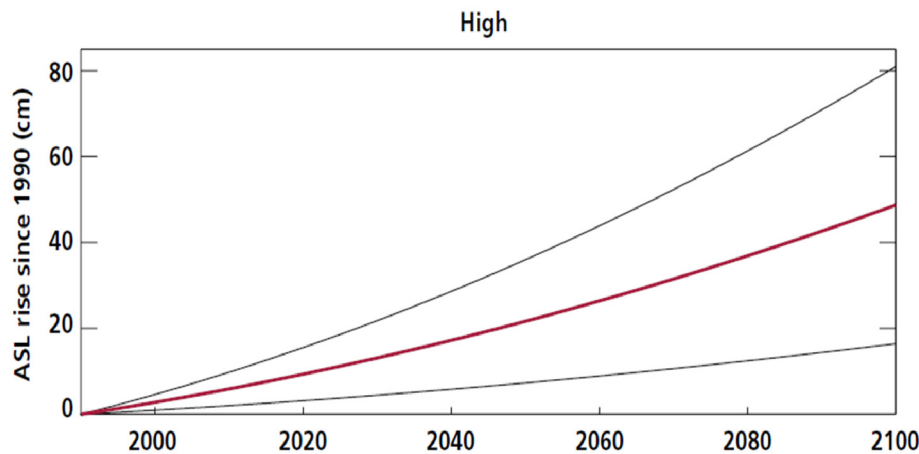


FIGURE 3: ESTIMATED UK ABSOLUTE SEA LEVEL (ASL) RISE TIME-SERIES FOR THE 21ST CENTURY. HIGH EMISSIONS SCENARIO. CENTRAL ESTIMATES (THICK LINES) ARE SHOWN TOGETHER WITH RANGE GIVEN BY 5TH AND 95TH PERCENTILES (THIN LINES). (LOWE *ET AL*, 2009).

The first issue is whether these global sea level rises apply locally to Southern Africa. Mechanisms for local sea level changes include vertical land movement, atmospheric pressure changes, ocean density variations, circulation changes and differential heating. Local sea level change due to ocean density and circulation change relative to the global average have been modelled (Meehl *et al*, 2007). For Southern Africa the predicted changes are approximately 0.05 m above the global average over the 21st century.

The rate of sea level rise measured by tide gauge between 1970 and 2003 at Durban is $+2.7 \pm 0.05$ mm/y, which is similar to recently published results of global sea-level rise calculations over the last ten years derived from worldwide tide gauge and TOPEX/Poseidon altimeter measurements, which range between 2.4 and 3.2 mm/y (Mather, 2007). An analysis of tide gauge records around Southern Africa (Mather *et al*, 2009) indicates that regional sea level trends vary, with the West Coast rising relative to land by +1.87 mm/y (1959–2006), the South Coast by +1.48 mm/y (1957 and 2006) and the East Coast by +2.74 mm/y (1967–2006). Vertical crust movements in Southern Africa are upwards (i.e. the sea level rise relative to land will be reduced compared to the global sea level rise) and increase from approximately +0.3 mm/y on the West Coast to +1.1 mm/y at Richards Bay (Mather *et al*, 2009). Mather *et al* (2009) also identify atmospheric pressure trends as contributing to the measured regional sea level trends given above.

Since the observed regional trends in relative sea level rise described above are relatively small compared to the uncertainties in the long-term global projections, for long-term design purposes it is proposed to apply the global sea level rise projections directly to Southern Africa.

Since the Intergovernmental Panel on Climate Change (IPCC) is the primary consensus reference on this subject, the sea level rise projections from the IPCC's Fourth Assessment Report (IPCC, 2007) are

summarised below. Referring to Table 1, the mid-point of the sea level rise projections for the worst emissions scenario is $(0.26 + 0.59) / 2 \approx 0.4$ m by 2100. The maximum sea level rise projection is $0.59 + 0.2 \approx 0.8$ m by 2100, which is the upper range modelled under the worst emissions scenario and includes a contribution due to increased ice flow from Greenland and Antarctica.

Since the IPCC's Fourth Assessment Report there has been an increased effort to understand the factors influencing sea-level rise, specifically the melting of the ice caps. The results of this research are summarised in Table 1 and provide an upper limit to sea level rise of 2.0 m by 2100.

Our recommended design approach (see Section 8) is to consider the implications for design of the following three sea level rise scenarios to 2100: the mid-point of the IPCC (2007) projections of 0.4 m, the upper end of the IPCC (2007) projections of 0.8 m, and in specific cases the design should also be evaluated for future design adaptations or contingency planning in the event of an extreme upper limit sea level rise of 2.0 m.

3. WIND

Based on a range of models, it is likely that future tropical cyclones (typhoons and hurricanes) will become more intense, with larger peak wind speeds associated with ongoing increases of tropical sea-surface temperatures. Extra-tropical storm tracks are projected to move poleward, with consequent changes in wind, precipitation and temperature patterns, continuing the broad pattern of observed trends over the last half century (IPCC, 2007).

For Cape Town, the south-east winds, which typically prevail along the Cape coast during the summer months, are projected to become stronger as climate change progresses and may become an increasing feature of the winter months. It is important to note that the north-west winds that prevail in winter do not, as yet, show a statistically discernable change as a result of climate forcing and are not projected in regional climate forecasts to change (MacDeevitt and Hewitson, 2007, cited in LaquaR Consultants, 2008).

The International Atomic Energy Agency (IAEA, 2003) recommends that an increase in wind strength between 5 and 10% be considered over a 100 year lifetime of a nuclear power plant. This is a global estimate from 2003.

The Department for Environment, Food and Rural Affairs of the UK Government (Defra, 2006) recommends that sensitivity testing be performed taking into account a 5% increase in offshore wind speed to the year 2055 and a 10% increase to the year 2115.

Due to the inherent uncertainties in long-term regional climate forecasts and the requirement for a precautionary approach, an increase in wind speed of 10% to the year 2100 is recommended for design, based on IAEA (2003) and Defra (2006). Ongoing research work on regional wind climate

projections should be reviewed annually, considering that the Ferrel Westerly winds are the main drivers for winter storm events along the South-Western and Southern Cape coastlines. Changes in wind direction are likely to be localised, with little information currently available.

4. STORM SURGE

Storm-induced surges can produce short-term increases in water level that rise to an elevation considerably above tidal levels. Storm surge is mainly composed of an atmospheric pressure component (low pressure for positive storm surge and high pressure for a negative storm surge) and a wind-induced component.

The gradient in atmospheric pressure and thus the atmospheric pressure component of storm surge is proportional to the wind speed, while the wind set-up component of storm surge is proportional to the square of the wind speed. With a 10% increase in wind speed due to climate change (see Section 3) the total storm surge is thus likely to increase by between 10% and 21%, depending on the relative contribution of the pressure and wind components, respectively.

The UK Climate Projections Report (Lowe *et al*, 2009) applied sophisticated surge models and found that around the United Kingdom the 1:50 year surge is projected to increase by less than 0.09 m by 2100 (not including the mean sea level change). In addition, a “High-plus-plus” (H++) model scenario was also considered (Lowe *et al*, 2009). Whilst the top end of this scenario cannot be ruled out based on current understanding, it is regarded as very unlikely to occur during the 21st century. For the H++ scenario the 1:50 year surge in the Thames Estuary is projected to increase by approximately 0.2 - 0.95 m.

In the absence of downscaled storm surge model data for Southern Africa, it is conservatively recommended to increase the storm surge by 21% to the year 2100, based on a 10% increase in wind speed.

Since shelf waves, edge waves and meteo-tsunamis have similar forcing mechanisms to storm surge, i.e. changes in wind or atmospheric pressure, is recommended to also increase the water level changes caused by these processes by 21%. Note that tsunamis due to geological forcing mechanisms, e.g. earthquakes, are unlikely to be influenced by climate change (IPPC, 2007).

5. WAVES

As part of the Fourth Assessment Report of the Intergovernmental Panel on Climate Change, Trenberth (2007) reports on historical trends in significant wave height (H_{m0}) obtained from Voluntary Observing Ships (VOS) data between 1950 and 2002 (see Figure 4). These results show that around Southern Africa the increase in H_s is around 0.4 cm/decade, whilst significantly higher increases up to

1.2 cm/decade are found in the Northern Atlantic and Northern Pacific Oceans. These results suggest that future wave height changes will not be uniform.

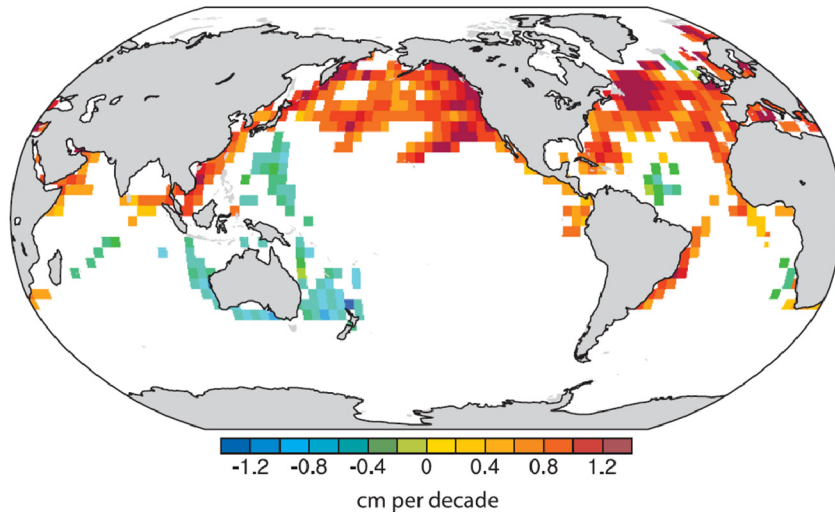


FIGURE 4: ESTIMATES OF LINEAR TRENDS IN SIGNIFICANT WAVE HEIGHT FOR REGIONS ALONG THE MAJOR SHIP ROUTES FOR 1950 TO 2002. TRENDS ARE SHOWN ONLY FOR LOCATIONS WHERE THEY ARE SIGNIFICANT AT THE 5% LEVEL. (TRENBERTH *ET AL*, 2007).

The UK Climate Projections Report (Lowe *et al*, 2009) applied sophisticated wave models and found that around the United Kingdom for the medium emissions scenario, the projected changes to 2100 in the winter mean H_{m0} are between -0.35 and $+0.05$ m. Changes in the annual maxima are projected to be between -1.5 and $+1.0$ m. Changes in wave period and direction were found to be rather small and more difficult to interpret.

The Department for Environment, Food and Rural Affairs of the UK Government (Defra, 2006) recommends sensitivity testing taking into account a 5% increase in wave height to the year 2055 and a 10% increase to the year 2115. These increases are the same as Defra recommends for wind.

The methods presented in Coastal Engineering Manual (CEM, 2003) have been used to analyse the impact of an increased wind speed on fetch-limited and duration-limited waves. Duration-limited waves show the largest increase, with a 10% increase in wind speed due to climate change (see Section 3) increasing the wave height by 13% for the lower wind speeds and 17% for the higher wind speeds.

Wave data measured offshore of Cape Town and Richards Bay have been analysed to investigate trends in the peak significant wave height of individual storm events (Guastella and Rossouw, 2009). The Cape Town data suggests an increasing trend during winter of approximately 0.5 m over the 14 year period from 1994 to 2008, and a general decreasing trend during summer. The Richards Bay data do not show any conclusive trends over the 30 year period from 1979 to 2008. The study also identifies

cold fronts and their associated low pressure systems as the major cause of extreme wave events along the South-Western Cape coastline. On the East Coast of South Africa tropical cyclones and cut-off lows were identified as being responsible for the extreme wave events.

In the absence of downscaled wave generation model data for Southern Africa, it is conservatively recommended to increase the wave height by 17% to the year 2100, based on a 10% increase in wind speed. The impact on wave period can be estimated from the present day H_{m0} - T_p relationship. We are not aware of data on changes in wave directions for South Africa. Sensitivity testing to wave direction should be considered on a project-specific basis.

6. CURRENTS

Ocean circulations could be affected by climate change, and these effects could be either gradual or sudden. For example, it is very likely that the Atlantic Ocean Meridional Overturning Circulation (MOC), which transports relatively warm upper-ocean waters northward (including the Gulf Stream), and relatively cold deep waters southward, will slow down during the course of the 21st century. It is however very unlikely that the MOC will undergo a large abrupt transition during the 21st century. (IPCC, 2007). No reference to possible changes in the Agulhas Current is made in IPCC (2007).

Coastal hydrodynamics will be affected by changes in wind, wave height, wave direction and sea level. Wind-driven currents will tend to increase linearly with wind speed, while wave-driven currents will depend both on wave height and wave direction. These changes will vary from one location to another and can only be quantified through detailed site-specific modelling.

7. SEAWATER TEMPERATURE

From a coastal engineering design perspective, seawater temperature is relevant for cooling water studies and also has a small effect on sediment settling velocities and thus sediment transport. Impacts on marine ecology are beyond the scope of this position paper.

The UK Climate Projections Report (Lowe *et al*, 2009) applied sophisticated hydrodynamic models and found that the seas around the UK are projected to be 1.5 - 4°C warmer, depending on location, and ~0.2 psu fresher by the end of the 21st century, using the medium emissions scenario. Seasonal stratification strength is projected to increase but not by as much as in the open ocean.

The International Atomic Energy Agency (IAEA, 2003) recommends an increase in sea temperature of 3°C be considered over a 100 year lifetime of a nuclear power plant.

Additional factors to be considered include:

- changes in large ocean currents on temperature, e.g. Agulhas Current

- changes in coastal upwelling due to changes in wind speed or direction.

8. RECOMMENDED DESIGN APPROACH

The recommended design approach is to first calculate the present day design parameters based on historical datasets, e.g. determine the 1:100 year wave height from an Extreme Value Analysis of measured Waverider data or wave hindcast data. The present day parameters should then be increased to account for climate change using the values in Table 2. In some cases a conservative design will be achieved by excluding the effect of climate change, e.g. for entrance channel depths and minimum seawater intake depths it is recommended not to include sea level rise.

Although the rate of change is expected to increase over time (see for example Figures 1 and 3), because of the uncertainty attached to these rates and to be conservative, we have assumed a linear increase over the 21st century, with 50% of the change predicted to the year 2100 occurring by 2050. The recommended increases are given in Table 2; refer to Sections 2 to 7 for the supporting information.

TABLE 2: RECOMMENDED INCREASE IN DESIGN PARAMETERS DUE TO CLIMATE CHANGE

Parameter		Increase to 2050	Increase to 2100
Sea level rise	Mid-point of projections ⁽¹⁾	+ 0.2 m	+ 0.4 m
	Upper end of projections ⁽²⁾	+ 0.4 m	+ 0.8 m
	Extreme upper limit ⁽³⁾	+ 1.0 m	+ 2.0 m
Wind speed		+ 5%	+ 10%
Storm surge (including shelf-waves, edge waves and meteo-tsunami)		+ 10%	+ 21%
Wave height		+ 8.5%	+ 17%
Wave period		Obtain from present day H_{m0} - T_p relationship.	
Wave direction		No data, consider sensitivity testing.	
Seawater temperature		+ 1.5°C	+ 3°C
Currents and sediment transport		Use site-specific modelling with the forcing parameters increased by the values given above.	

Notes:

- (1) Although engineering judgement is required on a case by case basis, this value would typically be recommended for minor structures with a short design life, or structures that can relatively easily be adapted to accommodate possible accelerated sea level rise in future.
- (2) Recommended for the majority of large coastal structures.
- (3) In specific cases the design should also be evaluated for future design adaptations or contingency planning in the event of an extreme upper limit sea level rise of 2.0 m by 2100. See below for further details.

In specific cases an extreme upper limit sea level rise of 2.0 m by 2100 should be considered as part of the design process. This will depend inter alia on the type of structure, the design life and the consequences of failure. Examples of the issues that should be considered include:

- The survivability of the structure under the extreme upper limit climate change projections.
- The design should consider making allowance for future adaptations, e.g. increase the breakwater crest width to allow for future raising of the crest level, allow space for future revetments in front of structure.
- Consider the cost implications of an adaptive versus precautionary approach (see Appendix A for more details).
- Consider the impacts of the structure on the adjacent coastline or adjacent structures, and vice versa, e.g. raising the structure levels may increase the flooding risk for adjacent structures.

REFERENCES

1. Ananthaswamy, A (2009) Sea level rise: It is worse than we thought. *New Scientist*, 2715, 28-33.
2. CEM (2003) CEM Part II Chapter 2 - Meteorology and Wave Climate, US Army Corps of Engineers, July 2003.
3. Defra (2006) Department for Environment, Food and Rural Affairs. Flood and Coastal Defence Appraisal Guidance: FCDPAG3 Economic appraisal: Supplementary note to operating authorities – Climate change impacts October 2006.” Defra, UK Government.
4. Deltacommissie (2008) Working together with water, A living land builds for its future, Findings of the Deltacommissie 2008.
5. Guastella, L A and Rossouw M (2009) Coastal Vulnerability: Are Coastal Storms Increasing in Frequency and Intensity along the South African Coast? International Multi-purpose reef conference, Jeffrey’s Bay, South Africa, May 2009.
6. IAEA (2003) Flood Hazard for Nuclear Power Plants on Coastal and River Sites. International Atomic Energy Agency. IAEA Safety Standards Series No. NS-G-3.5.
7. IPCC (2007) Climate Change 2007: Synthesis Report. Contribution of Working Groups I, II and III to the Fourth Assessment Report of the Intergovernmental Panel on Climate Change [Core Writing Team, Pachauri, R.K and Reisinger, A. (eds.)]. IPCC, Geneva, Switzerland, 104 pp.
8. LaquaR Consultants (2008) Global Climate Change and Adaptation - A Sea-Level Rise Risk Assessment, prepared by LaquaR Consultants CC for the City of Cape Town, 2008.
9. Lowe, J A, Howard, T P, Pardaens, A, Tinker, J, Holt, J, Wakelin, S, Milne, G, Leake, J, Wolf, J, Horsburgh, K, Reeder, T, Jenkins, G, Ridley, J, Dye, S, Bradley, S (2009). UK Climate Projections science report: Marine and coastal projections. Met Office Hadley Centre, Exeter, UK.
10. MacDeevit, C and Hewitson, B (2007) Sea-level Rise on the Cape Coast. Atmospheric Science Honours Thesis 2007. University of Cape Town.
11. Mather, A A (2007) Linear and nonlinear sea-level changes at Durban, South Africa, *South African Journal of Science*, 103, November/December 2007, 509-512.
12. Mather, A A, Garland G G and Stretch D D (2009). *African Journal of Marine Science* 2009, 31(2), in press.
13. Meehl, G.A., T.F. Stocker, W.D. Collins, P. Friedlingstein, A.T. Gaye, J.M. Gregory, A. Kitoh, R. Knutti, J.M. Murphy, A. Noda, S.C.B. Raper, I.G. Watterson, A.J. Weaver and Z.-C. Zhao, 2007: Global Climate Projections. In: *Climate Change 2007: The Physical Science Basis. Contribution of Working*

- Group I to the Fourth Assessment Report of the Intergovernmental Panel on Climate Change [Solomon, S., D. Qin, M. Manning, Z. Chen, M. Marquis, K.B. Averyt, M. Tignor and H.L. Miller (eds.)]. Cambridge University Press, Cambridge, United Kingdom and New York, NY, USA.
14. Rohling, E J, Grant, K, Hemleben, Ch, Siddal, M, Hoogakker, B A A, Bolshaw, M and Kucera, M (2008). High rates of sea-level rise during the last interglacial period, *Nature Geoscience*, 1, 38-42, 2008.
 15. PIANC (2008) Waterborne transport, ports and waterways: A review of climate change drivers, impacts, responses and mitigation. May 2008.
 16. Pfeffer, W. T., Harper, J. T. & O'Neel, S (2008). Kinematic constraints on glacier contributions to 21st-Century sea-level rise. *Science*, 321, 1340-1343.
 17. Rahmstorf, S. (2007) A Semi-Empirical Approach to Projecting Future Sea-Level Rise. *Science*, 315, 368-370.
 18. Trenberth, K.E., P.D. Jones, P. Ambenje, R. Bojariu, D. Easterling, A. Klein Tank, D. Parker, F. Rahimzadeh, J.A. Renwick, M. Rusticucci, B. Soden and P. Zhai, (2007). Observations: Surface and Atmospheric Climate Change. In: *Climate Change 2007: The Physical Science Basis. Contribution of Working Group I to the Fourth Assessment Report of the Intergovernmental Panel on Climate Change* [Solomon, S., D. Qin, M. Manning, Z. Chen, M. Marquis, K.B. Averyt, M. Tignor and H.L. Miller (eds.)]. Cambridge University Press, Cambridge, United Kingdom and New York, NY, USA.

APPENDIX A: ADAPTIVE VERSUS PRECAUTIONARY APPROACH

Our response to climate change requires appropriate decisions on whether to consider a managed adaptive approach or whether to adopt a more precautionary approach. The following (reproduced from Defra, 2006) provides a brief explanation of this.

Managed adaptive approach

A managed approach allows for adaptation in the future, and is wholly appropriate in the majority of cases where ongoing responsibility can be assigned to tracking the change in risk, and managing this through multiple interventions. This approach provides flexibility to manage future uncertainties associated with climate change, during the whole life of a flood risk management system. To consider a precautionary approach only, could lead to greater levels of investment at fewer locations. A managed approach is therefore important to ensure best value for money.

Both structural (e.g. physical changes to structures, upstream storage or a combination thereof) and non-structural solutions (e.g. land use changes, resilience, statutory objections, relocation, public awareness) are necessary to ensure cost effective adaptation can take place in future years. In order to fully explore non-structural options alongside structural options, the sensitivity analysis of these options should become a more important component of appraisal and decision making, with care needed at screening-out stages to avoid discarding non-structural options without strong justification. See Figure A.1 and the saw-tooth line to illustrate.

Precautionary approach

For some circumstances, future adaptation may be technically infeasible or too complex to administer over the long term of up to 100 years. These circumstances may occur where multiple interventions are not possible to manage the changes in risk. Therefore, a precautionary approach, perhaps with one-off intervention, may be the only feasible option, such as in the design capacity of a major culvert or in the span of a road bridge across a flood plain. See Figure A.1 and the dashed line to illustrate.

REFERENCES

- | | |
|--------------|---|
| Defra (2006) | Department for Environment, Food and Rural Affairs. Flood and Coastal Defence Appraisal Guidance: FCDPAG3 Economic appraisal: Supplementary note to operating authorities – Climate change impacts October 2006.” Defra, UK Government. |
|--------------|---|

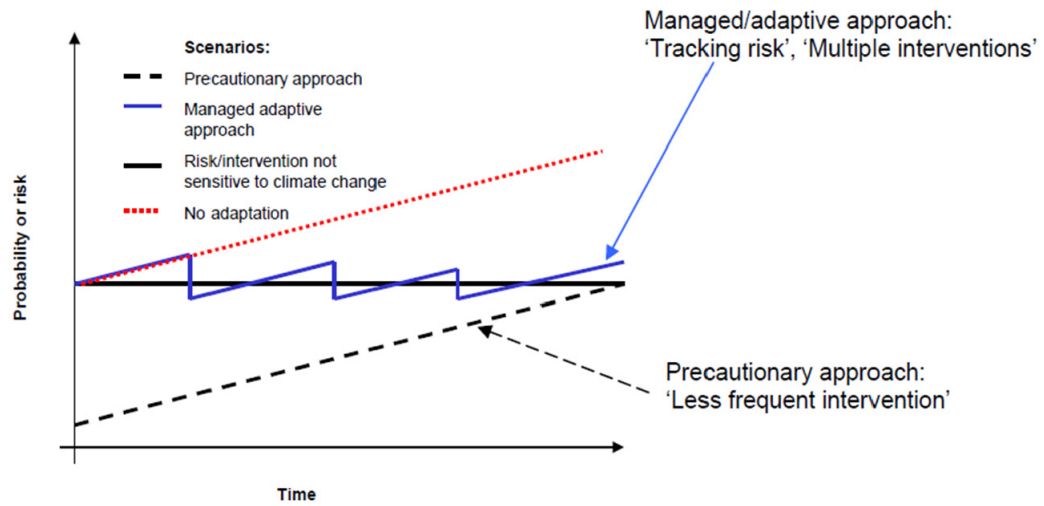


FIGURE A.1: COMPARISON BETWEEN MANAGED ADAPTIVE APPROACH AND PRECAUTIONARY APPROACH RESPONSE TO CLIMATE CHANGE. (DEFRA, 2006).